2008

Catalytic synthesis of ethanol from biomass-derived syngas

Adefemi Adelanwa Egbebi
Louisiana State University and Agricultural and Mechanical College

CATALYTIC SYNTHESIS OF ETHANOL FROM BIOMASS-DERIVED SYNGAS

A Dissertation

Submitted to the Graduate Faculty of the
Louisiana State University and
Agricultural and Mechanical College
in partial fulfillment of the
requirements for the degree of
Doctor of Philosophy

in

The Gordon A. and Mary Cain Department of Chemical Engineering

by
Adefemi Adelanwa Egbebi
B.Sc., Obafemi Awolowo University, Nigeria, 1999
December 2008

ACKNOWLEDGEMENTS

I wish to express my profound gratitude to Dr. James J Spivey, my advisor for his relentless support and guidance throughout the course of the research work. He was always ready to offer timely suggestions and share his ideas and I have learnt a lot from him.

I wish to thank Dr. K. Valsaraj, Dr. Gregory Griffin, Dr. Kerry Dooley and Dr Martin Hugh-Jones for being part of my examination committee. My appreciation goes to the chemical engineering department at LSU for giving me the opportunity to pursue this dream and for providing financial support. I also would love to thank everybody who has contributed in one way or the other to my experience at LSU: faculty, Dr Spivey's group members, fellow graduate students, student workers and the support staff at the chemical engineering department.

I would like to thank my lovely wife, Titilayo and our beautiful children, Oluwatoyosi and Opeyemi for their support, love and patience; and also my parents and siblings, for their prayers and encouragement.

Above all, I give thanks to God, for the gift of life, love, knowledge and understanding.

TABLE OF CONTENTS

LIST OF TABLES

LIST OF FIGURES

ABSTRACT

Syngas produced by gasification of biomass or coal can be converted directly to ethanol and higher alcohols by processes based on heterogeneous catalysts. In addition to its use as a neat fuel or fuel additive, ethanol can serve as a hydrogen carrier, which can be reformed to a hydrogen-rich gas at the point of use, and converted to electrical energy in a fuel cell. Rhodium-based catalysts have been found to be most selective for the formation of C_2 oxygenates from the hydrogenation of CO but the yield of ethanol is typically low in the absence of promoters. Improved yields can be achieved by suitable choice of promoter(s) and support.

Here, we explore the effects of Rh promoted with Mn, Fe, and Li and supported on TiO_2, which is an active support for CO hydrogenation reactions. Rh-TiO_2, Rh-Li/TiO_2, Rh-Mn/TiO_2, Rh-Mn-Li/TiO_2 and Rh-Mn-Li-Fe/TiO_2 catalysts were prepared using conventional incipient wetness impregnation and tested for the hydrogenation of CO and a mixture of CO and CO_2. Rh-Li/TiO_2 is the most active and selective of these catalysts for ethanol formation from CO hydrogenation, due to the interactions between Li and Rh resulting in enhanced Rh dispersion, which decreases CO dissociative adsorption activity on the catalysts. This allows for increased CO insertion and hydrogenation of surface species. Mn promotion leads to a weakening of the Rh-CO bond, this makes more CO available for CO insertion. However, the hydrogenation activity of this catalyst appears to be limited, so that the selectivity to acetaldehyde is relatively high. Multiple promotion by Mn+Li or Mn+Li+Fe leads to loss of overall activity although total oxygenates selectivity increases.

Despite increased methanation as a result of the addition of CO_2 to the feed, Rh-Mn-Li-Fe/TiO_2 catalysts produced ethanol at a higher selectivity during the hydrogenation of a CO/CO_2 mixture than for the hydrogenation of only CO, which was not observed on Rh/TiO_2, Rh-

Li/TiO_2, $Rh\text{-}Mn/TiO_2$ and $Rh\text{-}Mn\text{-}Li/TiO_2$. The Fe promoter is believed to increased reverse WGS reaction upon CO_2 addition, resulting in increased CO and decreased hydrogen species on the surface, leading to higher CO insertion activity than when Fe is not a promoter. The result is a higher increase in ethanol selectivity than in methanation activity, causing the $EtOH/CH_4$ to increase.

The hydrogenation of CO to form ethanol is thermodynamically limited if methane is allowed as a reaction product. Even on Rh-based catalysts - which are the most selective for ethanol - the selectivity to ethanol versus methane is limited in this work and in literature. Although it might be anticipated that increasing H_2/CO ratio would favor methane, the kinetic studies in the literature, and our results reported here, show that the point selectivity for ethanol ($\boldsymbol{S = r_{EtOH}/r_{CH_4}}$) actually increases with increasing H_2/CO ratio on Rh-based catalysts. This may be attributed to the increased hydrogenation of the surface acetaldehyde intermediate to ethanol.

CHAPTER 1 : INTRODUCTION

1.1 BIOMASS

The use of biomass and other renewables to provide energy and chemicals is receiving increased attention because these resources can supplement existing supplies of raw materials and have less net environmental impact, according to some studies[1]. Worldwide, renewable energy sources (including biomass) account for about 19% of total energy usage[2], and have the potential to supply 50% of world energy demand in the next century[3]. In the US, biomass supplied roughly 3% of a total energy demand of 98 quads in 2003[4], and is projected to grow to at a rate of 1.5%/yr through 2025[5, 6].

Virtually all of the energy derived from biomass (98% by one estimate[7]) is currently produced by direct combustion. Gasification is an alternative that offers a number of advantages, e.g., the potential for higher thermal efficiency[8, 9]. Large scale biomass gasification plants ranging in size from 15-70 MW_{th} [10] are being developed in Europe, primarily for power generation.

Gasification is a thermochemical process in which biomass reacts with air (or oxygen) and steam to produce synthesis gas, a mixture consisting primarily of CO, CO_2, H_2, and H_2O (Fig. 1.1). Table 1.1 shows typical compositions of syngas from various industrial gasifiers[11]. These compositions are mostly dependent on feedstock type, oxidant and the operating conditions of the gasifier among other factors. This mixture can be used to produce a range of products using well-established technologies, such as fuels via the Fischer-Tropsch process[12-15]. However, the use of biomass-derived syngas to produce higher alcohols has received relatively little attention, despite the potential to produce valuable compounds such as ethanol[14, 16, 17].

Challenges that remain include novel catalytic reactor designs tailored to the typically smaller scale of biomass conversion processes[18], catalysts for downstream adjustment of the

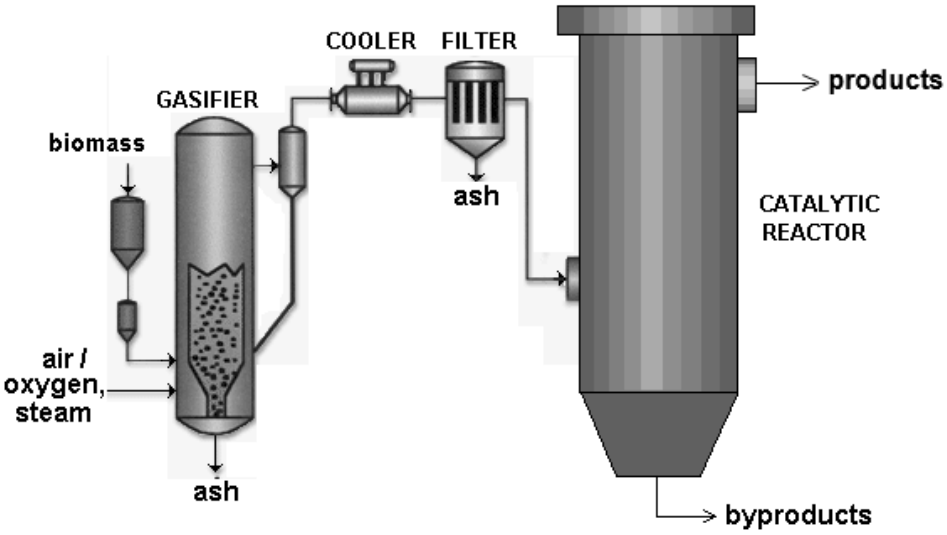

Figure 1.1: Generic biomass gasification process.

Table 1.1: Typical Compositions of Syngas from Various Industrial Gasifiers[11]

	BCL/FERCO	**MTCI**	**Purox**	**Shell**
gasifier type	CFB-IH[a].	BFB-IH[b]	FB[c]	FB-EF[d]
feedstock	wood	pulp	MSW[e]	coal
H_2 (%)	14.9	43.3	23.4	24
CO (%)	46.5	9.22	39.1	67
CO_2 (%)	14.6	28.1	24.4	4
H_2O (%)	dry	5.57	dry	3
CH_4 (%)	17.8	4.73	5.47	0.02
C_2+ (%)	6.2	9.03	4.93	0
Tars (%)	-	scrubbed	-	0
H_2S (%)	-	0.08	0.05	1
O_2 (%)	0	0	-	0
NH_3 (%)	0	0	-	0.04
N_2 (%)	0	0	-	1
H_2/CO Ratio	0.3	4.6	0.6	0.36
heating value (MJ/m^3)	18.0	16.7	-	9.51

[a] Circulating fluidized bed-indirectly heated.
[b] Bubbling fluidized bed- indirectly heated
[c] Fixed bed
[d] Fluidized bed - entrained flow
[e] Municipal solid waste

H_2/CO ratio for specific end products[19], and catalysts for the conversion of biomass-derived syngas to ethanol.

1.2 ETHANOL

Among other uses, ethanol has been used as a fuel in the US since at least 1908, although it was later displaced as a commodity fuel by petroleum-derived compounds[20]. Standard Oil marketed a 25% ethanol/gasoline mixture in the 1920's[20]. Recent incentives to use ethanol as a fuel additive in the US have led to an increase in production of about 12%/yr in recent years[20]. Current economic and process studies have shown that ethanol is an attractive end product because a widespread market exists for its use as a fuel additive[20], among other applications. In fact, over 2 billion gallons of ethanol were produced in the US in 2002, mostly for use as a fuel additive[21], with projections suggesting production of 5 billion gallons/yr by 2012[22]. Although this is a small fraction of the US consumption of 134 billion gallons/yr of gasoline, studies show that there is a potential to increase ethanol production to 34-75 billion gallons/yr (i.e., between 18 and 39% of US gasoline needs, on energy basis) if the necessary technology can be developed[23].

There are also clear environmental benefits of ethanol, both as a neat fuel and as a fuel additive. For example, Table 1.2 shows that biomass-derived ethanol transportation fuel results in lower net petroleum use and lower greenhouse gas emissions than gasoline per mile driven[24].

These facts suggest that there is a large potential market for ethanol, and that ethanol is a logical and environmentally favorable end product. Note that the catalysts used to produce ethanol from syngas typically form methanol and other higher alcohols as co-products.

Gasification routes to ethanol. Although most of the current research and development efforts are focused on biochemical routes to ethanol[20], thermochemical routes such as gasification can also produce these higher alcohols. Among the processes being studied to

Table 1.2: Comparison of Gasoline and Biomass-derived Ethanol [24]

Fuel	Petroleum use, Btu/mile	Greenhouse gas emissions, g/mile
Gasoline	5158	468
Bio-ethanol	258-758[1]	344-355[2]

[1]depends on specific source of ethanol, includes petroleum use in processing and transporting
[2]for ethanol from corn grain

produce ethanol are biomass gasification followed by:

- low-temperature fermentation to produce ethanol from CO and hydrogen[25], or
- catalytic synthesis of mixed alcohols[26] or mixed oxygenates[27].

Although biochemical processes are typically more selective to specific end products (including ethanol), the reaction rates of thermochemical processes are orders of magnitude higher and can be used to process a wide range of feedstocks (forest residues, animal wastes, etc.) into a syngas mixture of reasonably consistent composition. This can be a significant advantage in making these processes economically competitive.

1.3 CATALYSTS

Supported Rh has been known to have the ability to produce C_2^+ oxygenates such as ethanol, acetaldehyde and acetic acid selectively from syngas[28]. Rh is versatile because it can form methane, alcohols, or other oxygenates, from CO hydrogenation depending on support, promoter, and reaction conditions[29-34]. The selectivity to ethanol for unpromoted Rh catalysts is relatively low—the main products are hydrocarbons[28, 35] but the formation of ethanol can be greatly enhanced by the addition of promoters[36-38]. Some Rh-based catalysts have also been tested for CO_2 hydrogenation to ethanol, which is thought to proceed through a CO intermediate[39, 40].

We are aware of no systematic experimental studies of the catalytic synthesis of ethanol from gas mixtures that are designed to approximate those of gasified biomass. Most available

relevant literature has focused on the hydrogenation of either CO or CO_2, rather than mixtures of the two[28, 30, 36, 37, 41-43]. However, coal or biomass-derived syngas (as well as syngas from other sources) will contain significant levels of both as shown in Table 1.1.

1.4 OBJECTIVES

In this work we examined titania - supported Rh catalysts promoted with Mn, Li and Fe either individually or in combination for CO hydrogenation and also for hydrogenation of CO/CO_2 rich syngas, which is representative of a biomass-derived syngas. The goal is to study the effects of the promoters on Rh/TiO_2 for these hydrogenation reactions, with a view to determine the modifications necessary to produce catalysts with better yields to ethanol from biomass derived syngas.

1.5 OUTLINE OF THE DISSERTATION

Chapter 1 introduces the need to diversify our sources of energy by using more renewables like biomass which is abundant in nature. It also explains how ethanol can be produced from biomass (or coal) via the gasification process to produce syngas (a mixture of CO, H_2 and CO_2) which can be converted to high-value products like hydrocarbon fuels and ethanol in a catalytic reactor.

Chapter 2 examines the thermodynamics of the syngas reactions and reviews the extensive literature on the four major catalysts types that has been tested for the hydrogenation of CO and/or CO_2, namely: Rh-based, Cu-based, Mo-based and Fischer-Tropsch type catalysts. The effect of promoters, supports, preparation methods and other factors, which affect activity and selectivity of the catalysts, are discussed. It also discusses the reaction paths /mechanisms on each of these catalyst types.

Chapter 3 provides the details of the experimental design: the catalyst synthesis, testing and characterization methods used in this work. It also describes all the equipment used to carry

out the experiments.

Chapters 4-6 are written using the journal style. Each chapter is written is such a way that it can be sent for publication with little or no further editing. Each journal chapter has its own introduction, results and discussion, followed by references. This means that there is little duplication across the chapters in some subsections with regards to introduction and experimental methods used. It begins with **Chapter 4**, which examines the effects of selected promoters: Mn, Li and Fe on Rh/TiO_2 for CO hydrogenation reaction. These promoters are used individually and in combination and have been previously identified to help in ethanol forming reactions on Rh-based catalysts. **Chapter 5** focuses on the effect of CO_2 on the hydrogenation of CO on a series of Rh/TiO_2 catalysts. This not only examines the effect of CO_2 on product selectivity, but also serves as a comparison between product distribution of conventional syngas (with little or no CO_2 content) and a representative biomass/coal-derived syngas which typically has much higher CO_2 content. In **Chapter 6**, we looked at the effect of H_2/CO ratio on the selectivity of ethanol vs methane. This is necessary because methane formation is the most significant side reaction in the syngas to ethanol process.

Chapter 7 summarizes the conclusions drawn in the chapters 4 – 6 and offers recommendations for future work.

1.6 REFERENCES

1. S. Kim and B. E. Dale, *Journal of Industrial Ecology*, 2003, **7**, 147-162.
2. B. G. Park, *Korean Journal of Chemical Engineering*, 2004, **21**, 782-792.
3. IEA, International Energy Agency, Editon edn., 2005, vol. 2005.
4. DOE, *Annual Energy Review 2003* Report No. DOE/EIA-0384, 2004.
5. B. March, Energy Summit 2004, Louisiana State University, Baton Rouge, 2004.
6. DOE, ed. DOE, Editon edn., 2005.

7. D. J. Stevens, ed. National Renewable Energy Lab, Editon edn., Aug. 2001, p. 9.

8. Z. Wu, C. Wu, H. Huang, S. Zheng, X. Dai and Proceedings of the International Conference on Fluidized Bed Combustion, Jacksonville, Florida, 2003.

9. J. Andries and B. J. P. Buhre, *DGMK Tagungsbericht* 2000, 115-125.

10. H. Lampenius, *IMechE Conference Transactions*, 2003, **3,** , 99-111.

11. J. P. Ciferno and J. J. Marano, *Benchmarking Biomass Gasification Technologies for Fuels, Chemicals and Hydrogen Production.* , U. S Department of Energy, NETL, 2002.

12. W. H. Zimmerman, C. N. Campbell and J. L. Kuester, *Preprints of Papers - American Chemical Society, Division of Fuel Chemistry*, 1986, **31**, 116-123.

13. H. W. Parker, *Mechanical Engineering*, 1982, **104**, 54-59.

14. N. Koizumi, K. Murai, T. Ozaki and M. Yamada, *Catalysis Today*, 2004, **89**, 465-478.

15. K. W. Jun, H. S. Roh, K. S. Kim, J. S. Ryu and K. W. Lee, *Applied Catalysis a-General*, 2004, **259**, 221-226.

16. R. Breault, J. P. Hindermann, A. Kiennemann and M. Laurin, *Entropie*, 1986, **22** 7-16.

17. K. Klier, R. G. Herman and G. W. Simmons, *Catalysts for alcohols from biomass (DOE/CS/83001-T1; Order No. DE83003611), 12 pp. From: Energy Res. Abstr. 1983, 8(6), Abstr. No. 11970* DOE/CS/83001-T1; Order No. DE83003611, 1982.

18. C. Cao, Y. Wang, D. C. Elliott, J. Hu and D. Stevens, *Abstracts of Papers, 226th ACS National Meeting, New York, NY, United States*, 2003.

19. T. J. Wang, J. Chang, J. X. Zhu and Y. Fu, *Ranliao Huaxue Xuebao* 2004, **32**, 297-300.

20. J. DiPardo, *Outlook for Biomass Ethanol Production and Demand* http://www.eia.doe.gov/oiaf/analysispaper/biomass.html accessed Feb, 2005, US DOE, Energy Information Agency, 2002.

21. EERE/DOE, *Alternative Fuels Data Center www.afdc.doe.gov/altfuel/ediesel_general.html*, 2003.

22. K. Shaine Tyson, Joseph Bozell, Robert Wallace, E. Petersen and Luc Moens, *Biomass Oil Analysis:Research Needs and Recommendations* NREL/TP-510-34796, National Renewable Energy Lab (Golden, CO), 2004.

23. C. Riley, AIChE Spring Meeting, New Orleans, Louisiana, 2002.

24. M. Wang, C Seracks and D. Santini, *Near Future Cases for E-10 Use (ANL/ESD-38)* ANL/ESD-38, Argonne National Lab, Argonne, IL., 1999.

25. E. C. Clausen and J. L. Gaddy, *Preprints of Papers - American Chemical Society, Division of Fuel Chemistry*, 1993, **38**, 855-861.

26. E. S. Olson, R. K. Sharma and T. R. Aulich, *Applied Biochemistry and Biotechnology*, 2004, **113-16**, 913-932.

27. G. Claudet, *Clefs CEA* 2001, **2000-2001**, 16-20.

28. M. M. Bhasin, W. J. Bartley, P. C. Ellgen and T. P. Wilson, *Journal of Catalysis*, 1978, **54**, 120-128.

29. P. Forzatti, E. Tronconi and I. Pasquon, *Catalysis Reviews-Science and Engineering*, 1991, **33**, 109-168.

30. M. Ichikawa, T. Fukushima and K.Shikakura, Proc. 8th Int. Cong. Catal., Berlin, Germany, 1984.

31. M. Ichikawa, T. Fukushima, T. Yokoyama, N. Kosugi and H. Kuroda, *Journal of Physical Chemistry*, 1986, **90**, 1222-1224.

32. M. Ichikawa, *Chemtech*, 1982, **12**, 674-680.

33. M. Ichikawa, *Bulletin of the Chemical Society of Japan*, 1978, **51**, 2268-2272.

34. M. Bowker, *Catalysis Today*, 1992, **15**, 77-100.

35. W. M. H. Sachtler, *Berichte Der Bunsen-Gesellschaft-Physical Chemistry Chemical Physics*, 1995, **99**, 1295-1305.

36. S. C. Chuang, J. G. Goodwin and I. Wender, *Journal of Catalysis*, 1985, **95**, 435-446.

37. Y. H. Du, D. A. Chen and K. R. Tsai, *Applied Catalysis*, 1987, **35**, 77-92.

38. J. R. Katzer, A. W. Sleight, P. Gajardo, J. B. Michel, E. F. Gleason and S. Mcmillan, *Faraday Discussions*, 1981, 121-133.

39. T. Iizuka, Y. Tanaka and K. Tanabe, *Journal of Catalysis*, 1982, **76**, 1-8.

40. A. Trovarelli, C. Mustazza, G. Dolcetti, J. Kaspar and M. Graziani, *Applied Catalysis*, 1990, **65**, 129-142.

41. P. Gronchi, E. Tempesti and C. Mazzocchia, *Applied Catalysis A: General*, 1994, **120**, 115-126.

42. M. Ichikawa and T. Fukushima, *Journal of the Chemical Society-Chemical Communications*, 1985, 321-323.

43. A. Kiennemann, R. Breault, J. P. Hindermann and M. Laurin, *Journal of the Chemical Society-Faraday Transactions I*, 1987, **83**, 2119-2128.

CHAPTER 2 : LITERATURE REVIEW*

In order to understand the synthesis of ethanol from biomass-derived syngas it is necessary to examine the individual reactions leading to ethanol from the compounds present in syngas: CO, CO_2 and H_2. A great deal of literature has been published on these reactions, which are essentially hydrogenation reactions, i.e. hydrogenation of CO and/or CO_2 to C_2^+ products. Side reactions involving these compounds such as the water-gas shift and methanation reactions also occur. This chapter explores the thermodynamics of the reactions, effect of reactions, suitable catalysts types and possible reaction pathways.

2.1 THERMODYNAMICS

2.1.1 Hydrogenation of CO to Ethanol:

$$2CO + 4H_2 \rightarrow C_2H_5OH + H_2O \qquad (1)$$

ΔH_r° = -61.20 kcal/mol

ΔG_r° = -29.32 kcal/mol

This is a highly exothermic and favorable reaction. Thermodynamic analysis of the reaction assuming a stoichiometric mixture of CO and H_2 (H_2/CO = 2.0) at 20 bar shows that ethanol and water concentrations decrease with temperature while those of the reactants increase (Fig. 2.1). This suggests that ethanol formation from CO hydrogenation should be done at temperatures below roughly 300°C.

2.1.2 Hydrogenation of CO_2 to Ethanol:

$$2CO + 4H_2 \rightarrow C_2H_5OH + H_2O \qquad (2)$$

ΔH_r° = -41.54 kcal/mol, ΔG_r° = -15.70 kcal/mol

Reproduced by permission of The Royal Society of Chemistry. Most of this chapter has been published as J.J. Spivey and A.A. Egbebi, *Chemical Society Reviews*, 2007, 36, 1514 – 1528

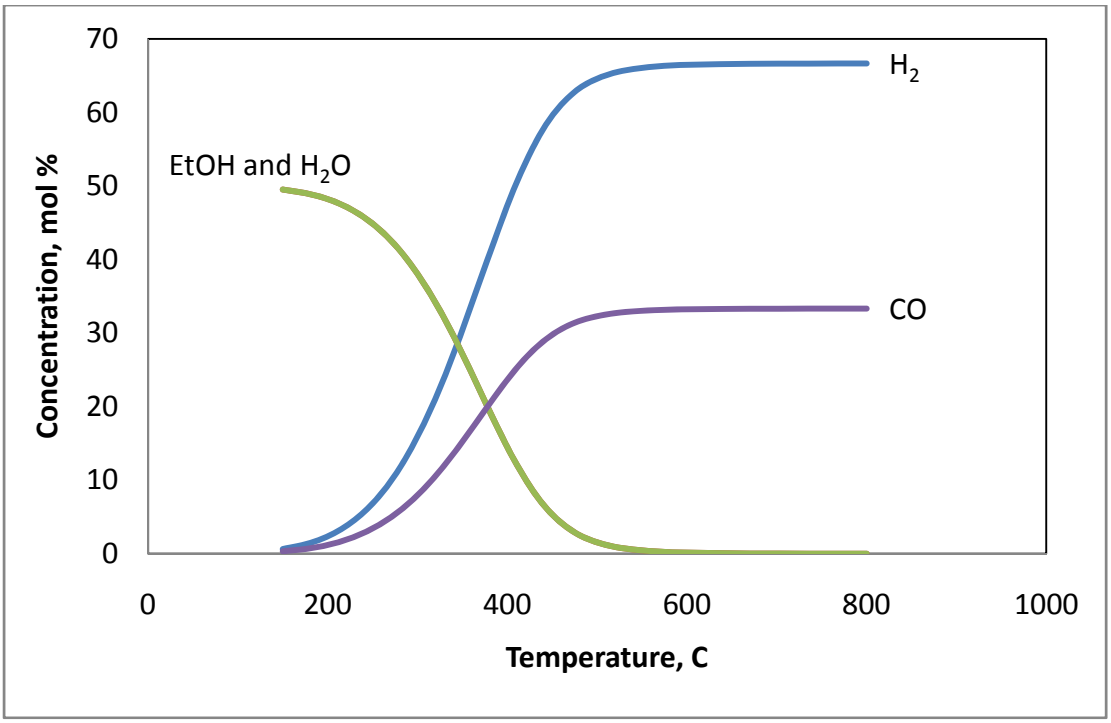

Figure 2.1: Equilibrium composition for the hydrogenation of CO to ethanol (H_2/CO = 2.0, 20 bar, calculated using HSC Chemistry software[1]).

This reaction is also exothermic and thermodynamically favorable. Fig. 2.2 shows that the concentration trends follow those of CO hydrogenation although the temperature window for substantial production of ethanol is not as wide. Ethanol and water concentrations decrease while those of CO_2 and H_2 increase with temperature. This result also suggests that ethanol synthesis from syngas should be carried out at low temperatures (~200°C) for reasonable conversion of reactants. However, substantial amount of water is formed in this reaction and might affect the temperature region we chose to run the reaction.

2.1.3 Side Reactions

The water gas shift (WGS) reaction;

$$CO + H_2O \rightleftarrows CO_2 + H_2O \qquad (3)$$

is a very important side reaction that affects the equilibrium of both CO and CO_2 hydrogenation reactions. In the hydrogenation of CO to ethanol, the H_2O formed readily can react with CO to

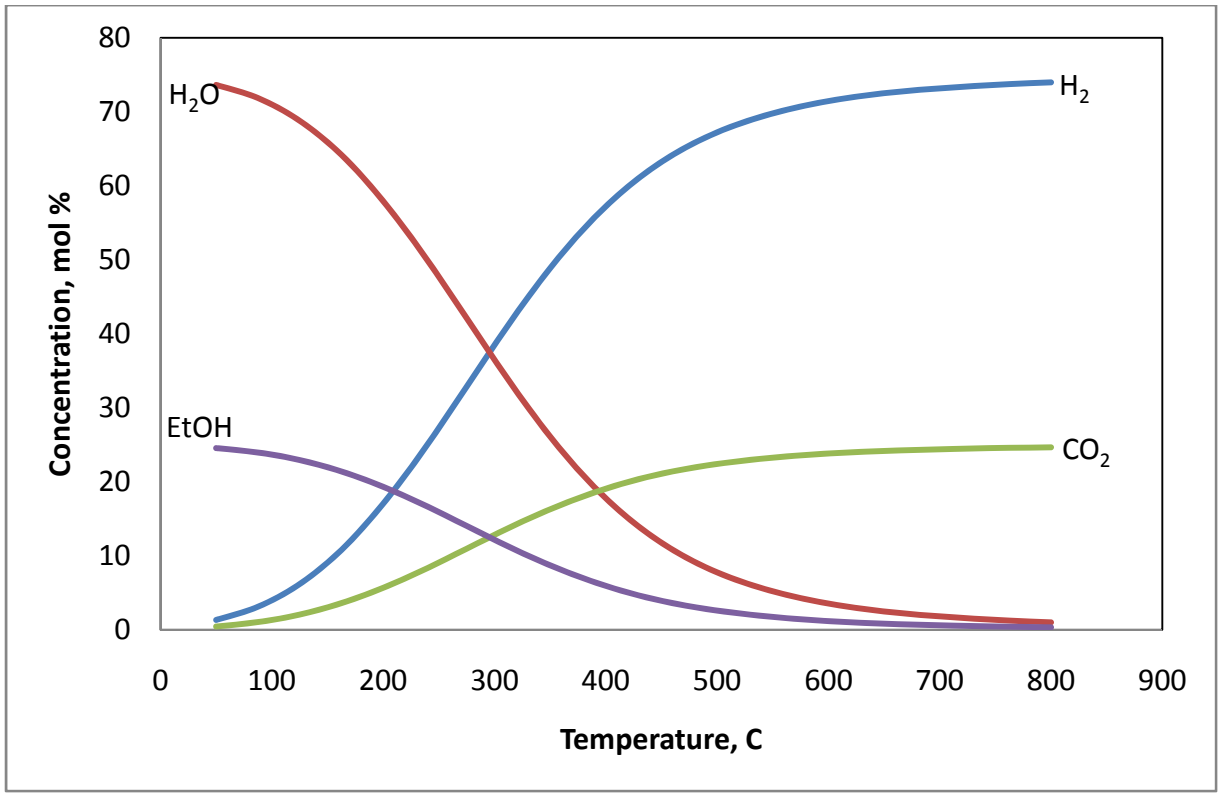

Figure 2.2: Equilibrium composition for the hydrogenation of CO to ethanol (H_2/CO_2 = 3.0, 20 bar, calculated using HSC Chemistry software[1]).

produce CO_2 and H_2, while in CO_2 hydrogenation the reverse WGS reaction may occur. The reverse WGS is essentially a partial reduction of CO_2 to CO, which has been identified as an elementary step involved in the synthesis of ethanol from CO_2 hydrogenation[2, 3]. This suggests that the hydrogenation of both CO and CO_2 to ethanol proceed through a common intermediate.

When methanation of CO and/or CO_2;

$$CO + 3H_2 \rightarrow CH_4 + H_2O \quad (4)$$

$$CO_2 + 4H_2 \rightarrow CH_4 + 2H_2O \quad (5)$$

are allowed to occur along with the hydrogenation reactions, methane is the most thermodynamically significant product[4]. Fig. 2.3 shows the equilibrium concentrations of a CO hydrogenation to ethanol reaction with stoichiometric mixture of CO and H_2 (H_2/CO = 2.0) at 20

bar when methane is allowed as a product. Ethanol mole fraction is virtually zero at all temperatures even though substantial amounts were formed at the same conditions when methane formation was not allowed (Fig. 2.1). This shows that the thermodynamically favored formation of methane must be kinetically limited if ethanol yield is to be significant.

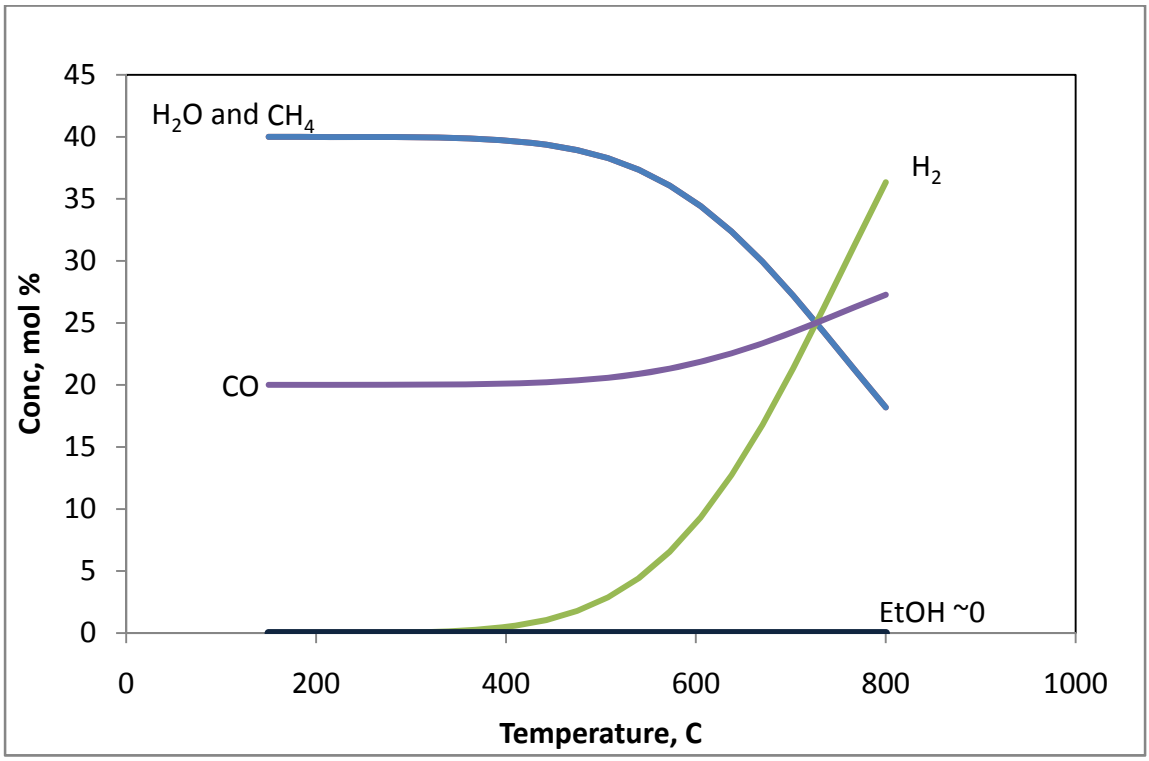

Figure 2.3: Equilibrium composition for the hydrogenation of CO to ethanol with methane allowed ($H_2/CO = 2.0$, 20 bar, calculated using HSC Chemistry software[1])

2.1.4 Effect of Pressure

Increasing pressure increases the equilibrium concentration of ethanol formation from the hydrogenation of CO. Formation of ethanol is favored at higher pressures, although the effect increasingly weakens at higher pressure in a logarithmic fashion (Fig. 2.4). This is in qualitative agreement with experimental results. For example, Chuang et al. show that increasing the pressure from 1 to 10 atm resulted in an increase in ethanol formation rate from zero to 0.44 mol/kg/h at 300 °C over a Rh/TiO_2 catalyst [5].

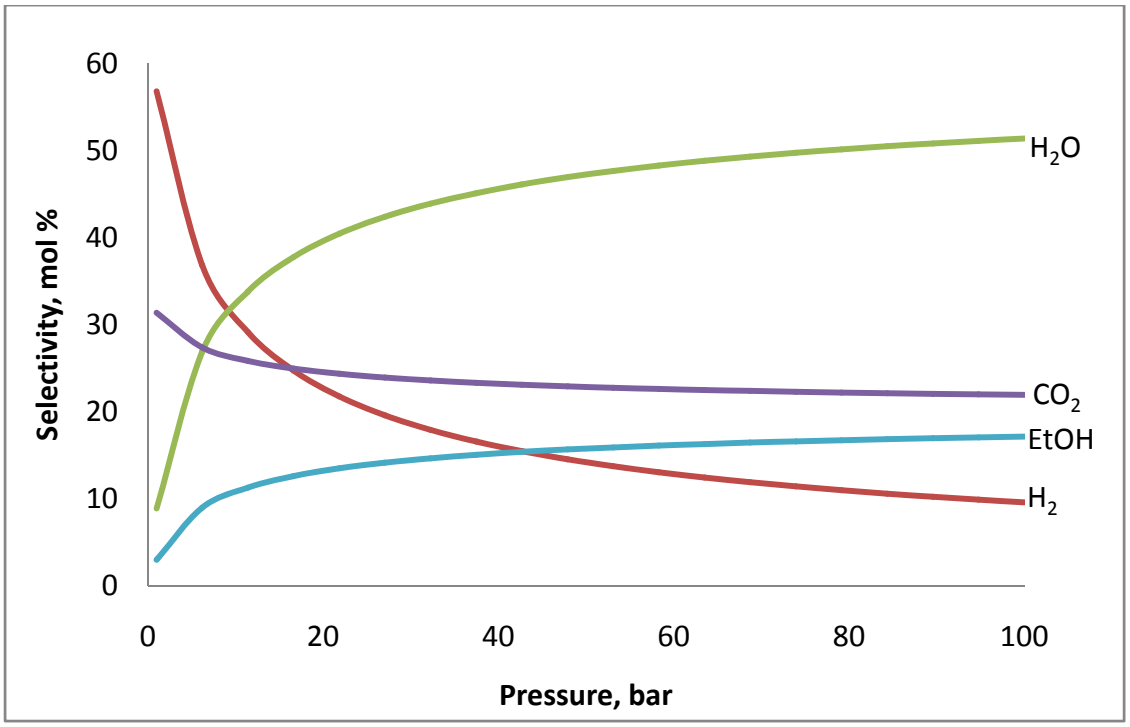

Figure 2.4: Equilibrium composition for the hydrogenation of CO to ethanol (H_2/CO = 2.0, 250°C, calculated using HSC Chemistry software[1]).

2.2 CATALYST TYPES

The vast majority of reported studies are based on the hydrogenation of CO. There are limited studies based on hydrogenation of CO_2, and even fewer on hydrogenation of mixtures of CO and CO_2. None of these studies contains realistic concentrations of H_2, CO, CO_2 and steam as contained in a product mixture of a steam gasified biomass.

Catalysts for ethanol synthesis from the hydrogenation of CO or CO_2 can be broadly grouped into four categories:

a) Rh-based catalysts

b) Modified methanol synthesis catalysts (based on Cu)

c) Modified Fischer-Tropsch type catalysts.

d) Modified Mo-based catalysts.

2.2.1 Rh-based Catalysts

2.2.1.1 CO Hydrogenation

By far the most widely studied catalysts for the hydrogenation of CO to oxygenates are based on Rh. Supported Rh has been known for decades to have the ability to produce C_2^+ oxygenates such as ethanol, acetaldehyde and acetic acid selectively from syngas[6]. Rh occupies an interesting position in the periodic table because it lies between metals that easily dissociate CO to form higher hydrocarbons (e.g., Fe and Co) and those which do not dissociate CO and produce methanol (e.g., Pd, Pt and Ir) [7, 8]. Rh can form methane, alcohols, or other oxygenates, from CO hydrogenation depending on support, promoter, and reaction conditions[7, 9-13].

Reaction sequence. Despite some differences in the details, the general mechanism proposed by a number of researchers for the formation of ethanol and C_3^+ oxygenates from CO hydrogenation can be represented by the sequence of reaction steps shown in Fig. 2.5[14, 15].

Steps 1 - 4 (CO and H_2 adsorption). First, in steps 1 and 2, CO and H_2 are adsorbed. The adsorbed, non-dissociated CO is then either hydrogenated to form methanol (step 3)[15, 16] or dissociated (step 4). The adsorption of CO on Rh is a key step because it is thought to be rate-determining in many cases[9, 17, 18]. CO adsorption is strongly affected by the presence of promoters[19-21], Rh cluster size and shape[22-24], support[25-27] pretreatment[28], and reaction conditions. These factors determine whether the adsorption is dissociative, non-dissociative, or both. Because a combination of both is required for ethanol synthesis (steps 4 and 7), it is not surprising that the activity and selectivity on Rh-based catalysts differ greatly depending on the exact preparation and history of the catalyst.

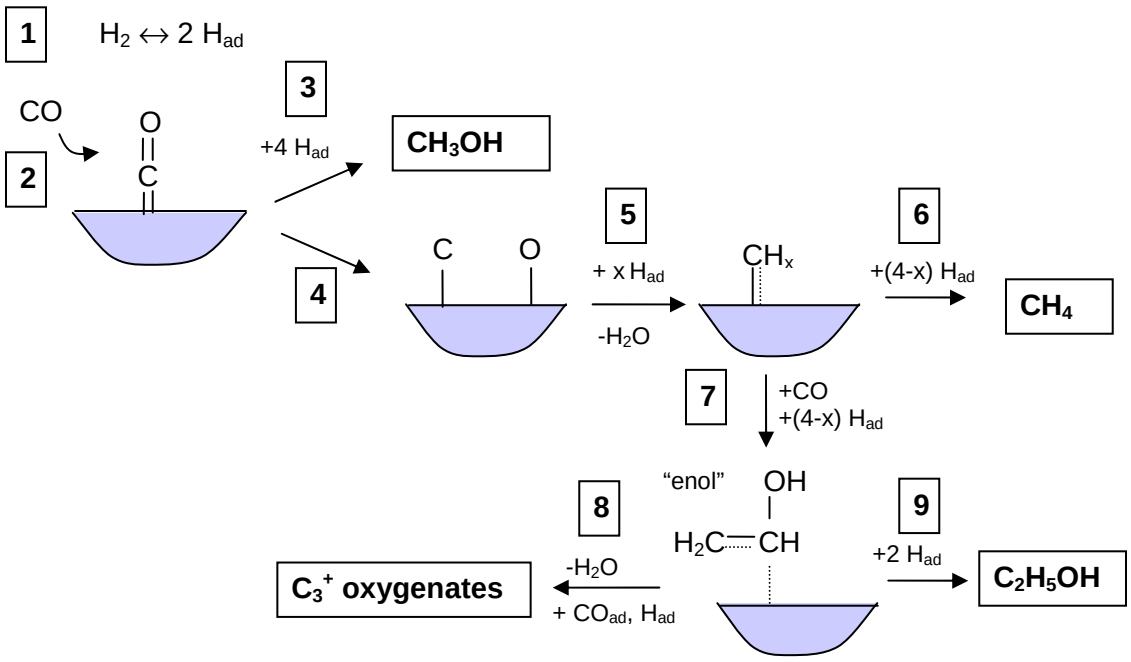

Figure 2.5: A simplified sequence for ethanol formation by CO hydrogenation on Rh-based catalysts. Individual reaction steps are indicated by boxed numbers

Several general conclusions regarding CO adsorption (steps 2 and 4) can be drawn from the literature:

(a) Promoter effects: transition metal promoters are thought to provide a site for interaction of the O atom in CO at the metal-promoter surface, as shown in Fig. 2.6[20, 21, 29]. During reduction, oxygen vacancies are created in the promoter, which allows for a strong (and controllable) interaction with the promoter. It seems that the most effective promoters decorate the surface of the Rh clusters, creating numerous sites for interaction between the promoter and Rh atoms. The stronger the M–O bond in Fig. 2.6, the more likely that CO will dissociate (e.g., Kato et al. observed a strong correlation between the heat of formation of the promoter oxide and CO dissociation[20]).

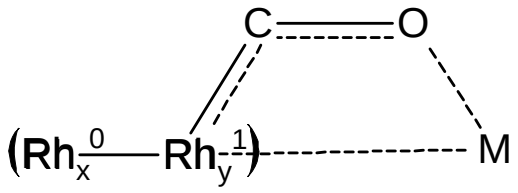

Figure 2.6: Interaction of CO with Rh-promoter surface; M = reduced metal oxide promoter (from Du et al. ref. [29]).

(b) Support effects: the support affects the Rh dispersion, which in turn affects the nature of the CO adsorption. For example, Trautmann and Baerns found that 0.5% Rh supported on SiO_2 produced Rh crystallites that adsorbed CO non-dissociatively, whereas the same metal loading on Al_2O_3 and TiO_2 formed more dispersed clusters that adsorbed CO dissociatively[30]. Qualitatively similar effects are reported by others[31], with TiO_2 typically being the most active support for dissociative adsorption[25].

Steps 5 – 9 (Ethanol and byproduct formation). The dissociated CO is then hydrogenated to form a surface hydrocarbon $(CH_x)_{ad}$ (x= 2 or 3; step 5). [Although not shown, another possibility is that the O_{ad} atom formed in step 4 reacts with CO to form CO_2[32].] This $(CH_x)_{ad}$ species can be hydrogenated to form methane (or higher hydrocarbons, not shown) in step 6[3, 33] or an undissociated CO can be inserted into the metal-carbon bond in $(CH_x)_{ad}$ [14] to form an "enol" intermediate in step 7. The resulting enol intermediate either reacts with adsorbed H atoms and CO to form higher oxygenates (step 8), or reacts only with adsorbed H atoms to form ethanol (step 9).

This reaction sequence is not intended to account for every elementary step, but does agree with most experimental results on Rh-based catalysts, and with the main features of mechanisms that have been postulated for these catalysts[14, 15]. The sequence does not explicitly

account for other C_2 oxygenates such as acetaldehyde or acetic acid, which are known byproducts. However, these compounds can be formed as byproducts in the sequence shown in Fig. 2.5. For example, acetaldehyde could be formed in step 7 by CO insertion into the $(CH_x)_{ad}$ species (as is required for ethanol formation), followed by mono-hydrogenation of the α- and β-carbon atoms without the formation of the hydroxyl group. Acetic acid could be formed by hydration of the enol intermediate by water formed in step 5.

Intermediates. Intermediates observed or postulated in mechanistic studies can also be explained by Fig. 2.5. For example, ketene ($H_2C=C=O$) has been shown to be a key intermediate[15, 34, 35]. Its formation is implicit in step 7, which is the sum of several single steps. Ketene can be formed by CO insertion into the $(CH_x)_{ad}$ species (x = 2), and would therefore be a precursor to the enol, which is formed by the hydrogenation of ketene. Acetyl intermediates ($H_3C–C=O$) have also been suggested [34, 35]. These species can also be formed in step 7 by CO insertion into $(CH_x)_{ad}$ in the case where x = 3. Formyl species ($H–C=O$)[36, 37] are possible in step 3, but lead only to methanol in the sequence shown in Fig. 2.5. This does not agree with the results of Wang et al. on promoted Rh/SiO_2 catalysts[37], which suggest that a formyl group is also an intermediate in ethanol synthesis. The difference may be due to the presence of the promoters in the Wang et al. study, which included Mn, Fe, Li, and Ti.

On virtually all catalysts on which high ethanol selectivities have been reported, CO conversions are low because hydrocarbon formation, which typically accompanies high catalyst activity, is suppressed. The observed trend is that selectivity to C_2 oxygenates decreases with increasing CO conversion. Therefore there has to be a balance between the catalyst activity and selectivity to obtain a high yield of ethanol.

Promoters. The selectivity to ethanol for unpromoted Rh catalysts is relatively low—the main products are hydrocarbons[6, 38]. The formation of ethanol can be greatly enhanced by the

addition of promoters[5, 29, 39]. The above reaction sequence (Fig. 2.5) suggests that Rh-based ethanol synthesis catalysts can be improved by promoters that increase CO dissociation and CO insertion activity while suppressing the hydrogenation of $(CH_x)_{ad}$ intermediate. The catalyst must dissociate only a portion of the CO molecules so that the catalyst surface contains both adsorbed molecular CO, and surface carbon species produced by dissociative adsorption[15]. There must also be a balance in hydrogenation activity—hydrogenation of the $(CH_x)_{ad}$ intermediate is undesirable, but hydrogenation of the enol is essential.

A variety of promoters including, transition metal oxides[3, 6, 14, 38, 40], rare earth oxides[29] (and combinations thereof[41]), alkalis[5] and noble metals[42] have been studied and found to exhibit significant enhancement of the ethanol yield. The effect of these promoters can be dramatic. Burch and Hayes examined the effect of Fe promotion on the selectivity to ethanol and other reaction products for a 2% Rh/Al_2O_3 catalyst[43]. The results show a substantial increase in ethanol selectivity with Fe addition up to 10% Fe. The authors of this study point out that the increase in ethanol selectivity corresponds directly to a decrease in methane selectivity, suggesting that one is at the expense of the other. This is consistent with the reaction scheme of Fig. 2.5: Fe promotes CO insertion (step 7) rather than hydrogenation of the $(CH_x)_{ad}$ species (step 6). A similar suppression of hydrogenation has been ascribed to the effect of alkali addition to a Rh/TiO_2 catalyst, leading to an increase in ethanol selectivity[5].

Similar increases in ethanol selectivity compared to an unpromoted supported Rh catalyst have been reported for lanthanides[29], and vanadium[3, 41], manganese[41], silver[42], ceria[44], and combinations of Ti, Fe, and Ir[45].

Supports. The support can also greatly affect the activity and selectivity of the reaction. The effect can be direct - e.g., when the support interacts directly with the metal in the catalytic

reaction or indirect - e.g., when the support affects the dispersion of the Rh or promoters, which then affects the reaction.

Most studies of supported Rh catalysts for CO hydrogenation to oxygenates use SiO_2 as a support, to which various promoters are added[14, 41, 45, 46]. However there are some studies which compared Rh on other supports for CO hydrogenation reactions[47-49]. As discussed above, unpromoted Rh seems to produce mostly hydrocarbons, irrespective of the support[50-53]. Rh/TiO_2 has been found to be more active for CO decomposition and hydrogenation than Rh/SiO_2 or Rh/Al_2O_3[47, 48], which generally leads to higher activity for hydrocarbon formation. Oxide supports like TiO_2, Al_2O_3, ZrO_2 and Nb_2O_5 have been reported to have a higher density of surface hydroxyls[43, 54] (than SiO_2) that allows for closer interaction between promoter and active metal (Rh), which is necessary for oxygenate synthesis. Recently, Pan et al [49] reported that yield of ethanol on Rh-Mn-Li-Fe in carbon nanotubes more than doubled that on $Rh\text{-}Mn\text{-}Li\text{-}Fe/SiO_2$. They attributed this to higher local pressure caused by the confinement metal particles inside the nanotubes leading to increased CO dissociation and hydrogenation activities.

2.2.1.2 CO_2 Hydrogenation

Because biomass-derived syngas contains CO_2 as well as CO, the hydrogenation of CO_2 to ethanol is also of interest. Hydrogenation of CO_2 to the products of interest here can, of course, proceed via the reverse water gas shift (r-WGS) reaction, followed by hydrogenation of CO to final products.

If so, then the reaction scheme in Fig. 2.5 would be modified only to account for the formation of surface C and O from CO_2 rather than CO, with the remaining steps being the same. There is experimental evidence to support this: adsorption of CO_2 results in the formation of linearly and bridge-bonded CO, which has been identified by IR spectroscopy on $Rh\text{-}Mo/ZrO_2$ [17], Rh/Al_2O_3[55], and Rh-Li/Y[56]. In one of these studies[55], the presence of hydrogen strongly

enhanced the formation of CO, possibly by reacting with the surface O atom formed in the initial adsorption of CO_2 and driving the adsorption process forward. As shown in Fig. 2.7, this suggests that CO_2 hydrogenation proceeds via the dissociative adsorption of CO_2 to form CO and O atoms on the surface[50, 57]. CO then dissociates to adsorbed C and O atoms, with final products being formed as shown in Fig. 2.5.

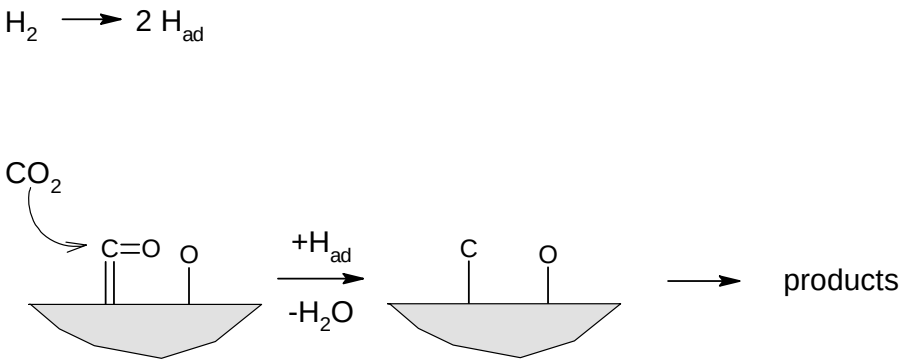

Figure 2.7 : Initial steps in the hydrogenation of CO_2, based on refs[50, 57]. Steps leading to the formation of final products are shown in Fig. 2.5

Essentially the same mechanism is proposed by Bando et al., who also studied the effect of Li promoters on CO_2 hydrogenation over a 5% Rh/Y catalyst[56]. They reported that the addition of Li monotonically increased the yield of methanol and ethanol, but also increased the yield of CO, probably by the desorption of CO formed in the dissociative adsorption of CO_2 in Fig. 2.7. They also observed that unpromoted Rh forms only methane which is consistent with other studies[50, 51, 58]. This agrees with a comprehensive study of 30 promoters for a 5% Rh/SiO_2 catalyst, which showed that the selectivity to ethanol was significant only for Li[58]. Methane was the primary product for most other promoters in this study, with significant levels of CO being formed (along with methane) in the case of Pt, Cu, Ag, Zn, and Sn promoters.

Mechanistic studies comparing CO + H_2 versus CO_2 + H_2 over Rh-based catalysts show substantial differences in these two reactions[50, 59-61]. Specifically, CO_2 hydrogenation seems to

take place at lower temperatures. Iizuka et al compared the two reactions for a 2.3% Rh/ZrO_2 catalyst and reported that only methane is formed in significant levels for both reactions, and that the rate of CO_2 hydrogenation is substantially greater than CO hydrogenation[50]. For identical levels of Rh (2.3%) supported on ZrO_2, Al_2O_3, SiO_2, and MgO, the activation energy for CO_2 hydrogenation was always less than for CO hydrogenation[50]- suggesting that dissociation of CO_2 is faster at a given temperature on all supports. Reaction orders were near zero in CO (consistent with Marengo et al[62]) and near 0.4 for CO_2, which means that that CO can act as a poison for H_2 adsorption and limit the observed reaction rate.

2.2.1.3 Hydrogenation of CO/CO_2 Mixtures

Virtually all the available relevant literature has focused on the hydrogenation of either CO or CO_2, rather than mixtures of the two. The effect of the mixture composition on the hydrogenation reaction is important, however, because biomass-derived syngas (as well as syngas from other sources) will contain significant levels of both. In addition, the high levels of steam in syngas will also affect the reaction, but we are aware of no literature in which the effects of varying levels of CO, CO_2, H_2 and H_2O on the synthesis of ethanol on Rh-based catalysts have been studied. Replacing a portion of CO in the feed with increasing concentrations of CO_2 on 1% $Rh\text{-}Mo/ZrO_2$ (Rh/Mo atomic ratio = 1/1)[62] leads to increasing yields of methanol and ethanol at low levels of CO_2, then reaching a maximum at about 5 - 10% CO_2. The authors attribute this to the r-WGS reaction[62], which presumably produces additional CO that is converted to the alcohols. However, methane yield increases continuously over the range of CO_2 concentrations studied. The decline in alcohol yield at higher levels of CO_2 is attributed to strong adsorption on sites that lead to the alcohols, with the reaction then being shifted toward methanation. An alternative explanation is that CO_2 reacts more readily to form methane than CO over the entire range of CO_2 concentrations, causing the monotonic increase in

methane yield with CO_2 content. Up to about 20% CO_2, the combined yields of methanol and ethanol follow the conversion quantitatively, meaning that the alcohol selectivity over this range is more constant than the yield alone would suggest. At CO_2 concentrations above ~20%, the r-WGS reaction may indeed produce sufficient strongly-adsorbing CO to inhibit the reactions leading to the alcohols[50].

Bando et al. added 1.8% CO to a CO_2 + H_2 mixture (H_2/CO = 3/1) and saw significant increases in methane selectivity (from 15 to 40%) and ethanol selectivity (~0 to 13%) over 5% Rh-Li/Y[56]. This can be explained by the strong adsorption and surface coverage of CO compared to CO_2. From Fig. 2.5, this could provide more surface coverage of C and O atoms, leading to an increase in both methanation (step 6) and CO insertion, step 7. A subsequent study by these same authors shows that Li stabilizes the Rh clusters compared to an identical catalyst without Li[63]. This apparently causes these changes in selectivity.

2.2.2 Modified Methanol Synthesis Catalysts

2.2.2.1 CO Hydrogenation

It was noted as early as the 1920's that the yield of higher alcohols increases during methanol synthesis on catalysts precipitated with alkali (as a result of the traces of alkali left on catalyst during preparation)[64]. This observation led to the use of alkali-doped Cu/Zn methanol catalysts for higher alcohol synthesis. The distribution of the higher alcohols mixture obtained on these catalysts depends on the promoter concentration, feed concentration (H_2/CO ratio) and the reaction conditions. However, no matter what the choice of catalyst or conditions, methanol remains the dominant product on these catalysts[65]. Most of the work reported on modified methanol catalysts for CO hydrogenation to higher alcohols has been on Cu-based catalysts. Alkali-doped binary Cu/Zn system and ternary Cu/Zn/Al or Cu/Zn/Cr (a third component of

either Al or Cr is always added to stabilize against sintering[66]) system have been extensively studied by Smith et al[64, 67] and Nunan et al[68-70].

Reaction Sequence / mechanism. A chain growth mechanism has been proposed for the formation of higher alcohols on modified Cu/Zn catalysts. The chain growth mechanism was first proposed by Frohlich and Cryder[71], who reported that higher alcohols are formed by the successive condensations of two lower alcohols with H loss from either the hydroxylated (α) carbon or adjacent (β) carbon atoms. It was assumed that hydrogen loss from the β-carbon is faster than the α-carbon[72]. This mechanism suggests that methanol with only an α-carbon will slowly react to form ethanol, while ethanol that has both α- and β- carbons react to form propanol at a faster rate. The effect is that large amounts of methanol and small amounts of ethanol are formed on these catalysts.

Different modifications have been made to this mechanism to account for branched and linear alcohols found in the product stream. Smith and Anderson[64], working with K/Cu/Zn/Al, assumed the simple case of a single carbon addition with no α-addition beyond the first step and no addition to a - CH group. This mechanism is limited because it predicts only methanol, ethanol and 1-propanol with a chain termination at 2-methyl-1-propanol because β-addition cannot occur [64]. They later modified this scheme to include α-addition beyond the first step but no more than two-carbon addition[67].

While there are various reports that describe the chain growth schemes to account for linear and branched alcohols[66, 69, 73], we shall limit the review here to the mechanism of the formation of the initial C-C bond and ethanol only. The coupling reaction of two methanol molecules was identified as the predominant mechanism to form ethanol over Cu/ZnO catalyst (doped with Cs) after isotopic labeling and NMR studies eliminated the other possible routes

from CO hydrogenation to ethanol[68]. Schematically, the proposed mechanism of ethanol formation over Cs doped Cu/ZnO catalyst is shown in Fig. 2.8.

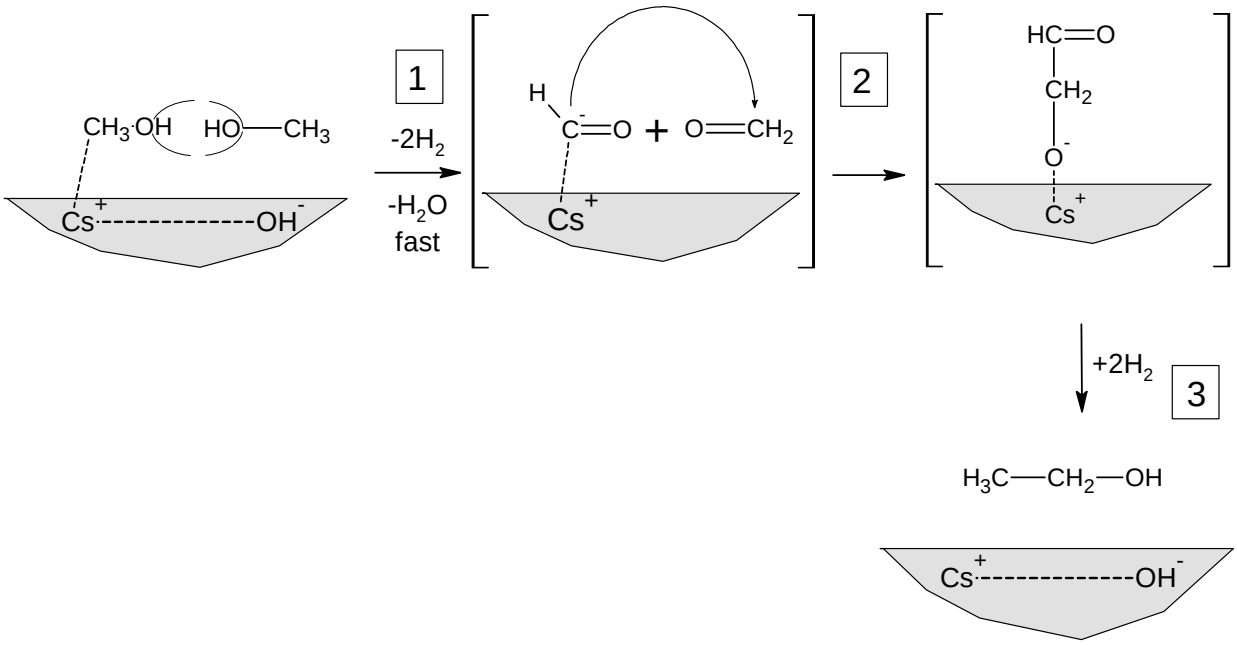

Figure 2.8. Mechanism for ethanol formation from methanol condensation on Cu-based catalysts.[68]. Boxed numbers refer to reaction steps.

The coupling reaction of two methanol molecules to form ethanol involves a nucleophilic attack of an adsorbed formyl on formaldehyde[68] to generate the C_2 precursor with two oxygen atoms (step 2). Both the adsorbed formyl and formaldehyde are believed to be formed preferentially from methanol[74] (step 1). An alternative methanol coupling mechanism that also involved an adsorbed formyl was proposed as well, but was considered as less likely because of steric hinderance.

The proposed mechanism of methanol formation on this catalyst as presented by these same authors is depicted in Fig. 2.9 [68]. CO is activated by Cs^+ and its associated OH^- ions to form an adsorbed formate species (step 1). This is followed by slow hydrogenation (step 2) to produce an adsorbed formyl, further hydrogenation to formaldehyde (step 3) and transformation to a methoxide (step 4) leading to methanol. Interestingly, formaldehyde and adsorbed formyl are

also intermediates in the methanol coupling reaction to ethanol (Fig. 2.8).

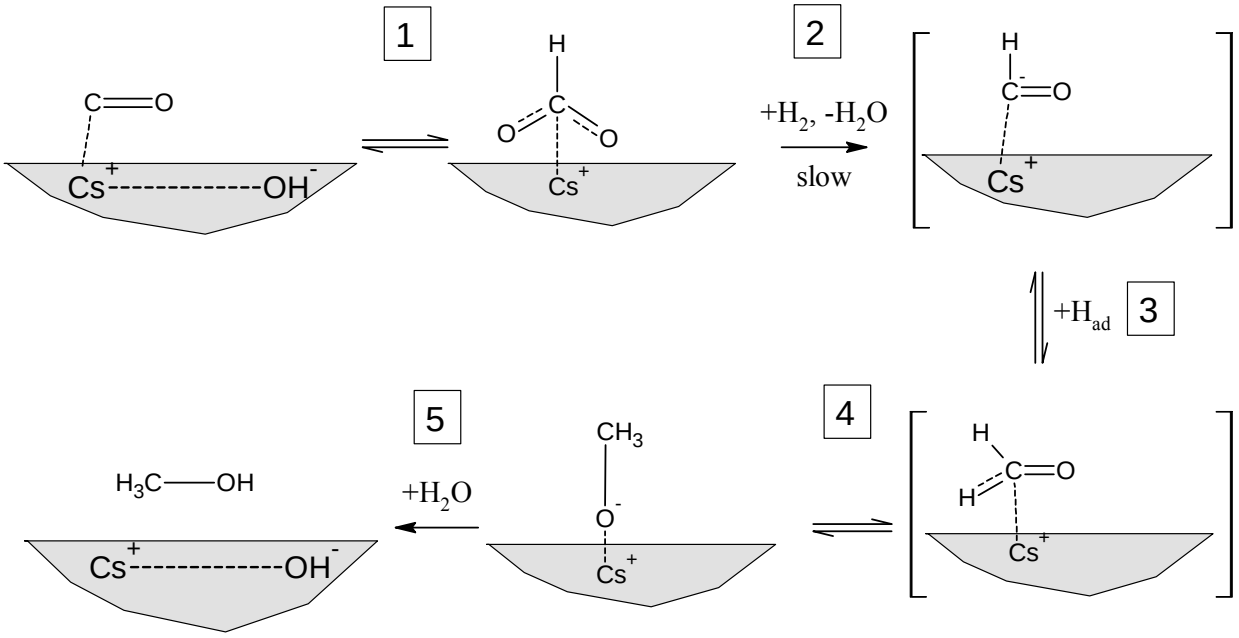

Figure 2.9. Mechanism for methanol formation from CO hydrogenation on Cu-based catalysts[68]. Boxed numbers refer to reaction steps.

Methanol has been shown to decompose to formaldehyde via a methoxide intermediate on various metals[75-77]. This is therefore a likely pathway through which the adsorbed formyl and formaldehyde intermediates are formed in the first step of the ethanol-forming reaction (Fig. 2.8). These intermediates can also be formed directly from CO and H_2, but it is a very slow step compared to their formation from the condensation of two methanol molecules[68].An alternative explanation is provided by Elliot and Pennella[65] who argued that the ethanol does not form from a methanol intermediate but from a surface-bound C_1 precursor (**I** below) which can be formed from either syngas (CO + H_2) or methanol. Such a precursor can also be the intermediate for methanol formation from syngas:

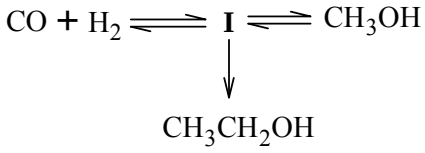

This pathway shows that the C_1 intermediate (I) could be the adsorbed formyl or formaldehyde, shown in Fig. 2.8 and Fig. 2.9 to be intermediates for both methanol and ethanol. These intermediates can also be formed from either syngas or methanol.

Promoters and their effects. Alkali promotion of Cu-based catalysts for has been found to increase higher alcohol synthesis with increasing alkali atomic size, in the order Li < Na < K < Rb < Cs[78]. K and Cs have been extensively used on these catalysts and their functions have been suggested to be dual in nature: the first is the suppression of surface acidity by the titration of acid sites that leads to dimethylether (DME)[73]. Reducing DME selectivity effectively leads to higher alcohol selectivity because DME is also formed by the condensation reaction of methanol. The second function is to provide basic sites (in association with its counter-ion) necessary for the various C-C and C-O bond forming reactions[70]. The degree of promotion is however dependent on the promoter type, concentration and catalyst support, among other factors. The yield of higher alcohols has been shown to go through a maximum as the promoter concentration is increased[70, 79].

This is because as the promoter concentration increases, more alkali sites are created thereby increasing the yield of higher alcohols but eventually the promoter block sites to the Cu/Zn portion of the catalyst that are required for methanol synthesis. When this occurs, it hinders methanol formation thereby reducing the driving force for higher alcohol synthesis[79]. However, methanol yield has also been found to pass through a maximum as promoter concentration increases, in the same manner as for higher alcohols[68, 79]. This suggests that methanol and higher alcohols are likely formed at same sites (alkali-Cu interfaces) on the catalyst and contradicts the earlier proposal[79] that methanol and higher alcohol synthesis require different sites.

Even though alkalis promote the formation higher alcohols on Cu catalysts, the effect of alkali doping on ethanol yield is not significant[69]. The addition of 0.25mol% Cs to unpromoted Cu/ZnO leads to an insignificant increase in ethanol yield, but 1-propanol and isobutanol yields increase considerably. In fact ethanol yield decreases while other higher alcohols yields increase at higher levels of Cs doping[69].

Effect of CO/H_2 ratio. Besides process conditions like temperature, pressure and space velocity, the feed H_2/CO ratio also affects the higher alcohol selectivity over alkali-doped Cu based catalysts. Higher alcohols are favored by CO-rich feed mixtures because the rate of chain growth increases with increasing partial pressure of CO while termination rate varied with H_2 partial pressure [64, 67]. High H_2 partial pressures have the effect of inhibiting the rate of $C_1 - C_2$ chain growth step by enhancing the conversion of C_1 intermediates to methanol[80].

2.2.2.2 Hydrogenation of $CO + CO_2$ Mixtures

Little literature is available on the hydrogenation of CO_2 to ethanol on modified methanol synthesis catalysts. However, CO_2 has been co-fed with syngas mixtures to probe its effect on catalyst activity and selectivity on these catalysts. CO_2 when co-fed with CO and H_2 has a promoting effect on methanol synthesis on Cu/ZnO. Klier et al reported a peak in methanol synthesis rate at CO_2 concentration of 2% and a progressive decrease in the promotion effect as CO_2 gradually replaces CO in the feed mixture for up to 20% CO_2 concentration [81]. They claimed that this effect is mainly promotional because CO hydrogenation is the primary source of methanol in a $CO/CO_2/H_2$ feed mix and that CO_2 only becomes a significant source of carbon when the syngas feed is CO_2-rich[81]. However Chinchen et al [82] arrived at a different conclusion using ^{14}C tracer studies: that on $Cu/ZnO/Al_2O_3$ methanol is made predominantly from CO_2 hydrogenation for all mixtures tested.

The explanation given for the promotional effect of CO_2 is that a surface formate intermediate is formed by either CO_2 and H or CO and H_2O (suggesting that CO_2 and H_2O probably have the same effect on methanol synthesis)[81]. Without CO_2 in the feed the formate would not be formed and with high CO_2 concentrations, the active catalyst surface is blocked by the strongly adsorbed CO_2, retarding surface formate formation[81]. This formation of a surface formate species in methanol synthesis from CO_2 hydrogenation is consistent with Chinchen et al[83] as shown in the reaction following reaction sequence:

$$H_2 \rightarrow 2H_{(ad)}$$

$$CO_2 \rightarrow CO_{2(ad)}$$

$$H_{(ad)} + CO_{2(ad)} \rightarrow HCO_{2(ad)}$$

$$HCO_{2(ad)} + H_{(ad)} \rightarrow H_2CO_{(ad)} + O_{(ad)}$$

$$H_2CO_{(ad)} + H_{(ad)} \rightarrow H_3CO_{(ad)}$$

$$H_3CO_{(ad)} + H_{(ad)} \rightarrow CH_3OH$$

$$CO + O_{(ad)} \rightarrow CO_2$$

$$H_2 + O_{(ad)} \rightarrow H_2O$$

Elliot also reported an increase in both methanol as well as higher alcohols synthesis rate using a CO + H_2 feed containing 6% CO_2[84]. Conversely, over alkali promoted catalysts, Hilmen et al [73]reported inhibition effects of CO_2 on both methanol and higher alcohols synthesis by increasing oxygen coverages on Cu surfaces and titrating the basic sites necessary for condensation reactions. The degree of inhibition depended on the concentration of Cu sites on the catalyst – the inhibition for methanol synthesis is weaker on catalysts with high Cu sites density while those with lower Cu sites densities are more affected. Calverley and Smith [79]on the other hand reported that the effect of CO_2 added to CO + H_2 depended on the alkali concentration for K_2CO_3-promoted $Cu/ZnO/Cr_2O_3$. At a 0.5% K_2CO_3 loading, CO_2 in the feed enhance methanol formation while at 4.0% K_2CO_3 the yield of methanol is depressed.

In summary, CO_2 seems to have a promoting effect for methanol synthesis, but it inhibits higher alcohol formation on modified methanol catalysts. No higher alcohols were formed on Cu/ZnO when a feed mix containing only CO_2 and H_2 (with no CO) was used [85].

2.2.3 Modified Fischer-Tropsch Catalysts

2.2.3.1 CO hydrogenation

Evidence that alcohols, with ethanol present in the largest proportion, are precursors to the formation of hydrocarbons on Fischer-Tropsch type catalysts has been presented since 1952[86]. These types of catalysts, based on Co, Ru and Fe, have been reported to give higher alcohols when suitably modified with additives[87-91]. Some authors reported that the synthesis of higher alcohols on Ir/Ru-SiO2[92] and Ir/Co-SiO2[93] might have been caused by a synergistic interaction between metals that readily dissociate CO (Ru and Co) and Ir, which does not dissociate CO. A combination of two such metals might produce a catalyst that has the proper combination of CO dissociation and CO insertion, which are necessary for higher alcohol formation on some catalysts (Fig. 2.5).

Reaction sequence. The mechanism for alcohol formation on modified Fisher Tropsch catalysts is essentially same as the one described for Rh catalysts. It starts with CO dissociation and hydrogenation of the adsorbed carbon into CH_x surface species, followed by CO insertion into the CH_x species as shown in Fig. 2.5[94].

Promoters and effects. Kintaichi et al[95] tested a series of bimetallic catalysts containing a pair of group VIII metals; one which dissociates CO and one which does not. They reported that Ir-Ru/SiO_2 gives the highest CO conversion, least methanol selectivity and the highest selectivity for higher alcohols. The addition of alkali improved C_2-oxygenate selectivity. The properties of these catalysts are said to be largely affected by the preparation procedure especially factors like impregnation sequence[95], precursors [90, 91, 96], metal and promoter loading[95].

A close interaction between the catalysts and promoter is important for higher alcohol yield – TPR profiles of a co-impregnated Ir-Ru/SiO_2 showed[95] a single Ir-Ru reduction peak, indicating a close interaction. A similar, single Pd-Co reduction peak is shown for Pd-Co/CeO_2 [97]. A co-impregnated Ir-Ru/SiO_2 catalyst showed greater higher alcohol selectivity than those in which Ir and Ru were sequentially impregnated.

Matsuzaki et al reported the effects of Co and promoter precursors on the catalysts performance - they reported that ethanol selectivity on Co-Re-Sr/SiO_2 increased from 1.3% to 20% when the precursors are changed from nitrates to acetates[96]. Interestingly, unpromoted Co/SiO_2 catalyst from an acetate precursor, and those promoted with Sr prepared from chlorides, nitrates or carbonyl precursors were largely inactive for ethanol synthesis. This clearly shows the importance of preparation materials and procedure.

Different promoters have been shown to have different effects on Fischer-Tropsch type catalysts. On a Co/SiO_2 catalyst promoted with Re-Sr [91]and Sr [98], Takeuchi et al. reported deviations from the Schulz-flory distribution of C_2 hydrocarbon and C_2 oxygenates, where they witnessed a deficit in C_2 hydrocarbon and an excess in C_2 oxygenates and suggested a mechanism in which oxygenates and hydrocarbons are formed through the same intermediates. This is consistent with the mechanism of Fig. 2.5. The effect of the promoters therefore would be the preferential conversion of the intermediate to ethanol at the expense of C_2 hydrocarbons.

Alkali dopants promote activity and selectivity to C_2^+ oxygenates by depressing hydrocarbon formation[95]. Transition metals like Ir, Re, Pt and Os help to reduce inactive Co (II) acetate species to the active metallic state by activating H_2 (during pretreatment) for Co reduction while keeping it highly dispersed. High Co dispersion is absolutely necessary for oxygenate synthesis; agglomeration of Co particles tends to catalyze hydrocarbon formation[96].

Although the promoted Co catalysts showed enhanced selectivity towards ethanol, hydrocarbon selectivities remain high (above 60 %) in virtually all reported studies[87, 90-92, 99].

2.2.3.2 CO_2 Hydrogenation

Inui and co-workers report the synthesis of ethanol via CO_2 hydrogenation using multifunctional catalysts [2, 100-103]. These catalysts are a mixture of Rh, Fe and Cu designed to partially reduce CO_2 to CO, propagate chain growth (C-C bond formation), and insert an –OH group. The Fischer-Tropsch type Fe-Cu-Al-K catalyst gave 8% ethanol selectivity from a CO_2/H_2 (25:75) mixture. The selectivity increased to 11% when 3% CO was substituted for CO_2. While the increase in CO concentration increased the ethanol yield, a CO-rich gas reduced ethanol selectivity because CO_2 was formed (rather than ethanol) via the shift reaction. The performance of this catalyst is said to be dependent on the oxidation-reduction state of the Fe catalyst during reaction - the active phase for CO_2 hydrogenation to ethanol is Fe_3O_4 and is a function of the reduction temperature. Reduction at about 450°C gives Fe_3O_4, insufficient reduction leaves Fe in the inactive Fe_2O_3 phase and over-reduction leads to the metallic Fe. Combining Fe with other catalysts and suitable promotion from metals like Pd and Ga (which have the H_2 spillover and reverse-spillover, respectively) maintains the oxidation state of the catalysts during reaction conditions[2].

The importance of choice of precursors for oxygenate formation was also mirrored by Okabe et al for CO_2 hydrogenation - acetate-derived $Co(A)/SiO_2$ promoted with Ir and Na from acetate precursors showed improved alcohol selectivity over nitrate-derived $Co(N)/SiO_2$[104].

2.2.4 Modified Mo-based Catalysts

2.2.4.1 CO Hydrogenation

When alkali metals are added to Mo-based catalysts, the selectivity for CO hydrogenation has been shown to shift from hydrocarbons to alcohols[105]. The promoting effect of alkalis (on

MoS_2) for alcohol formation was found to increase in the order Li < Na < Cs < Rb < K, suggesting that moderate basic promotion is desired[106]. Muramatsu et al claimed that the role of K on Mo/SiO_2 is to preserve the surface MoO_2 species which is active for alcohols by retarding the reduction of Mo to metal[107]. Selectivity to alcohols on alkali promoted Mo catalysts normally follows the Schulz-Flory distribution, which limits higher alcohol formation. However, further promotion with transition metals like Co and Ni has been shown to improve C_2^+ alcohol selectivity[108-110]. When K/MoS_2 catalyst is co-modified with Ni and Mn, the synergistic effect of both promoters is said to enhance the catalytic activity and the formation of $C_2 – C_3$ alcohols. Ni is thought to enhance the $C_1 \longrightarrow C_2$ homologation step that might explain the high ethanol selectivity. The further addition of Mn inhibits the enrichment of Ni, leading to the suppression of methanation functions of Ni while improving the dispersion of the catalyst[108]. The main mechanism for ethanol formation on alkali promoted Mo-based catalyst is via the insertion of CO into the metal-CH_x bond as depicted in Fig. 2.5[111, 112].

Preparation techniques have been reported by a number of authors to affect the selectivity and activity of Mo catalysts. KCl promoted Mo/SiO_2, which was prepared by the successive impregnation K and Mo solutions on silica gel, was found to give higher activity and selectivity for alcohol formation than when the order of impregnation was reversed i.e. Mo was added first. The sequence was found to greatly affect the activity and selectivity because certain interactions between Mo and SiO_2, which inhibits higher alcohol formation, is said to be less pronounced when K was added first[113]. A rapid drying procedure instead of a slow one was found to improve alcohol selectivity and activity on K-Mo/C catalyst[114]. A modified Mo/SiO_2 catalyst prepared using the metal oxide vapor synthesis (MOVS) exhibited much higher activity and selectivity to higher alcohols than a nominally similar catalyst prepared by the conventional impregnation

method[109]. These improved activities and selectivities result from better dispersion of active species.

2.2.4.2 Hydrogenation of CO/CO_2 Mixture

Significant amounts of CO_2 are formed on MoS_2 catalyst when the feed is CO_2-free because of its high activity for the water–gas shift (WGS) reaction[114, 115]. However the inclusion of CO_2 in a syngas feed shifts the WGS reaction equilibrium toward H_2O formation causing large amounts of water to be formed instead of CO_2. CO_2 in feed also reduces the formation of higher alcohols which might be due to the inhibition of the chain growth process by CO_2 or the reverse effect of the large amounts of water formed[114].

In summary, modified methanol synthesis catalysts give the highest activity for ethanol formation in terms of CO conversion, but methanol remains the dominant alcohol product. Ethanol selectivities are very low on these catalysts because of the chain growth mechanism for the formation of higher alcohols. While ethanol is formed from methanol via a slow difficult reaction, ethanol is quickly converted to higher alcohols via a faster chain growth mechanism. Rh-based catalysts give the highest ethanol selectivities, albeit at lower CO conversions. Methanol formation is very low but high CH_4 formation is thermodynamically favorable and seems to be inevitable on these catalysts. Modified Fischer-Tropsch catalysts give moderate ethanol selectivities but methane formation is dominant and methanol selectivities are significant.

2.3 REFERENCES

1. A. Roine, *HSC Chemistry 5.11*, (2003) Outokumpu Research Oy., Pori, Finland.
2. T. Inui, T. Yamamoto, M. Inoue, H. Hara, T. Takeguchi and J. B. Kim, *Applied Catalysis a-General*, 1999, **186**, 395-406.
3. P. Gronchi, E. Tempesti and C. Mazzocchia, *Applied Catalysis A: General*, 1994, **120**, 115-126.

4. S. Mawson, M. S. Mccutchen, P. K. Lim and G. W. Roberts, *Energy & Fuels*, 1993, **7**, 257-267.

5. S. C. Chuang, J. G. Goodwin and I. Wender, *Journal of Catalysis*, 1985, **95**, 435-446.

6. M. M. Bhasin, W. J. Bartley, P. C. Ellgen and T. P. Wilson, *Journal of Catalysis*, 1978, **54**, 120-128.

7. P. Forzatti, E. Tronconi and I. Pasquon, *Catalysis Reviews-Science and Engineering*, 1991, **33**, 109-168.

8. M. L. Poutsma, L. F. Elek, P. A. Ibarbia, A. P. Risch and J. A. Rabo, *Journal of Catalysis*, 1978, **52**, 157-168.

9. M. Ichikawa, T. Fukushima and K.Shikakura, Proc. 8th Int. Cong. Catal., Berlin, Germany, 1984.

10. M. Ichikawa, T. Fukushima, T. Yokoyama, N. Kosugi and H. Kuroda, *Journal of Physical Chemistry*, 1986, **90**, 1222-1224.

11. M. Ichikawa, *Chemtech*, 1982, **12**, 674-680.

12. M. Ichikawa, *Bulletin of the Chemical Society of Japan*, 1978, **51**, 2268-2272.

13. M. Bowker, *Catalysis Today*, 1992, **15**, 77-100.

14. M. Ichikawa and T. Fukushima, *Journal of the Chemical Society-Chemical Communications*, 1985, 321-323.

15. A. Takeuchi and J. R. Katzer, *Journal of Physical Chemistry*, 1982, **86**, 2438-2441.

16. A. Takeuchi and J. R. Katzer, *Journal of Physical Chemistry*, 1981, **85**, 937-939.

17. E. Guglielminotti, E. Giamello, F. Pinna, G. Strukul, S. Martinengo and L. Zanderighi, *Journal of Catalysis*, 1994, **146**, 422-436.

18. A. Kohl, C. Linsmeier, E. Taglauer and H. Knozinger, *Physical Chemistry Chemical Physics*, 2001, **3**, 4639-4643.

19. D. R. Mullins, *Surface Science*, 2006, **600**, 2718-2725.

20. H. Kato, M. Nakashima, Y. Mori, T. Mori, T. Hattori and Y. Murakami, *Research on Chemical Intermediates*, 1995, **21**, 115-126.

21. A. B. Boffa, C. Lin, A. T. Bell and G. A. Somorjai, *Catalysis Letters*, 1994, **27**, 243-249.

22. J. Libuda, M. Frank, A. Sandell, S. Andersson, P. A. Bruhwiler, M. Baumer, N. Martensson and H. J. Freund, *Springer Series in Solid-State Sciences* 1996, 210-216.

23. S. Andersson, M. Frank, A. Sandell, A. Giertz, B. Brena, P. A. Bruhwiler, N. Martensson, J. Libuda, M. Baumer and H. J. Freund, *Journal of Chemical Physics*, 1998, **108**, 2967-2974.

24. M. Frank, S. Andersson, J. Libuda, S. Stempel, A. Sandell, B. Brena, A. Giertz, P. A. Bruhwiler, M. Baumer, N. Martensson and H. J. Freund, *Chemical Physics Letters*, 1997, **279**, 92-99.

25. A. Erdohelyi and F. Solymosi, *Journal of Catalysis*, 1983, **84**, 446-460.

26. P. Gelin, J. F. Dutel and Y. B. Taarit, *Journal of the Chemical Society-Chemical Communications*, 1990, 1746-1747.

27. G. Bergeret, P. Gallezot, P. Gelin, Y. Bentaarit, F. Lefebvre, C. Naccache and R. D. Shannon, *Journal of Catalysis*, 1987, **104**, 279-287.

28. T. Maillet, J. Barbier, P. Gelin, H. Praliaud and D. Duprez, *Journal of Catalysis*, 2001, **202**, 367-378.

29. Y. H. Du, D. A. Chen and K. R. Tsai, *Applied Catalysis*, 1987, **35**, 77-92.

30. S. Trautmann and M. Baerns, *Journal of Catalysis*, 1994, **150**, 335-344.

31. F. Solymosi and M. Lancz, *Journal of the Chemical Society-Faraday Transactions I*, 1986, **82**, 883-897.

32. Y. Tanaka, T. Iizuka and K. Tanabe, *Journal of the Chemical Society-Faraday Transactions I*, 1982, **78**, 2215-2225.

33. F. Solymosi and A. Erdohelyi, *Surface Science*, 1981, **110**, L630-L633.

34. H. Wang, J. Liu, J. Fu, J. Cai, H. Zhang, Q. Cai and *Journal of Natural Gas Chemistry* 1993, **2**, 13-18.

35. J. Liu, H. Wang, J. Fu, Y. Li and K. Tsai, Proc. - Int. Congr. Catal., 9th, Calgary, Canada, 1988.

36. H. Y. Wang, J. P. Liu, J. K. Fu, H. B. Zhang and K. R. Tsai, *Research on Chemical Intermediates* 1992, **17**, 233-242.

37. H. Y. Wang, J. P. Liu, J. K. Fu, H. L. Wan and K. R. Tsai, *Catalysis Letters*, 1992, **12**, 87-96.

38. W. M. H. Sachtler, *Berichte Der Bunsen-Gesellschaft-Physical Chemistry Chemical Physics*, 1995, **99**, 1295-1305.

39. J. R. Katzer, A. W. Sleight, P. Gajardo, J. B. Michel, E. F. Gleason and S. Mcmillan, *Faraday Discussions*, 1981, 121-133.

40. S. Ishiguro, S. Ito and K. Kunimori, *Catalysis Today*, 1998, **45**, 197-201.

41. H. Y. Luo, W. Zhang, H. W. Zhou, S. Y. Huang, P. Z. Lin, Y. J. Ding and L. W. Lin, *Applied Catalysis a-General*, 2001, **214**, 161-166.

42. R. Krishnamurthy and S. S. C. Chuang, *Fuel Science & Technology International*, 1995, **13**, 1215-1236.

43. R. Burch and M. J. Hayes, *Journal of Catalysis*, 1997, **165**, 249-261.

44. A. Kiennemann, R. Breault, J. P. Hindermann and M. Laurin, *Journal of the Chemical Society-Faraday Transactions I*, 1987, **83**, 2119-2128.

45. H. Arakawa, T. Fukushima, M. Ichikawa, S. Natsushita, K. Takeuchi, T. Matsuzaki and Y. Sugi, *Chemistry Letters*, 1985, 881-884.

46. H. M. Yin, Y. J. Ding, H. Y. Luo, D. P. He, W. M. Chen, Z. Y. Ao and L. W. Lin, *Journal of Natural Gas Chemistry*, 2003, **12**, 233-236.

47. I. Mochida, N. Ikeyama, H. Ishibashi and H. Fujitsu, *Journal of Catalysis*, 1988, **110**, 159-170.

48. T. Ioannides and X. Verykios, *Journal of Catalysis*, 1993, **140**, 353-369.

49. X. L. Pan, Z. L. Fan, W. Chen, Y. J. Ding, H. Y. Luo and X. H. Bao, *Nature Materials*, 2007, **6**, 507-511.

50. T. Iizuka, Y. Tanaka and K. Tanabe, *Journal of Catalysis*, 1982, **76**, 1-8.

51. T. Iizuka, Y. Tanaka and K. Tanabe, *Journal of Molecular Catalysis*, 1982, **17**, 381-389.

52. M. A. Baltanas, J. H. Onuferko, S. T. Mcmillan and J. R. Katzer, *Journal of Physical Chemistry*, 1987, **91**, 3772-3774.

53. F. Solymosi, I. Tombacz and M. Kocsis, *Journal of Catalysis*, 1982, **75**, 78-93.

54. I. E. Wachs, G. Deo, M. A. Vuurman, H. C. Hu, D. S. Kim and J. M. Jehng, *Journal of Molecular Catalysis*, 1993, **82**, 443-455.

55. T. Iizuka and Y. Tanaka, *Journal of Catalysis*, 1981, **70**, 449-450.

56. K. K. Bando, K. Soga, K. Kunimori and H. Arakawa, *Applied Catalysis a-General*, 1998, **175**, 67-81.

57. M. F. H. Vantol, A. Gielbert and B. E. Nieuwenhuys, *Applied Surface Science*, 1993, **67**, 166-178.

58. H. Kusama, K. Okabe, K. Sayama and H. Arakawa, *Applied Organometallic Chemistry*, 2000, **14**, 836-840.

59. F. Solymosi, A. Erdohelyi and T. Bansagi, *Journal of Catalysis*, 1981, **68**, 371-382.

60. B. A. Sexton and G. A. Somorjai, *Journal of Catalysis*, 1977, **46**, 167-189.

61. F. Solymosi and A. Erdohelyi, *Journal of Molecular Catalysis*, 1980, **8**, 471-474.

62. S. Marengo, S. Martinengo and L. Zanderighi, *Chemical Engineering Science*, 1992, **47**, 2793-2798.

63. K. K. Bando, N. Ichikuni, H. Arakawa and K. Asakuara, *Molecular Crystals and Liquid Crystals*, 2000, **341**, 1277-1282.

64. K. J. Smith and R. B. Anderson, *Canadian Journal of Chemical Engineering*, 1983, **61**, 40-45.

65. D. J. Elliott and F. Pennella, *Journal of Catalysis*, 1988, **114**, 90-99.

66. J. C. Slaa, J. G. Vanommen and J. R. H. Ross, *Catalysis Today*, 1992, **15**, 129-148.

67. K. J. Smith and R. B. Anderson, *Journal of Catalysis*, 1984, **85**, 428-436.

68. J. G. Nunan, C. E. Bogdan, K. Klier, K. J. Smith, C. W. Young and R. G. Herman, *Journal of Catalysis*, 1988, **113**, 410-433.

69. J. G. Nunan, C. E. Bogdan, K. Klier, K. J. Smith, C. W. Young and R. G. Herman, *Journal of Catalysis*, 1989, **116**, 195-221.

70. J. G. Nunan, R. G. Herman and K. Klier, *Journal of Catalysis*, 1989, **116**, 222-229.

71. P. K. Frolich and D. S. Cryder, *Industrial and Engineering Chemistry*, 1930, **22**, 1051-1057.

72. G. D. Graves, *Industrial and Engineering Chemistry*, 1931, **23**, 1381-1385.

73. A. M. Hilmen, M. T. Xu, M. J. L. Gines and E. Iglesia, *Applied Catalysis a-General*, 1998, **169**, 355-372.

74. J. R. Fox, F. A. Pesa and B. S. Curatolo, *Journal of Catalysis*, 1984, **90**, 127-138.

75. D. C. Foyt and J. M. White, *Journal of Catalysis*, 1977, **47**, 260-268.

76. I. E. Wachs and R. J. Madix, *Journal of Catalysis*, 1978, **53**, 208-227.

77. E. I. Ko, J. B. Benziger and R. J. Madix, *Journal of Catalysis*, 1980, **62**, 264-274.

78. G. A. Vedage, P. B. Himelfarb, G. W. Simmons and K. Klier, *Acs Symposium Series*, 1985, **279**, 295-312.

79. E. M. Calverley and K. J. Smith, *Journal of Catalysis*, 1991, **130**, 616-626.

80. L. Majocchi, L. Lietti, A. Beretta, P. Forzatti, E. Micheli and L. Tagliabue, *Applied Catalysis a-General*, 1998, **166**, 393-405.

81. K. Klier, V. Chatikavanij, R. G. Herman and G. W. Simmons, *Journal of Catalysis*, 1982, **74**, 343-360.

82. G. C. Chinchen, P. J. Denny, D. G. Parker, M. S. Spencer and D. A. Whan, *Applied Catalysis*, 1987, **30**, 333-338.

83. G. C. Chinchen, K. C. Waugh and D. A. Whan, *Applied Catalysis*, 1986, **25**, 101-107.

84. D. J. Elliott, *Journal of Catalysis*, 1988, **111**, 445-449.

85. C. Kuechen and U. Hoffmann, *Chemical Engineering Science*, 1993, **48**, 3767-3776.

86. D. Gall, E. J. Gibson and C. C. Hall, *Journal of Applied Chemistry*, 1952, **2**, 371-380.

87. A. Razzaghi, J. P. Hindermann and A. Kiennemann, *Applied Catalysis*, 1984, **13**, 193-210.

88. M. Pijolat and V. Perrichon, *Applied Catalysis*, 1985, **13**, 321-333.

89. K. Fujimoto and T. Oba, *Applied Catalysis*, 1985, **13**, 289-293.

90. M. Inoue, T. Miyake, Y. Takegami and T. Inui, *Applied Catalysis*, 1984, **11**, 103-116.

91. K. Takeuchi, T. Matsuzaki, H. Arakawa and Y. Sugi, *Applied Catalysis*, 1985, **18**, 325-334.

92. H. Hamada, Y. Kuwahara, Y. Kintaichi, T. Ito, K. Wakabayashi, H. Iijima and K. Sano, *Chemistry Letters*, 1984, 1611-1612.

93. Y. Kintaichi, Y. Kuwahara, H. Hamada, T. Ito and K. Wakabayashi, *Chemistry Letters*, 1985, 1305-1306.

94. S. A. Hedrick, S. S. C. Chuang, A. Pant and A. G. Dastidar, *Catalysis Today*, 2000, **55**, 247-257.

95. Y. Kintaichi, T. Ito, H. Hamada, H. Nagata and K. Wakabayashi, *Sekiyu Gakkaishi-Journal of the Japan Petroleum Institute*, 1998, **41**, 66-70.

96. T. Matsuzaki, K. Takeuchi, T. Hanaoka, H. Arawaka and Y. Sugi, *Applied Catalysis a-General*, 1993, **105**, 159-184.

97. H. Idriss, C. Diagne, J. P. Hindermann, A. Kinnemann and M. A. Barteau, *Studies in Surface Science and Catalysis*, 1993, **75**, 2119-2122.

98. K. Takeuchi, T. Matsuzaki, T. A. Hanaoka, H. Arakawa, Y. Sugi and K. Wei, *Journal of Molecular Catalysis*, 1989, **55**, 361-370.

99. T. Matsuzaki and T. A. Hanaoka, *Abstracts of Papers of the American Chemical Society*, 1996, **211**, 14-Petr.

100. T. Inui, *Catalysis Today*, 1996, **29**, 329-337.

101. T. Inui and T. Yamamoto, *Catalysis Today*, 1998, **45**, 209-214.

102. T. Yamamoto and T. Inui, *Advances in Chemical Conversions for Mitigating Carbon Dioxide*, 1998, **114**, 513-516.

103. T. Inui, *Abstracts of Papers of the American Chemical Society*, 2000, **219**, U250-U250.

104. K. Okabe, H. Yamada, T. Hanaoka, T. Matsuzaki, H. Arakawa and Y. Abe, *Chemistry Letters*, 2001, 904-905.

105. T. Tatsumi, A. Muramatsu and H. O. Tominaga, *Chemistry Letters*, 1984, 685-688.

106. H. C. Woo, T. Y. Park, Y. G. Kim, I. S. Nam, J. S. Lee and J. S. Chung, *Studies in Surface Science and Catalysis*, 1993, **75**, 2749-2752.

107. A. Muramatsu, T. Tatsumi and H. Tominaga, *Bulletin of the Chemical Society of Japan*, 1987, **60**, 3157-3161.

108. H. J. Qi, D. B. Li, C. Yang, Y. G. Ma, W. H. Li, Y. H. Sun and B. Zhong, *Catalysis Communications*, 2003, **4**, 339-342.

109. E. C. Alyea, D. He and J. Wang, *Applied Catalysis a-General*, 1993, **104**, 77-85.

110. J. G. Santiesteban, C. E. Bogdan, R. G. Herman and K. Klier, 9th Int. Congr. Catal, 1988.

111. K. J. Smith, R. G. Herman and K. Klier, *Chemical Engineering Science*, 1990, **45**, 2639-2646.

112. D. B. Li, C. Yang, W. H. Li, Y. H. Sun and B. Zhong, *Topics in Catalysis*, 2005, **32**, 233-239.

113. T. Tatsumi, A. Muramatsu and H. Tominaga, *Journal of Catalysis*, 1986, **101**, 553-556.

114. G. Lu, C. F. Zhang, Y. Q. Gang, Z. B. Zhu, Y. H. Ni, L. J. Cheng and F. Yu, *Applied Catalysis a-General*, 1997, **150**, 243-252.

115. Y. M. Li, R. J. Wang and L. Chang, *Catalysis Today*, 1999, **51**, 25-38.

CHAPTER 3 : EXPERIMENTAL DESIGN

This chapter describes the experimental set up including the equipment and the techniques involved in catalysts preparation, testing and characterization.

3.1 EXPERIMENTAL SET-UP

3.1.1 Fixed Bed Reactor System

The catalysts activity tests are carried out in an Altamira™ AMI200R-HP reactor system, which has the capacity to blend four feed gases at a time. The schematic of the fixed bed reactor system and the analytical equipment is shown in Figure 3.1. Feed gases of ultra high purity (UHP) grade are delivered from compressed cylinders without further purification to the reactor at appropriate inlet pressures. Flow rates of the feed gases are measured and controlled by *Brooks Instruments* Model 5850E mass flow controllers (MFCs).

Powder catalyst samples (200 – 300mg) are placed in the center of a glass-lined stainless steel reactor tube (0.25”OD, 0.15” ID, 12” length), which is mounted vertically in a furnace and held in place by quartz wool plugs. An electronic temperature controller drives the single zone split tube vertical furnace. The temperature of the catalytic bed is monitored with a K-type thermocouple. The reactor pressure is controlled by a back pressure regulator located downstream of the reactor tube. The feed mixture enters the bottom of the tube and flows upward through the catalyst bed. Downstream of the back pressure regula*t*or, the product gases flows via a heated line into an Agilent gas chromatograph 6980N / mass spectrometer MSD 5968 (GC/MS) for analysis. A slipstream of reaction products is also taken via capillary tubing into an Ametek Dycor Quadlink Residual Gas Analyzer / Quadrupole Mass Spectrometer (RGA/QMS) for real time monitoring of mass fractions during temperature-programmed experiments.

The reactor system is controlled with the AMI 2000 software that allows for the automated control of the gas flow rates, temperature of the furnace and pressure of the reactor.

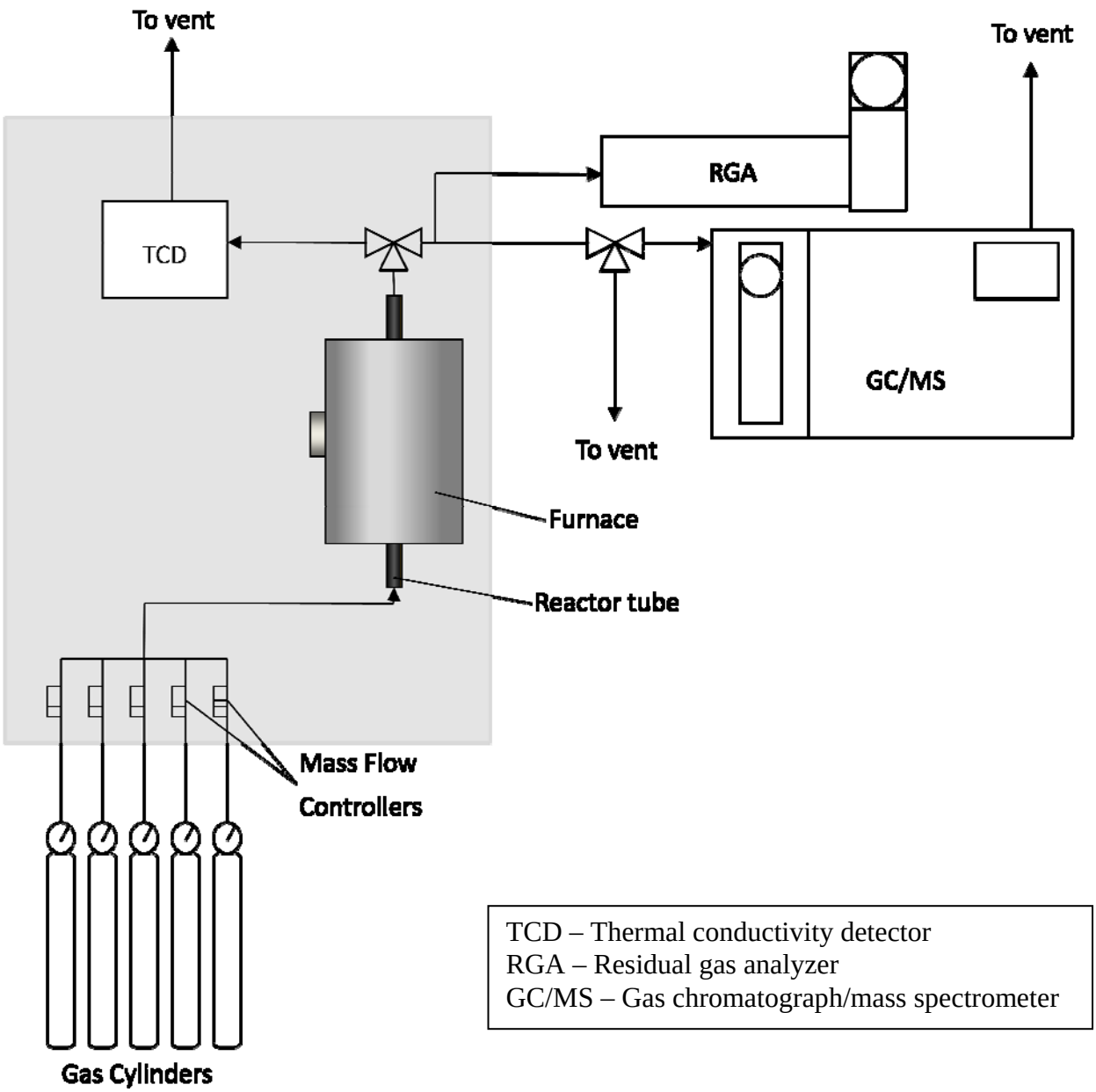

Figure 3.1: Schematic of the reactor and the analytical equipment.

3.1.2 Gas Chromatograph/Mass Spectrometer*

The Agilent 6890N series gas chromatograph (GC) has been configured by Wasson ECE Instrumentation (Wasson) for the analysis of various hydrocarbons, light molecular weight oxygenates, and some fixed gases and water.

* Adapted from Wasson-Agilent manual

An auxiliary isothermal oven is mounted on top of the GC to provide housing for columns and valve locations. The oven is connected to a heated chase which provides a heated zone between the auxiliary oven and the programmable oven. It also maintains the carrier gas/sample components in a vapor state as they pass between ovens. The instrument is equipped with a hot injector oven to receive the gas sample stream from the Altamira reactor system. This is always kept at a temperature of 250°C, ensuring that any condensable in our product stream is kept in the vapor state as it is transported into the GC/MS.

The instrument has been supplied with three detectors for this application: an Agilent 5975N mass selective detector (MSD), and two thermal conductivity detectors (TCD). The MSD is connected to the GC via a heated transfer line through the left side of the primary oven. The GC/MS requires two career gases: helium and nitrogen. Helium is the carrier selected for the analysis of oxygenated and light hydrocarbons which require the use of the MSD and also for the front TCD (TCD A) analysis of water. Helium of UHP grade is supplied from a gas cylinder and cleaned to remove oxygen, moisture, and hydrocarbons by using appropriate gas traps. Nitrogen is used as the carrier gas for the hydrogen analysis on the rear TCD (TCD B); Nitrogen is the choice here (in lieu of He) because its thermal conductivity is farther away from that of hydrogen than He, thereby yielding more amplified TCD signal for hydrogen. UHP grade nitrogen is used without further purification. Table 3.1 shows the carrier gases employed for our analyses.

Table 3.1. Carrier Gases

gas	grade	detector	set pressure
He	UHP	MSD, TCD A	100 psig
N_2	UHP	TCD B	60 psig

The instrument is equipped with air-actuated Valco gas sampling and switching valves to

effect sample injection as well as column and detector selection. Air is delivered to the GC from gas cylinder for valve actuation. The rotary valves are located in the auxiliary and programmable ovens of the GC, and the two high temperature gas sample valves, V1 and V2 are located in the injector oven mounted above the inlets (injection ports) to introduce gaseous samples to the three analytical subsystems, as dictated by the detectors: one in line with the TCD A with nitrogen as the carrier gas, the second with the TCD B having helium as the carrier gas and the third in line with the MSD, also with helium carrier gas. The 10-port rotary valve (V4), located in the programmable oven, controls the choice of capillary column effluents sent to the MSD.

Each subsystem has its own set of columns: guard columns are positioned upstream of the main column to retain the heavier components from getting to the main column for the analysis. Using a combination of valves and switches, carrier gas flows can be reversed at specific times to sweep the heavy components being retained on the guard columns back into the sample vent.

3.1.3 Residual Gas Analyzer

Ametek Residual Gas Analyzer (Dycor Quadlink) is a quadrupole mass spectrometer system which allows for real time mass fractions data acquisition in the 2 - 100 AMU range. It is used during temperature-programmed experiments. It is connected to the Altamira reactor system via a 1-meter long fused silica capillary tubing with an inside diameter of 50 microns, through which a slipstream of gaseous sample passes from the reactor to the filament/ detector chamber under vacuum. The residual gas analyzer is made up of the quadrupole mass spectrometer, electron multiplier detector, power supply and the pressure reduction subsystem. The pressure reduction subsystem consists of the roughing and turbomolecular pumps to maintain the low operating pressure of 1.0E-6 Torr range in the sampling chamber. Data acquisition and system control is accomplished via the Dycor System 2000 software. The software is integrated with the

AMI 2000 software of the reactor, which allows for mass fraction signals to be recorded as a function of reactor temperature.

3.1.4 Drying Oven and Calcination Furnace

The drying oven and calcination furnace are used during catalyst preparation. The Lindberg/Blue M Mini-Mite™ calcination furnace is tube furnace with a single zone heater and a programmable digital control. The sample holder is a 1-inch diameter quartz tube with gas connection through a mass flow controller on one side while the other end is opened to allow for gas exhaust. The Fisher Scientific Isotemp oven is used for the drying of freshly impregnated catalysts samples at fixed temperatures.

3.2 CATALYST PREPARATION

The catalysts are prepared by the incipient wetness impregnation method. The pore volume of the support is estimated prior to impregnation by drying a known weight of titania support in the oven at 120°C for 1 h to remove any residual moisture from the pores. It is cooled to room temperature in a desiccator and water is added drop-wise until the pores are just fully saturated, the porosity is then calculated by dividing the volume of water added by the weight of the support.

With the porosity known, the volume of the impregnating solution is calculated for any given weight of support. The quantities of the metal and promoter precursor compounds dissolved are determined by the desired active metal and promoter loading respectively. The promoter precursor solution is added drop-wise onto the dry support and mixed until a homogeneous paste is formed. It is allowed to sit for 2 h to allow for adequate contact before overnight drying at 120°C in an oven. The dried sample is then crushed back into powder form and placed in the calcination tube furnace. The catalyst is calcined at 500°C for 4 hours in a flow of air. If more than one promoter is desired, they can be co-impregnated or sequentially

impregnated. We used co-impregnation method, in which all the promoter metal precursors are dissolved in a solution along with the Rh metal. For sequential impregnation, the same sequence of steps are repeated for other promoter(s) each ending with drying in the oven or calcination in a flow of air.

3.2.1 Support Choice

Most of the previous work done in this area has been on SiO_2 supports[1-4]. Relatively less focus has been on other supports like Al_2O_3 and TiO_2, which have been reported to have a high density of surface hydroxyls[5, 6]. It is worth noting that catalysts precursors are anchored on the surface of metal oxide supports via reaction with surface hydroxyl groups[5, 7, 8]. Therefore, the population of such hydroxyls affects the particle size of the supported phase while their density may affect the interactions between the supported metals[6]. Titania was used in this studies because it possesses high surface density of reactive hydroxyls (relative to SiO_2) which allows for the formation of a close-packed monolayer of the supported metals[5, 6]. The rationale is that this may lead to an increased rhodium–promoter interface which is thought to accommodate chemisorbed CO that is carbon-bound to a rhodium atom and oxygen-bound to a promoter ion as shown in Figure 2.6, resulting in improved metal-promoter interaction. This mode of CO adsorption is thought to be important in the catalytic synthesis of oxygenates from CO/H_2 mixtures[9, 10].

Rh/TiO_2 has also been found to be more active for CO decomposition and hydrogenation than Rh/SiO_2 or Rh/Al_2O_3[11], although titania also leads to higher activity for methanation and water gas shift. With suitable promotion we can modify the properties of Rh/TiO_2 to shift selectivity more towards C_2+ oxygenates in general and ethanol in particular while minimizing methanation activity. Table 3.2 shows the properties of the TiO_2 support (Degussa P25) as provided by the manufacturer.

Table 3.2: Properties of the TiO_2 Support.

Properties	Unit	Typical Value*
TiO_2-content	wt. %	> 99
Anatase content	wt. %	> 70
Specific pore volume	ml / g	0.35 – 0.45
BET surface area	m^2 / g	40 - 50
Median Pore Diameter	nm	31

* from Degussa Aerolyst 7710 catalyst product information sheet

3.2.2 Choice of Promoters

As explained in the literature review section, the formation of ethanol can be enhanced on Rh catalysts by the addition of promoters[12-14]. Mn promoters have been used widely studied with Rh-based catalysts and have been reported to increase overall activity as well as improve selectivity towards C_2-oxygenates[10, 15, 16]. Several mechanisms for Mn promotion have been reported: some proposed that Mn enhances CO dissociation by forming tilt-adsorbed CO species that is C-bonded to Rh and O-bonded to Mn, resulting in weakening of the C-O bond, thereby increasing activity[17]. Others thought that Mn weakens the adsorption strength of CO (i.e. Rh-CO bond) leading to less carbon coverage, allowing for increased surface concentration of H_2 species necessary for increased activity[10, 16, 18].

Alkali promoters have been used to enhance oxygenate formation by suppressing the hydrogenation activity of Rh (and other group VIII metals)[12]. However oxygenates also require their intermediates/precursors to be hydrogenated. Alkali promotion is therefore only effective if the hydrogenation suppression decreases the formation of methane more than C_2 oxygenates[19].

Chuang et al[12] tested a series of alkali promoters on Rh/TiO_2 and reported that their ability to enhance selectivity of oxygenates increased in the order: unpromoted < Li < K = Cs while overall catalyst activity decreases in the order: unpromoted > Li > K > Cs. The activity of the catalyst is thus correlated with the ability to enhance oxygenate selectivity.

Li has been reported to produce the highest ethanol selectivity among 30 different promoters tested for CO_2 hydrogenation on Rh/SiO_2[20]. Li (as well as other alkalis) is believed to;

- change the electronic state of Rh on SiO_2, causing a change in the balance of CO species on the surface[20];
- physically blocks the surface of active sites, inhibiting reaction steps like CO dissociation that requires large ensemble of atoms[21]; or
- create active sites for C_2-oxygenates on Rh/TiO_2[22].

Regardless of the mechanism of promotion, Li generally suppresses methanation and also reduces CO conversion[12, 20, 23, 24].

A catalysts containing a combination of both promoters (on $Rh\text{-}Li\text{-}Mn/SiO_2$) have shown higher yield and selectivity for C_2-oxygenates from CO hydrogenation than when the promoters are used individually[25]. These observations were attributed to reduced CO dissociation and increased CO insertion. Yin et al reported a further increase in the yield of C_2-oxygenates when Fe was added unto $Rh\text{-}Mn\text{-}Li/SiO_2$, even for a loading as little as 0.05 wt %, but a decrease was observed when Fe amount exceeded 1.0%[26]. It is known that Fe promoted Rh catalysts can increase ethanol selectivity from CO hydrogenation[2, 6] and from CO_2 hydrogenation, as reported by Kusama et al[20].

In this work, Rh/TiO_2, $Rh\text{-}Li/TiO_2$, $Rh\text{-}Mn/TiO_2$, $Rh\text{-}Mn\text{-}Li/TiO_2$ and $Rh\text{-}Mn\text{-}Li\text{-}Fe/TiO_2$ catalysts were prepared using co-impregnation methods. Aqueous solutions of $Rh(NO_3)_3$,

$Mn(NO_3)_2$, $LiNO_3$ and $Fe(NO_3)_3$ were co-impregnated (depending on the catalyst composition) on the support, which is TiO_2 (Degussa Aerolyst, ~50m^2/g), dried overnight at 110°C and calcined under air flow for 4 hr at 500°C. Table 3.3 shows the target compositions of the catalysts.

Table 3.3: Target Compositions of the Catalysts

Catalyst	Metal	Target composition (wt %)
Rh/TiO_2	Rh	1.00
$Rh\text{-}Li/TiO_2$	Rh Li	1.00 0.10
$Rh\text{-}Mn/TiO_2$	Rh Mn	1.00 0.55
$Rh\text{-}Mn\text{-}Li/TiO_2$	Rh Mn Li	1.00 0.55 0.10
$Rh\text{-}Mn\text{-}Li\text{-}Fe/TiO_2$	Rh Mn Li Fe	1.00 0.55 0.10 0.50

For the reason of practicality, Rh was used at a moderate loading of 1 wt % on all catalysts because of the high price of Rh metal. The loadings of the other metals were chosen so as to approximate a 1:1 atomic ratio between Rh and each of the promoter metals.

3.3 REACTION TESTS

Reaction tests at differential conditions were carried out in a ¼" glass-lined stainless steel fixed bed *Altamira 200R-HP* micro-reactor system at a total pressure of 20 bar. Prior to reaction tests the catalyst was reduced in-situ for 2 h in 75% H_2/25% He mixture. CO (or CO_2) hydrogenation [H_2/CO (or CO_2) = 2/1] reactions were run at GHSVs of about 52800 scc hr^{-1} $gcat^{-1}$. For each run the syngas feed was diluted with He to reduce heat effects within the bed and

to ensure that the conversion is low enough to keep the oxygenated products in vapor state for online GC/MS analysis. The total flow rate of the feed gas was maintained at 220 scc/min. The sum of the flow rates of H_2 + CO (or CO_2) was 120 scc/min, with a constant flow rate of 100 scc/min He. For the hydrogenation of CO/CO_2 mixture, equimolar substitution of half of feed CO with CO_2 resulted in reactant feed rate of 80, 20 and 20 sccm/min for H_2, CO and CO_2 respectively keeping the GSHV (52800 $scchr^{-1}gcat^{-1}$) and H/C ratio [$H_2/(CO+CO_2)$ = 2] the same. In between these experiments, catalyst regeneration was done via an oxidation step at 450°C in 10% O_2/He, to remove surface carbon, followed by a reduction in diluted 75% H_2 /25% He gas stream at 350°C. Data were collected at furnace temperatures of 260°C and 270°C; reactions were allowed to run for at least 1.5 h at each temperature level to attain steady state before samples are injected into the GC for analysis.

3.4 PRODUCT ANALYSIS

Included in this section are the sampling procedure and the description of analytical methods. Calibration and method development information are given in Appendix 1.

3.4.1 Gas Sample And Standard Injection

Reactor gas samples (or gas phase standards during calibration) enter the GC from the reactor via a heat traced sample line that travels into the injector oven. The sample line is connected to the dual injection gas sampling valves via $^1/_{16}$" tubing, filling the sample loops in the process and the excess gas sample purges from the instrument to vent. The sampling valve then switches to allow the carrier gas to sweep the sample to be analyzed into the GC for analysis via split/splitless injector ports. Sample gas is separated according to their retention/elution times as it is transported through the GC columns to the detector. Prior to sample injection, the reactor flow is used to purge sample through the sampling valves and then shut off (diverted to vent).

GC is controlled with Agilent ChemStation software that also handles the data analysis. It

is necessary to choose and load the appropriate method for the analytes to be determined via the computer software prior to sample injection. Three methods are developed for the complete analysis of our products. Method development involves selection of columns and setting of flows and oven temperature program that gives the best separation between components of interest. It also involves the calibration of the GC, which is done by analyzing gas standards of known concentrations in order to get response factors that enable the correlation of response signals to composition of analytes injected. Below, we discuss the methods developed for the GC. Table 3.4 shows a list of the columns installed in the GC/MS.

Table 3.4. Columns installed in the GC/MS

column no.	length (m)	inner diameter (mm)	column code[1]	mesh size	max. temp (°C)	type[2]
1	1	0.53	KC134	-	165	C
2	13	0.53	KC134	-	165	C
3a	15	0.53	KC090	-	220	C
3b	1	0.53	KC134	-	165	C
4	50	0.53	KC080	-	210	C
5	100	0.25	KC 066	-	210	C
6a	6''	1/8"	K1	80/100	150	P
6b	7"	1/8"	K2	80/100	330	P

[1] Wasson Instrumentation ECE internal codes for columns
[2] C = capillary, P = packed

3.4.2 GC Methods

3.4.2.1 Analysis of Oxygenates and Heavier Hydrocarbons by MSD

The analysis of the oxygenated components and heavier hydrocarbons is achieved with the MSD. When this method is loaded, valve switches to place column 5 is series with the gas sample valve and the MSD. At the start of the run, the sampling valve injects its volume of gas sample into the carrier stream traveling to the front injector which is a Split/Splitless type. The sample is split accordingly at the front inlet and is then swept onto column 5. All components in the sample travel through column 5 to the MSD which selectively quantifies the analytes

assigned to this method: Acetaldehyde, acetone, methanol, ethanol, i-propanol, n-propanol, i-butanol, n-butanol as well as i-Butane, n-Butane or any C_4 olefins that may be present.

3.4.2.2 Analysis of Light Components by MSD

The lighter components are best separated by column 4. Column 4, however, strongly retains any heavy components in the sample, and for that reason, a guard column combination is used, The set column 3a & 3b are used to keep heavies from column 4 by using a pressure switch to reverse flow at the prescribed time, sending the heavies back into the front Inlet and out to vent, not being detected. The light components are allowed to travel from columns 3a & 3b to column 4 where they are separated and detected by the MSD. The light components assigned to this method include CO, CO_2, methane, ethane, propane, propylene, and propadiene.

3.4.2.3 Analysis of Hydrogen and Water by TCD

This method uses both TCDs: TCD B uses nitrogen as a carrier gas and its used for the analysis of hydrogen, when the method is run, valves turn to bring columns 6a & 6b in line to receive the sample. Sampling valve then switches to flush a volume of sample onto columns 6a & 6b via the back inlet. The sample components travel forward down columns 6a & 6b, with hydrogen eluting first to TCD B. Once hydrogen has been detected, valve switches to back flushing the remaining heavies to vent.

Simultaneously, a second volume of sample (all the same components) is injected onto the column set, column 1 & column 2. Column 2 is a longer column, which is needed to perform the necessary separation prior to detection by TCD A. This detector uses helium as a carrier gas, and is used for the quantification of higher amounts of water in the sample. Column 1 is a guard column and protects Column 2 from seeing heavy components which would otherwise take too long to elute from Column 2. A pressure switch is employed that effectively reverses flow in Column 1, while maintaining forward flow in Column 2, at a prescribed time. Thus, the earlier

the pressure switch the fewer the heavy components are seen on TCD A.

3.5 CATALYST CHARACTERIZATION

3.5.1 Temperature Programmed Reduction (TPR)

TPR is a useful technique for the characterization of metal oxide catalysts. TPR profile of a catalyst contains qualitative information on the oxidation state of the reducible catalyst. In essence, it shows the ease of reducibility of such catalyst and the extent of reduction. TPR provides information on the temperatures needed for the complete reduction of a catalyst and for bimetallic catalysts, it often reveals whether the two metals are in contact or not.

In order to generate this profile, a known weight of the catalyst is placed in the center of the reactor tube and held in place by the 2 quartz wool plugs, degassed with He flow at 120°C for 30 minutes to remove moisture that might be on the catalysts during storage and allowed to cool to room temperature under He flow. The sample is then exposed to 100 sccm flow of 10% H_2/Ar gas mixture, as the reactor temperature, ramped to 500°C from room temperature at the desired heating rate. TCD signal corresponding to H_2 consumption is then recorded as a function of temperature a function of temperature. In this work, TPR 250mg of the catalyst sample is used in the reactor tube, degassed at 120°C, reducing gas mixture is 10% H_2/Ar while the temperature ramp rate is 5°C/min from room temperature to 500°C.

3.5.2 Temperature Programmed Desorption (TPD)

TPD experiments offer a means of obtaining quantitative information about the number of surface sites exposed and available for chemisorption and for supported metal catalysts, it may be used to calculate an average metal crystallite size. Such information provides a basis for comparing the activity and selectivity of different catalysts. In addition, it can also give a qualitative measure of the variation in the strength of adsorption for different sites on the surface.

The catalyst sample is placed in the reactor tube held in place by the two quartz plugs as usual. It was pre-reduced in 100sccm of H_2 flow at 350°C for 2 hr and flow switched to He while the sample is allowed to cool to room temperature. The chemisorbing gas, in this case CO, was then allowed to flow over the sample for 1 hour at room temperature. Prior to the desorption step, the system is flushed with He for 2 hr to sufficiently remove gas phase CO and physisorbed CO. Still under He flow, the temperature was linearly ramped from room temperature (RT) to 500°C at 5°C/min. A quadrupole mass spectrometer (QMS) at the exit of the reactor was used to continuously monitor CO (m/z = 28), CO_2 (44) and H_2 (2) as a function of temperature.

3.5.3 Temperature Programmed Oxidation (TPO)

Temperature programmed oxidation (TPO) was done on used catalysts. At the end of a CO and/or CO_2 hydrogenation experiment, the reactor was cooled down to RT in He flow to flush out any residual product within the bed. The flow is then switched to a 10% O_2/He mixture while the temperature is ramped from RT to 500°C at 5°C/ min. A quadrupole mass spectrometer (QMS) at the exit of the reactor was used to continuously monitor CH_4 (m/z = 16), CO (28), CO_2 (44), H_2 (2) as a function of temperature.

3.6 REFERENCES

1. H. Y. Luo, W. Zhang, H. W. Zhou, S. Y. Huang, P. Z. Lin, Y. J. Ding and L. W. Lin, *Applied Catalysis a-General*, 2001, **214**, 161-166.

2. H. Arakawa, T. Fukushima, M. Ichikawa, S. Natsushita, K. Takeuchi, T. Matsuzaki and Y. Sugi, *Chemistry Letters*, 1985, 881-884.

3. M. Ichikawa and T. Fukushima, *Journal of the Chemical Society-Chemical Communications*, 1985, 321-323.

4. H. M. Yin, Y. J. Ding, H. Y. Luo, D. P. He, W. M. Chen, Z. Y. Ao and L. W. Lin, *Journal of Natural Gas Chemistry*, 2003, **12**, 233-236.

5. I. E. Wachs, G. Deo, M. A. Vuurman, H. C. Hu, D. S. Kim and J. M. Jehng, *Journal of Molecular Catalysis*, 1993, **82**, 443-455.

6. R. Burch and M. J. Hayes, *Journal of Catalysis*, 1997, **165**, 249-261.

7. M. P. Cabero, M. J. Holgado and V. Rives, *Materials Chemistry and Physics*, 1991, **27**, 181-188.

8. U. Usman, M. Takaki, T. Kubota and Y. Okamoto, *Applied Catalysis a-General*, 2005, **286**, 148-154.

9. A. Kiennemann, R. Breault, J. P. Hindermann and M. Laurin, *Journal of the Chemical Society-Faraday Transactions I*, 1987, **83**, 2119-2128.

10. F. G. A. van den Berg, J. H. E. Glezer and W. M. H. Sachtler, *Journal of Catalysis*, 1985, **93**, 340-352.

11. T. Ioannides and X. Verykios, *Journal of Catalysis*, 1993, **140**, 353-369.

12. S. C. Chuang, J. G. Goodwin and I. Wender, *Journal of Catalysis*, 1985, **95**, 435-446.

13. Y. H. Du, D. A. Chen and K. R. Tsai, *Applied Catalysis*, 1987, **35**, 77-92.

14. J. R. Katzer, A. W. Sleight, P. Gajardo, J. B. Michel, E. F. Gleason and S. Mcmillan, *Faraday Discussions*, 1981, 121-133.

15. K. P. De Jong, J. H. E. Glezer, H. P. C. E. Kuipers, A. Knoester and C. A. Emeis, *Journal of Catalysis*, 1990, **124**, 520-529.

16. M. Ojeda, M. L. Granados, S. Rojas, P. Terreros, F. J. Garcia-Garcia and J. L. G. Fierro, *Applied Catalysis a-General*, 2004, **261**, 47-55.

17. M. Ichikawa and T. Fukushima, *Journal of Physical Chemistry*, 1985, **89**, 1564-1567.

18. A. S. Lisitsyn, S. A. Stevenson and H. Knozinger, *Journal of Molecular Catalysis*, 1990, **63**, 201-211.

19. S. S. C. Chuang, R. W. Stevens and R. Khatri, *Topics in Catalysis*, 2005, **32**, 225-232.

20. H. Kusama, K. Okabe, K. Sayama and H. Arakawa, *Catalysis Today*, 1996, **28**, 261-266.

21. S. C. Chuang, J. G. Goodwin and I. Wender, *Journal of Catalysis*, 1985, **92**, 416-421.

22. H. Orita, S. Naito and K. Tamaru, *Chemistry Letters*, 1983, 1161-1164.

23. R. Burch and M. I. Petch, *Applied Catalysis a-General*, 1992, **88**, 39-60.

24. B. J. Kip, E. G. F. Hermans and R. Prins, *Applied Catalysis*, 1987, **35**, 141-152.

25. H. M. Yin, Y. J. Ding, H. Y. Luo, W. M. Chen and L. W. Lin, in *Natural Gas Conversion Vii*, Editon edn., 2004, vol. 147, pp. 421-426.

26. H. M. Yin, Y. J. Ding, H. Y. Luo, H. J. Zhu, D. P. He, J. M. Xiong and L. W. Lin, *Applied Catalysis a-General*, 2003, **243**, 155-164.

CHAPTER 4 : EFFECT OF Li, Mn AND Fe PROMOTERS ON TITANIA-SUPPORTED Rh CATALYST FOR ETHANOL FORMATION FROM CO HYDROGENATION

4.1 INTRODUCTION

It is well know that rhodium-based catalysts are active for the formation of C_2 oxygenates from the hydrogenation of CO[1]. Thermodynamics have shown that ethanol selectivity is very low unless the formation of methane can be eliminated. The use of suitable promoters and supports has been shown to shift selectivities towards ethanol and other C_2 oxygenates.[2]

Mn promoters have been used widely studied with Rh-based catalysts and have been reported to increase overall activity as well as improve selectivity towards C_2-oxygenates[3-5]. Several mechanisms for Mn promotion have been reported: some proposed that Mn enhances CO dissociation by forming tilt-adsorbed CO species that is C-bonded to Rh and O-bonded to Mn resulting in the weakening of the C-O bond thereby increasing activity[6]. Others thought that Mn weakens the adsorption strength of CO (i.e. Rh-CO bond) leading to less carbon coverage, allowing for increased surface concentration of H_2 species necessary for increased activity[3, 5, 7]. On Rh/SiO_2, oxides of Mn along with those of Ti and Al have been reported to have contrasting effects on the dissociation of CO: first a promoting effect (when on the surface of the Rh) by bounding with the O atom of adsorbed CO, thereby weakening the C=O bond and second, an inhibiting effect by covering the surface of Rh ensembles necessary for CO dissociation[8]. The overall effect is determined by which of the two effects is dominant. It has also been reported that Mn oxide weakens CO chemisorption either by suppressing the formation of more thermally stable CO species[4] or by forming a mixed oxide with Rh which does not completely reduce at 500°C[3]

Alkali promoters have been used to enhance oxygenate formation by suppressing the hydrogenation activity of Rh (and other group VIII metals)[9]. However oxygenates also require

their intermediates/precursors to be hydrogenated. Alkali promotion is therefore only effective if the hydrogenation suppression decreases the formation of methane more than C_2 oxygenates[10]. Chuang et al[9] tested a series of alkali promoters on Rh/TiO_2 and reported that their ability to enhance selectivity of oxygenates increased in the order: unpromoted < Li < K = Cs while overall catalyst activity decreases in the order: unpromoted > Li > K > Cs. Activity of the catalyst is thus correlated with the ability to enhance oxygenate selectivity. Li (as well as other alkalis) is believed to; change the electronic state of Rh on SiO_2, causing a change in the balance of CO species on the surface[11]; physically blocks the surface of active sites, inhibiting reaction steps like CO dissociation that requires large ensemble of atoms[12]; or create active sites for C_2-oxygenates on Rh/TiO_2[13]. Regardless of the mechanism of promotion, Li generally suppresses methanation and also reduces CO conversion[9, 11, 14, 15].

However, most of these previous work done has been on SiO_2 supports[1, 16-18], with relatively less literature on Al_2O_3-supported Rh and very few on Rh/TiO_2. Both Al_2O_3 and TiO_2 supports have been reported to have a high density of surface hydroxyls. Such surface hydroxyl groups[19-21] provide anchors for catalysts precursors on the surface of metal oxide supports by reacting with them (precursors). Therefore, the population of such hydroxyls affects the particle size of the supported phase while their density may affect the interactions between the supported metals[22]. In this work, we use TiO_2 as the support because of it high surface density of reactive hydroxyls (relative to SiO_2) which allows for the formation of a close-packed monolayer of the supported metals[21, 22]. Rh/TiO_2 has also been found to be more active for CO decomposition and hydrogenation than Rh/SiO_2 or Rh/Al_2O_3[23], although titania also leads to higher activity for methanation and water gas shift. With suitable promotion we can modify the properties of Rh/TiO_2 to shift selectivity more towards C_2+ oxygenates in general and ethanol in particular while minimizing methanation activity.

A catalysts containing a combination of both promoters (on Rh-Li-Mn/SiO_2) have shown higher yield and selectivity for C_2-oxygenates from CO hydrogenation than when the promoters are used individually[24]. These observations were attributed to reduced CO dissociation and increased CO insertion. Yin et al reported a further increase in the yield of C_2-oxygenates when Fe was added unto Rh-Mn-Li/SiO_2, even for a loading as little as 0.05 wt %, but a decrease was observed when Fe amount exceeded 1.0%[25]. It is known that Fe promoted Rh catalysts can increase ethanol selectivity from CO hydrogenation[1, 22].

To this end, we have synthesized a series of Rh catalysts supported on TiO_2 catalysts using Fe, Mn, and Li as promoters. The purpose of the present research is to explore how Mn, Li and Fe promoters, which have been found to improve (either individually or in combination) C_2+ oxygenate selectivity, affect the selectivity/activity of Rh/TiO_2 catalysts for ethanol (or C_2^+ oxygenates) production from synthesis gas.

4.2 EXPERIMENTAL

Reaction tests at differential conversions were carried out in a ¼" glass-lined stainless steel fixed bed *Altamira 200R-HP* micro-reactor system at a total pressure of 20 bar. Prior to reaction tests the catalyst was reduced in-situ for 2 h in 75% H_2/25% He mixture. CO hydrogenation (H_2/CO = 2/1) reactions were run at GHSVs of 52800 scc hr^{-1} $gcat^{-1}$. For each run the syngas feed was diluted with He to reduce heat effects within the bed and to ensure that the conversion is low enough to keep the oxygenated products in vapor state for online GC/MS analysis. The total flow rate of the feed gas was maintained at 220 scc/min. The sum of the flow rates of H_2 + CO was 120 scc/min, with a constant flow rate of 100 scc/min He. Data were collected at furnace temperatures of 260°C and 270°C; reactions were allowed to run for at least 1.5 h at each temperature level to attain steady state before samples are injected into the GC for analysis

4.3 RESULTS AND DISCUSSION

The composition of the synthesized catalysts measured by ICP-OES* is shown in Table 4.1. The measured composition is close the target composition is all cases except for the Rh-Mn-Li-Fe/TiO_2 which shows composition close to half of what was targeted on all the components.

Table 4.1: Measured Composition of the Catalysts

Catalyst	Metal	Composition (wt %)	BET surface area (m_2/g)
Rh/TiO_2	Rh	0.90	45
Rh-Mn/TiO_2	Rh	1.03	45
	Mn	0.48	
Rh-Li/TiO_2	Rh	1.16	43
	Li	0.09	
Rh-Mn-Li/TiO_2	Rh	1.07	43
	Mn	0.47	
	Li	0.08	
Rh-Mn-Li-Fe/TiO_2	Rh	0.66	42
	Mn	0.27	
	Li	0.05	
	Fe	0.16	

*Inductively-Coupled Plasma Optical Emission Spectroscopy

4.3.1 XRD

X-ray diffraction patterns of the catalysts shows only peaks consistent with TiO_2 phases of rutile and anatase. The XRD patterns of unpromoted Rh/TiO_2 and the promoted catalysts exactly overlap that of a blank Titania support as shown in Figure 4.1, suggesting that the Rh is highly dispersed and could not be observed by XRD[1], consistent with the TPR results. An argument can also be made that at 1 wt% Rh content in the catalysts, it is virtually impossible to detect Rh because it is too close to the typical detection limit by powder X-ray diffraction, which is also about 1.0%.

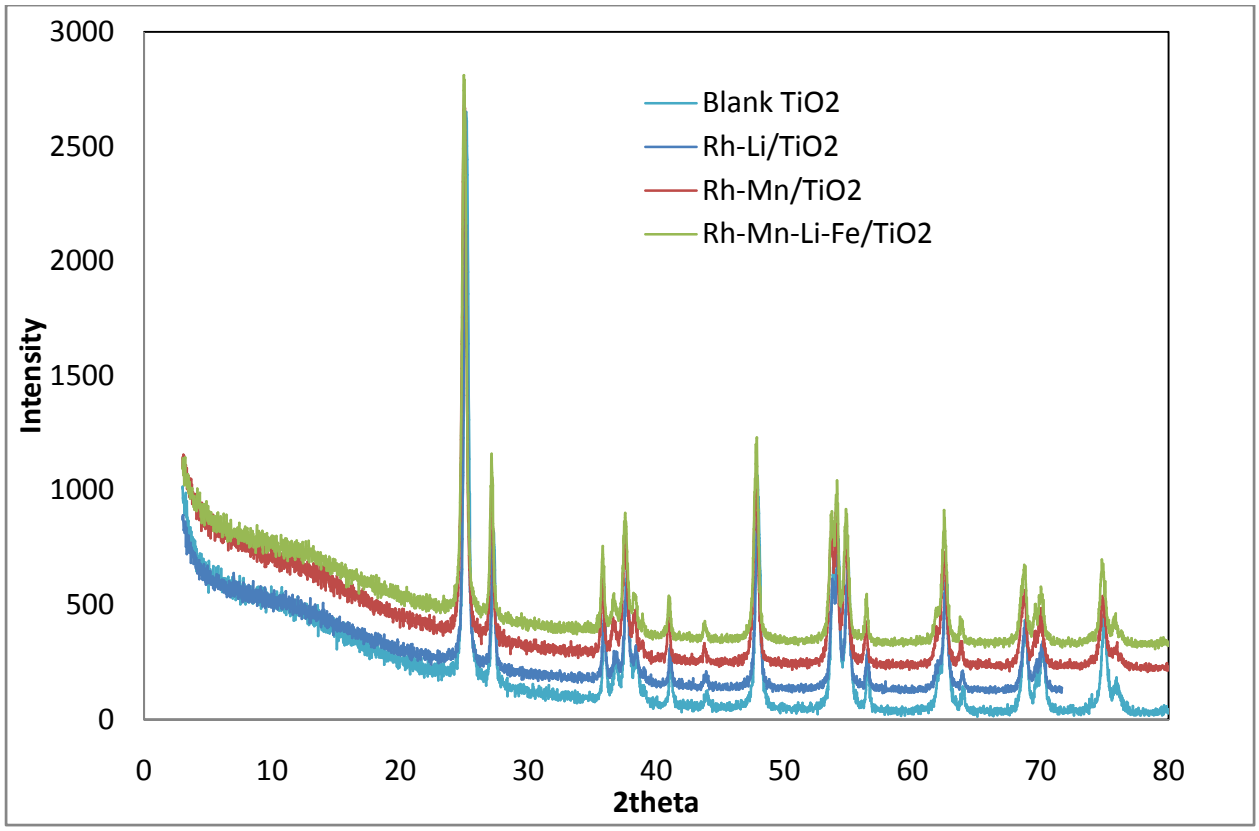

Figure 4.1. XRD profiles of selected catalysts

4.3.2 Reaction Tests

Table 4.2 shows the selectivity of products for the CO hydrogenation reaction at 260°C and 270°C on the five synthesized catalysts. In general, the major products formed are methane, acetaldehyde, ethanol and methanol with trace amounts of n-propanol, n-butanol and n-butane. The selectivity and activity largely depend on promotion although there are only slight changes in selectivity patterns within the small temperature range explored. The activity increases with increase in temperature as expected for an exothermic reaction. On all the catalysts, increasing the reaction temperature from 260 to 270°C has the effect of reducing the total oxygenates, C_2^+ oxygenates and ethanol selectivities, while increasing methane formation.

Methanation remains dominant on all the catalysts though the promoters (individually or in combination) seem to have the desired effect reducing methane selectivity. However, Rh-

Mn/TiO_2 showed very minimal changes in product selectivities with temperature changes within the small temperature range investigated here (260 – 270°C). The most dominant oxygenate formed on all the catalysts is acetaldehyde, except $Rh\text{-}Li/TiO_2$ on which ethanol has the highest selectivity among the oxygenated products. Unpromoted Rh/TiO_2 gave the highest methane selectivity of 71% at 260°C, while selectivities to methanol, ethanol and acetaldehyde are 8.3%, 7.2% and 5.1% respectively. High CH_4 suggests pronounced CO dissociation and less CO insertion than the promoted catalysts. Methanol, another C_1 species, is the most dominant of the oxygenate products, which is consistent with the previous statement of low catalyst activity for CO insertion.

Table 4.2: Products Selectivity (mol %) for CO Hydrogenation over Promoted Rh/TiO_2 Catalysts (reaction conditions: 20 bar, 52,800scc/hr-gcat., $H_2/CO = 2/1$)

	Rh/ TiO_2		Rh-Li/ TiO_2		Rh-Mn/ TiO_2		Rh-Mn-Li/ TiO_2		Rh-Mn-Li-Fe/TiO_2	
	260°C	**270°C**	**260°C**	**270°C**	**260°C**	**270°C**	**260°C**	**270°C**	**260°C**	**270°C**
methanol	8.3	6.6	5.0	3.6	4.4	4.2	10	6.5	9.1	7.5
acetaldehyde	5.1	5.5	10	10	12	11	17	19	10	13
ethanol	7.2	6.2	16	11	9.0	8.1	12	8.1	8.5	9.2
methane	71	74	62	70	69	71	56	58	63	62
CO_2	3.0	2.8	3.3	2.6	2.5	2.6	3.0	3.4	3.8	5.4
Total Oxy.	21	19	33	25	26	24	41	35	29	31
EtOH/Tot. Oxy	0.33	0.32	0.48	0.42	0.34	0.34	0.29	0.23	0.30	0.30
EtOH /CH_4	0.10	0.08	0.25	0.15	0.13	0.11	0.21	0.14	0.13	0.15
Conversion, *% mol C*	**0.8**	**1.0**	**2.0**	**2.5**	**1.4**	**2.1**	**0.6**	**0.7**	**0.6**	**0.8**

4.3.2.1 $Rh\text{-}Li/TiO_2$: Effect of Li on Rh/TiO_2 for CO Hydrogenation

In the CO hydrogenation reaction, C_2+ oxygenate selectivity on $Rh\text{-}Li/TiO_2$ is twice that of Rh/TiO_2 while methane selectivity decreases from 71% to 62% (although the difference is within the margin of error) (Figure 4.2). Ethanol is the most prevalent oxygenated product and its selectivity (16%) is twice that of the unpromoted catalyst (7.2%). Generally, more C_2+

oxygenated species are produced at the expense of C_1 species (methanol and methane). This can be attributed to the moderation effect of Li on the CO dissociation ability of the Rh/TiO_2. Li promotion also increases the CO conversion from 0.8% to 2.0%. This enhancement of activity on Li promotion is unexpected because the opposite is typically reported in literature[9, 12, 15].

Alkali metals have been known to enhance catalyst activity or oxygenate formation from CO hydrogenation on promoted catalysts via electronic effects[26]. This effect involves the donation of electrons from alkali to Rh metal and the back-donation of electrons from the metal to CO leading to a stronger bond between CO and the promoted metal. However, previous reports have shown that the presence of both metallic Rh^0 and oxidized Rh^+ is necessary for oxygenates formation[3, 27, 28]. Oxidized Rh^+ sites are thought to be responsible for CO insertion (which is necessary for oxygenate formation) while metallic Rh^0 sites are favorable for CO dissociation[3, 29]. Van der Berg et al suggested that CO chemisorbs more strongly Rh^0 sites than on Rh^+ sites supported on SiO_2 [3], therefore the ratio of these Rh species goes a long way in determining the product distribution. The electron donation effect of Li also tends to the increase the population of metallic Rh^0 on the support surface[30]. If this phenomenon solely explains our result, the addition of Li would increase Rh^0 and reduce Rh^+, thereby increasing CO dissociation leading to increased methanation and reduced ethanol selectivity. This suggests that Li effect on Rh/TiO_2 may not be electronic.

Our TPR results (Figure 4.8) show no bulk Rh peak on $Rh\text{-}Li/TiO_2$, suggesting that Rh is more dispersed on this catalyst than on Rh/TiO_2. The more dispersed the Rh is on the surface, the less the CO dissociation activity of the catalyst, because CO dissociation on transition metal oxides generally requires an ensemble of metal atoms[3]. Less CO dissociation has the effect of limiting surface carbon species on the reaction sites (which inhibits the adsorption of hydrogen) thereby increasing the surface concentration of hydrogen which is important for improved

activity[31]. It is also possible that Li physically blocks the surface of active sites thereby inhibiting reaction steps like CO dissociation which requires an ensemble of Rh atoms[8, 15]. This would be expected to coincide with reduced CO conversion due to loss of sites, which is not consistent with our results. Reduced CO dissociation also increases number CO molecules available for insertion into the Rh-$(CH_x)_{ad}$ bond, leading to higher chance of C-C bond formation versus the hydrogenation of $(CH_x)_{ad}$ to form methane.

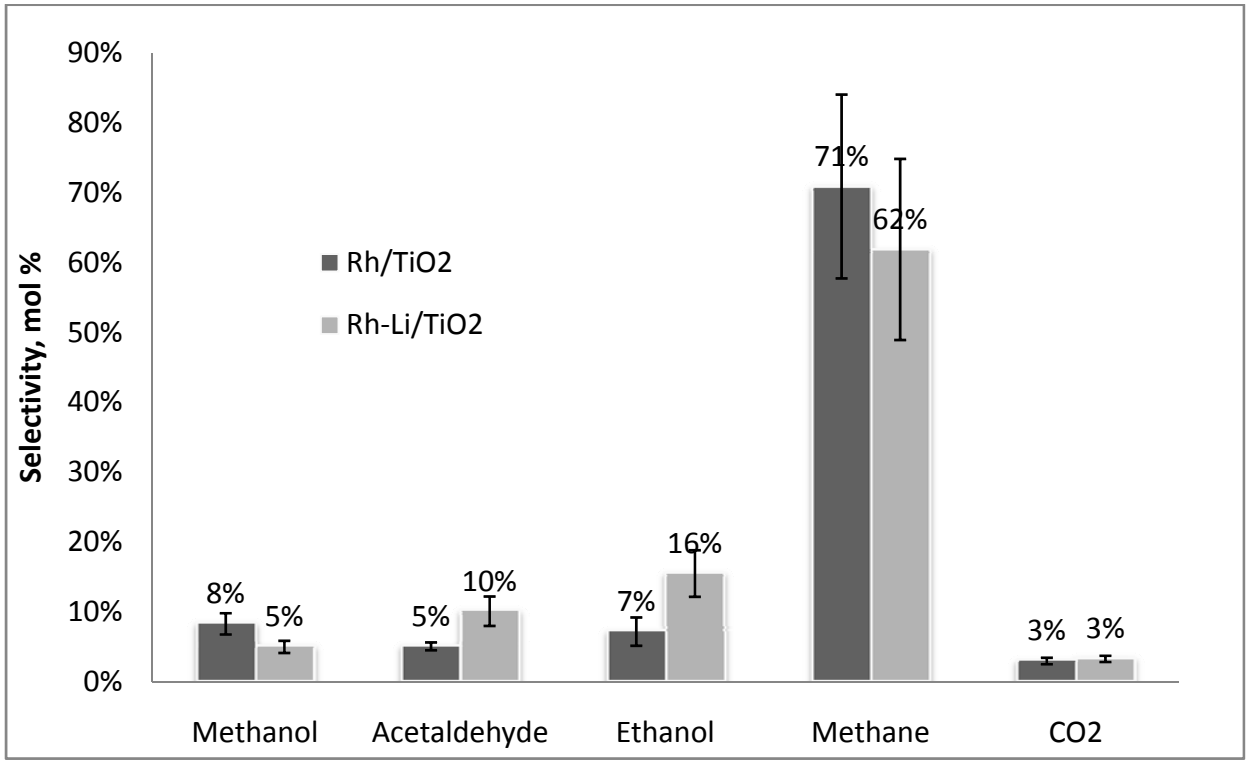

Figure 4.2: Products selectivity (mol %) for CO hydrogenation over Rh/TiO_2 vs $Rh-Li/TiO_2$ catalysts (reaction conditions: 260°C, 20 bar, 52,800scc/hr-gcat., $H_2/CO = 2/1$)

4.3.2.2 Rh-Mn/TiO_2: Effect of Mn on Rh/TiO_2 for CO Hydrogenation

During CO hydrogenation, CO conversion on $Rh-Mn/TiO_2$ is nearly twice as that on Rh/TiO_2, with increased oxygenates formation and essentially the same selectivity to CH_4 (71% and 69% on Rh/TiO_2 and $Rh-Mn/TiO_2$ respectively). Acetaldehyde is the most prevalent oxygenate on $Rh-Mn/TiO_2$; selectivity to acetaldehyde more than double from 5.1% on Rh/TiO_2 to 12% $Rh-Mn/TiO_2$ while methanol selectivity is halved from 8.3% to 4.4% correspondingly.

However, ethanol selectivity shows no significant change on Mn promotion (Figure 4.3). This suggests increased CO insertion activity leading to increased acetaldehyde formation at the expense of methanol. The little or no significant increase in ethanol and methane selectivity indicates that Mn has not enhanced the hydrogenation activity of catalysts which could have resulted in the hydrogenation of surface intermediates to either of them. It is also evident in the higher selectivity of acetaldehyde than ethanol on the Mn promoted catalyst because the hydrogenation of acetaldehyde (which previous work shows to be an intermediate[32]) to ethanol is limited.

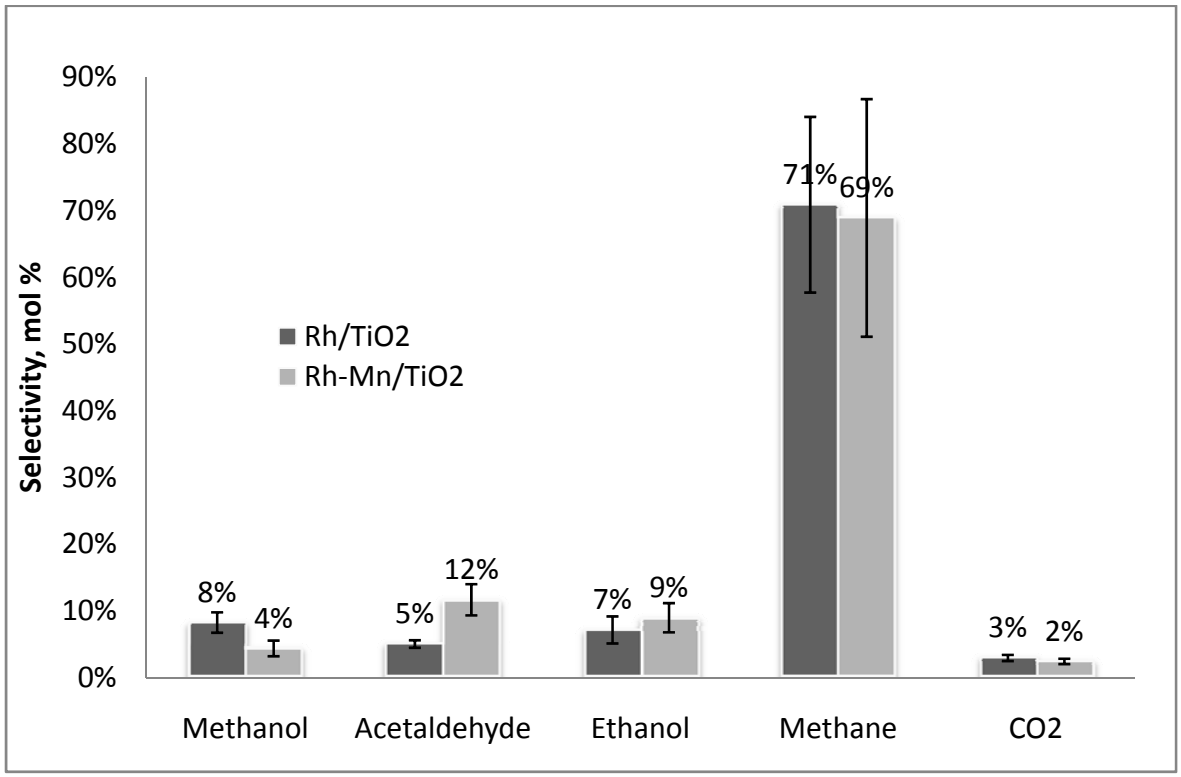

Figure 4.3: Products selectivity (mol %) for CO hydrogenation over Rh/TiO_2 and $Rh\text{-}Mn/TiO_2$ catalysts (reaction conditions: 260°C, 20 bar, 52,800scc/hr-gcat., $H_2/CO = 2/1$)

From literature, Mn, as a promoter, acts as an electron acceptor, in contrast with Li or other alkalis[30]. It withdraws electrons from the Rh, resulting in a partially oxidized Rh at the Rh-Mn interface. Mn is thought to form a mixed oxide with Rh, thereby stabilizing the Rh^+ species

which are thought to be responsible for CO insertion[3, 30]. Rh^+ sites supported on SiO_2 are thought to chemisorb CO less strongly than metallic Rh^0 because they have less capacity for back-donation of electrons to CO[3]. Therefore, the Rh-CO bond is effectively weaker in Mn-promoted catalyst because of increased population of Rh^+ on the surface. This explanation seems consistent with our results.

4.3.2.3 Rh-Mn-Li/TiO_2: Effect of Combining Li and Mn as Promoters on Rh/TiO_2

Combined Li and Mn promotion showed slightly less activity than the unpromoted Rh/TiO_2 catalysts and even much less than the individually promoted catalysts (Rh-Li/TiO_2 and Rh-Mn/TiO_2) probably because the Rh-Mn and Rh-Li interactions has been weakened or the promoters combined to partially cover up the surface Rh, leading to fewer reaction sites (Table 4.2). However the selectivity pattern shows that ethanol increased from 7.2% to 12% and acetaldehyde from 5% to 17% on the dual promoted Rh-Li-Mn/TiO_2 promoted catalyst (Figure 4.4). Methanol and methane selectivities remain statistically the same virtually the same upon promotion of Rh/TiO_2 with Li and Mn. The total oxygenate selectivity however increased from 21% to 41%, which is the highest among the catalysts tested here, suggesting that CO insertion activity is greatest on this catalyst. The changes in selectivities resulted in an increase in EtOH/CH_4 ratio increase to 0.21 from 0.10 on Rh/SiO_2. All these suggest a catalyst with relatively low hydrogenation activity and higher CO insertion properties than the other.

4.3.2.4 Rh-Mn-Li-Fe/TiO_2: Effect of Fe on Rh-Mn-Li/TiO_2 for CO Hydrogenation

During CO hydrogenation at 260° and 20 bar pressure, the addition of Fe to Rh-Mn-Li/TiO_2 caused no significant change methanol and methane selectivities. However, ethanol and acetaldehyde are more sensitive to Fe addition as their selectivities decreased from 12% to 8.5% and 17% to 10% respectively (Figure 4.5).

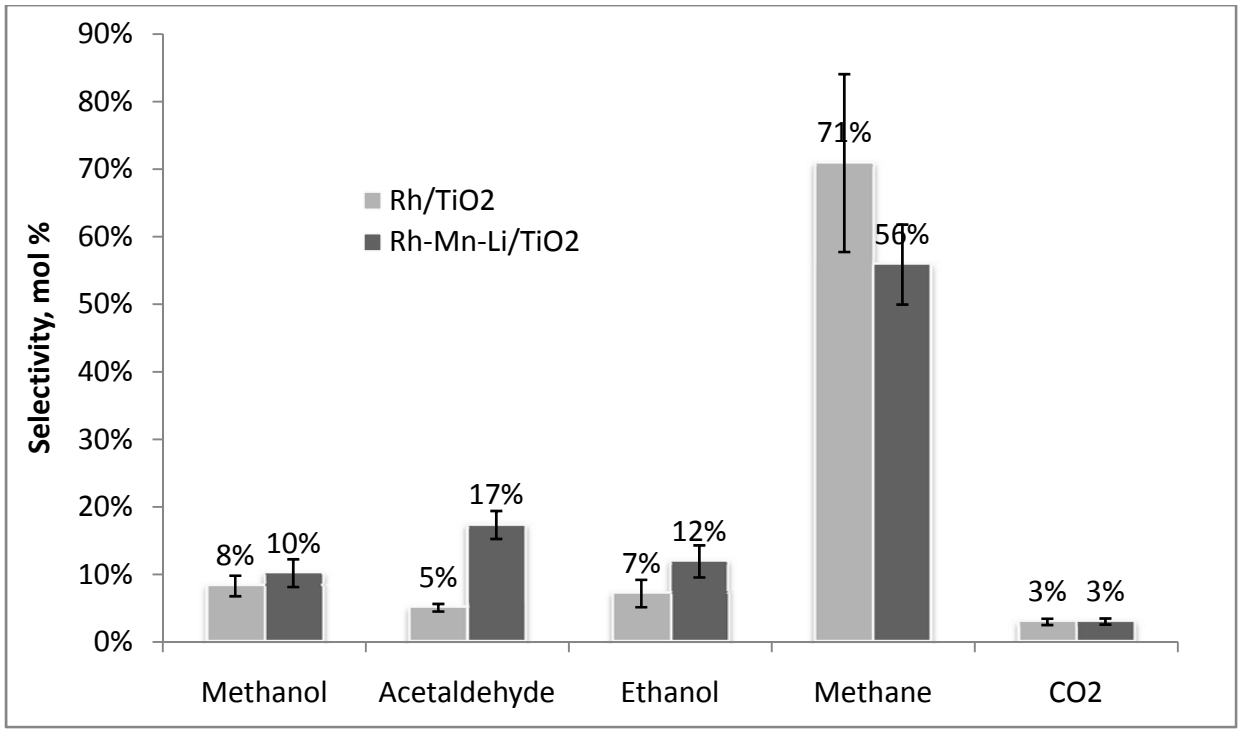

Figure 4.4: Products selectivity (mol %) for CO hydrogenation over Rh/TiO_2 vs $Rh\text{-}Mn\text{-}Li/TiO_2$ catalysts (reaction conditions: 260°C, 20 bar, 52,800scc/hr-gcat., $H_2/CO = 2/1$)

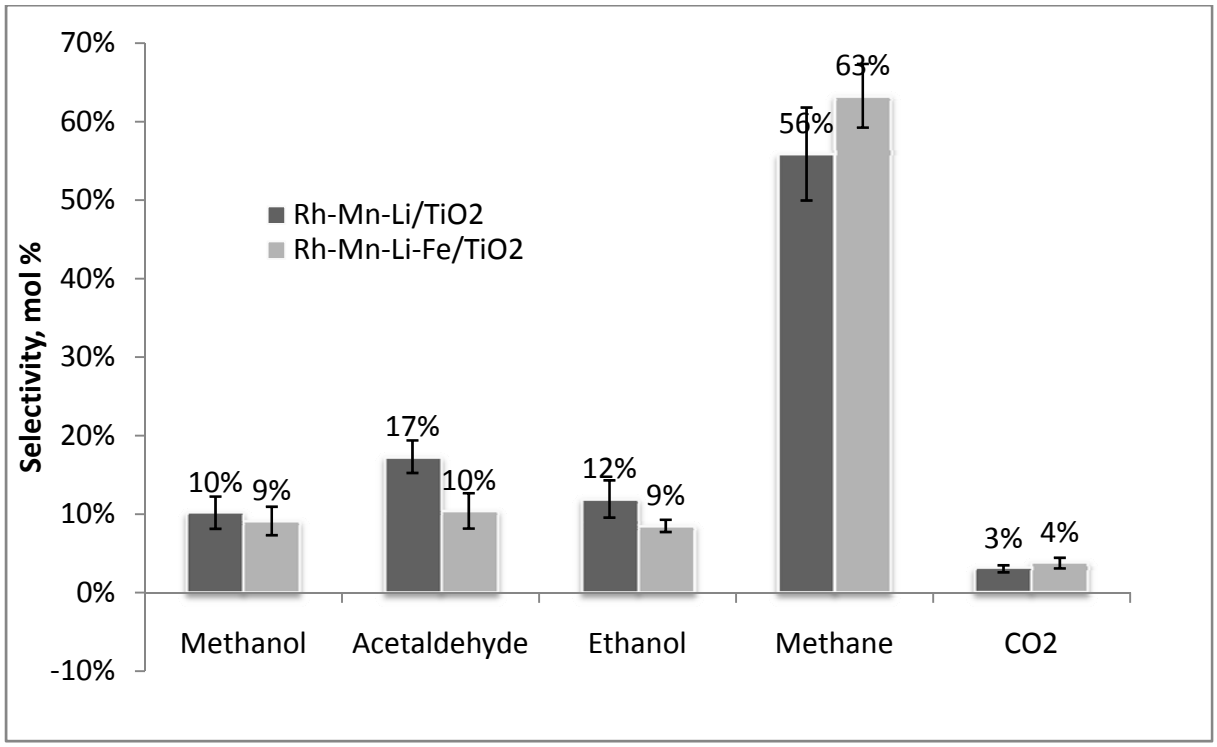

Figure 4.5: Products selectivity (mol %) for CO hydrogenation over $Rh\text{-}Mn\text{-}Li/TiO_2$ vs $Rh\text{-}Mn\text{-}Li\text{-}Fe/TiO_2$ catalysts (reaction conditions: 260°C, 20 bar, 52,800scc/hr-gcat., $H_2/CO = 2/1$)

With methane selectivity of 56% on Rh-Mn-Li/TiO_2 and 63% on Rh-Mn-Li-Fe/TiO_2, methanation activity remains essentially the same within the margin of error, although the EtOH/CH_4 ratio reduced from 0.21 to 0.14 on Rh-Mn-Li-Fe/TiO_2. These selectivity trends suggests a decrease in the CO insertion activity resulting in reduced C-C formation, coupled with increased hydrogenation, on Fe promotion. This leads to reduced C_2-oxygenates selectivity while C_1 (CH_4 and methanol) species showed higher (but not significant) selectivities for CO hydrogenation on Rh-Mn-Li-Fe/TiO_2.

The Fe promoted catalyst shows essentially the same CO conversion as Rh-Mn-Li/TiO_2 at the conditions used in this experiment although the turnover frequency for the Fe-promoted catalyst is higher because Table 4.1 shows that there are less amounts of Rh and promoters on Rh-Mn-Li-Fe/TiO_2 compared to the other catalysts tested. Therefore, a higher catalyst activity would be expected if the composition levels were comparable to those of others catalysts tested.

This is somewhat similar to the Yin et al. work on the influence of Fe promoter on Rh-Mn-Li/SiO_2 for CO hydrogenation (H_2/CO = 2/1, 320°C, 30 bar) in which they reported an increase in catalyst activity with Fe loading of 0.05% with reduction in ethanol selectivity[25]. At higher (than 0.05%) Fe content, they observed reduced catalyst activity, decreasing EtOH and acetaldehyde with increasing methane and methanol selectivities. Conversely, Burch and Hayes[22] reported increasing ethanol selectivity with Fe loading on Rh/Al_2O_3 for up to 10wt % Fe from CO hydrogenation (H_2/CO = 1/1, 270°C, 10 bar), which they calculated to be the amount required for complete monolayer coverage of the surface. What these show is that there is a limit beyond which an increase in Fe (or any metal promoter) promotion is no longer beneficial to either ethanol selectivity or catalyst activity. This amount is characteristic of support, Rh amount, reaction conditions and the presence/absence of other promoters among other factors.

In summary, promotion effects seem to be interplay between CO dissociation, CO insertion and the hydrogenation of surface intermediates. Overall Rh-Li/TiO_2 is the most active and the most selective for ethanol. An important parameter to measure is the ratio of the selectivity of EtOH to methane[33] – this ratio is also highest on Rh-Li/TiO_2. Among the catalyst tested here, it is only the promoted catalyst that produces more ethanol than acetaldehyde. The interaction between Rh and Li only seems to be weakened with the addition of other promoters.

4.3.3 CO TPD

Figure 4.6 shows the desorption profiles of CO (m/z = 28) from the CO-TPD experiment for the five catalysts. The single CO peak shows slight differences between the Mn promoted catalysts and those with no Mn. On Rh-Mn/TiO_2, Rh-Mn-Li/TiO_2 and Rh-Mn-Li-Fe/TiO_2, the CO peak emerged at the same temperature of 85°C; this is 7°C lower than the peaks on Rh/TiO_2 and Rh-Li/TiO_2 which emerged at 92°C.

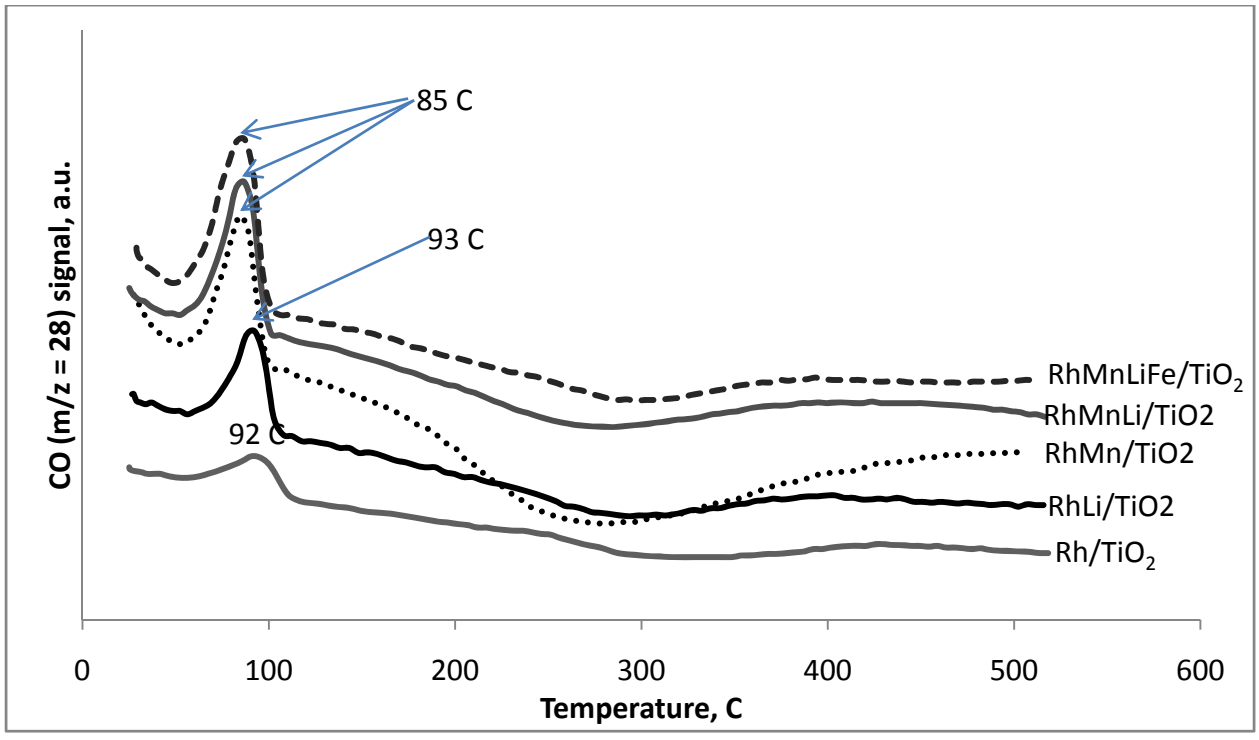

Figure 4.6: Desorption profiles of CO from CO TPD of various promoted Rh/TiO_2 catalysts, following continuous CO adsorption at room temperature.

This means that the CO adsorption is slightly weaker on the Mn-containing catalysts and that the addition of Li or Fe does not have much as effect on the strength of the Rh-CO bond. We do not know if the effect of Li and Fe on CO adsorption would become pronounced at higher loadings of these promoters. The weakening of the Rh-CO bond by Mn is consistent with the electron-withdrawing effect explained earlier which results in increase in the population of Rh^{+} species on the catalysts surface, these are thought to chemisorb CO less strongly that Rh^{0} sites[3]. The CO peak on Rh-Mn/TiO_2, Rh-Mn-Li/TiO_2 and Rh-Mn-Li-Fe/TiO_2 is bigger in size that the peak on either Rh/TiO_2 or Rh-Li/TiO_2. Two observations can be inferred: first, increased CO chemisorption because Mn provides more sites for CO adsorption and second, CO dissociation is less on the Mn-containing catalysts making most of the adsorbed CO desorb as associated CO species. The latter point is consistent with the effect of Mn on Rh/SiO_2, as previously reported, where Mn oxide weakened the adsorption of CO [3, 7]. Unpromoted Rh/TiO_2 gave the lowest CO peak area while Rh-Li/TiO_2 showed an intermediate CO desorption peak area suggesting that Li promotion, when in close contact with Rh, increases its dispersion leading to more sites for CO adsorption. The stronger the adsorption between CO and metal the more likely it is to be dissociated, suggesting that CO is less likely to dissociate on the Mn-containing catalysts than on those with no Mn because of the slightly lower CO peak temperature indicative of more weakly adsorbed CO.

There was no CO peak at higher temperatures on any of the catalysts consistent with the results of Ioannides and Verykios on Rh/TiO_2 [23] although at higher temperatures, a large CO_2 (Figure 4.7) peak was observed for all the five catalysts. It appears as if the Rh/TiO_2 catalysts in this work have more CO dissociation activity than that of Ioannides and Verykios leading to less CO molecules desorption. The CO_2 and H_2 desorption peaks from CO-TPD experiments as shown in Figure 4.7 is for the Rh-Mn-Li/TiO_2 catalyst. It is representative of all the catalysts

because the peaks are similar and are positioned at almost the same temperature. The small low temperature CO_2 peak at 85°C seems to be associated with the single CO peak and can be attributed to the reaction between dissociated CO species (Boudouard / disproportionation reaction):

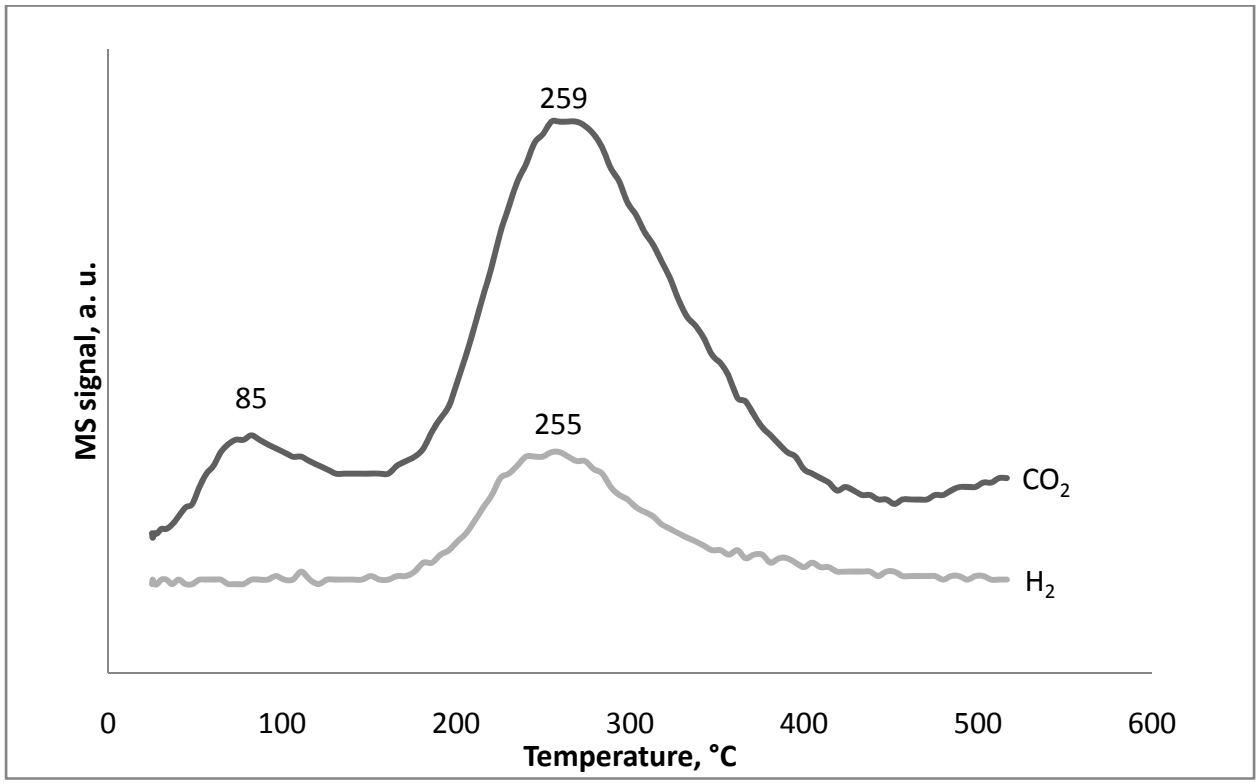

Figure 4.7: CO_2 and H_2 desorption from CO TPD of Rh-Mn-Li/TiO_2 catalyst, following continuous CO adsorption at room temperature

$$2CO_{(ad)} \rightarrow C_{(s)} + CO_2 \qquad (3)$$

while the bigger peak at ~260°C can be attributed to the reaction between CO and the surface hydroxyl species on the TiO_2 support. This is consistent with the fact that the 260°C peak on the CO_2 spectra is accompanied by a peak on the H_2 (mass 2) spectrum. CO_2 desorption and H_2 evolution from CO-TPD would suggest a reaction such as:

$$CO_{(ad)} + OH_{(s)} \rightarrow CO_2 + ½H_2 \qquad (4)$$

This reaction has been reported on Al_2O_3 and TiO_2 supported Rh catalysts and the CO_2 is said to originate from the interaction between hydroxyl groups and CO species strongly adsorbed to metallic surface as the latter travels through the particle upon desorption [23].

In summary, on all the catalysts here, the weakly adsorbed CO desorbs as CO while the strongly adsorbed CO forms CO_2.

4.3.4 TPR

The TPR profile of the catalysts is shown in Figure 4.8. All the catalysts show two reduction peaks except for Rh-Li/TiO_2 which shows a single Rh reduction peak. The low-temperature peak corresponds to the reduction of surface Rh oxide species and the smaller high-temperature peak for the reduction of bulk Rh species[25, 34]. The position of the low-temperature peak shifts slightly to higher temperatures in the order Rh/TiO_2 (55°C) < Rh-Mn-Li/TiO_2 (80°C), Rh-Mn/TiO_2 (83°C), Rh-Li/TiO_2 (85°C), < Rh-Mn-Li-Fe/TiO_2 (104°C). The shift in peak position with the addition Mn, Li and Fe promoters is indicative of decreased reducibility of Rh as a result of the interaction between Rh and the promoters on the surface. Such interactions can be in form on surface alloys, leading to shifts in reduction temperatures to an intermediate value between those of the components of the alloy.

Two peaks of Mn reduction at 317ºC and 403ºC has been observed from TPR results of 10% Mn/TiO_2 – these were assigned to the reduction of $MnO_2/Mn_2O_3 \rightarrow Mn_3O_4$ and of $Mn_3O_4 \rightarrow$ MnO respectively[35]. Same authors showed two peaks at slightly higher temperatures for 10% Mn/Al_2O_3 and 10% Mn/SiO_2, indicative of the same two-step reduction process[35]. When Mn was used as a promoter on Rh/SiO_2, the TPR peaks for both Rh and Mn have been shown emerge at intermediate temperatures between Rh and Mn reduction peaks on Rh/SiO_2 and Mn/SiO_2 respectively[25, 36]. We do not observe a distinct peak for Mn reduction probably because Mn content in our catalysts is small; the peaks associated with Mn reduction could be broadened

and might have been "swallowed" by the baseline. Mn is at best partly reduced to Mn^{2+} under reaction conditions and could not be reduced to the metallic state[25]. Li would generally not reduce at our temperature range of choice, i.e. below 500°C[25].

The high temperature (bulk Rh) peaks for Rh/TiO_2, $Rh\text{-}Mn/TiO_2$ and $Rh\text{-}Mn\text{-}Li\text{-}Fe/TiO_2$ are at 190°C, except for the Fe promoted catalysts, where it shifts to 250°C. The absence of any difference in the bulk Rh peak positions of Rh/TiO_2, $Rh\text{-}Mn/TiO_2$ and $Rh\text{-}Mn\text{-}Li\text{-}Fe/TiO_2$ means that Mn and Li promoters show negligible interaction with Rh in the bulk phase. It appears as if Fe inhibits bulk Rh reduction (or Rh makes Fe more reducible) because of the marked shift in both peak positions of $Rh\text{-}Mn\text{-}Li\text{-}Fe/TiO_2$. Fe has multiple oxidations between There are conflicting reports about the oxidation state of Fe in literature.

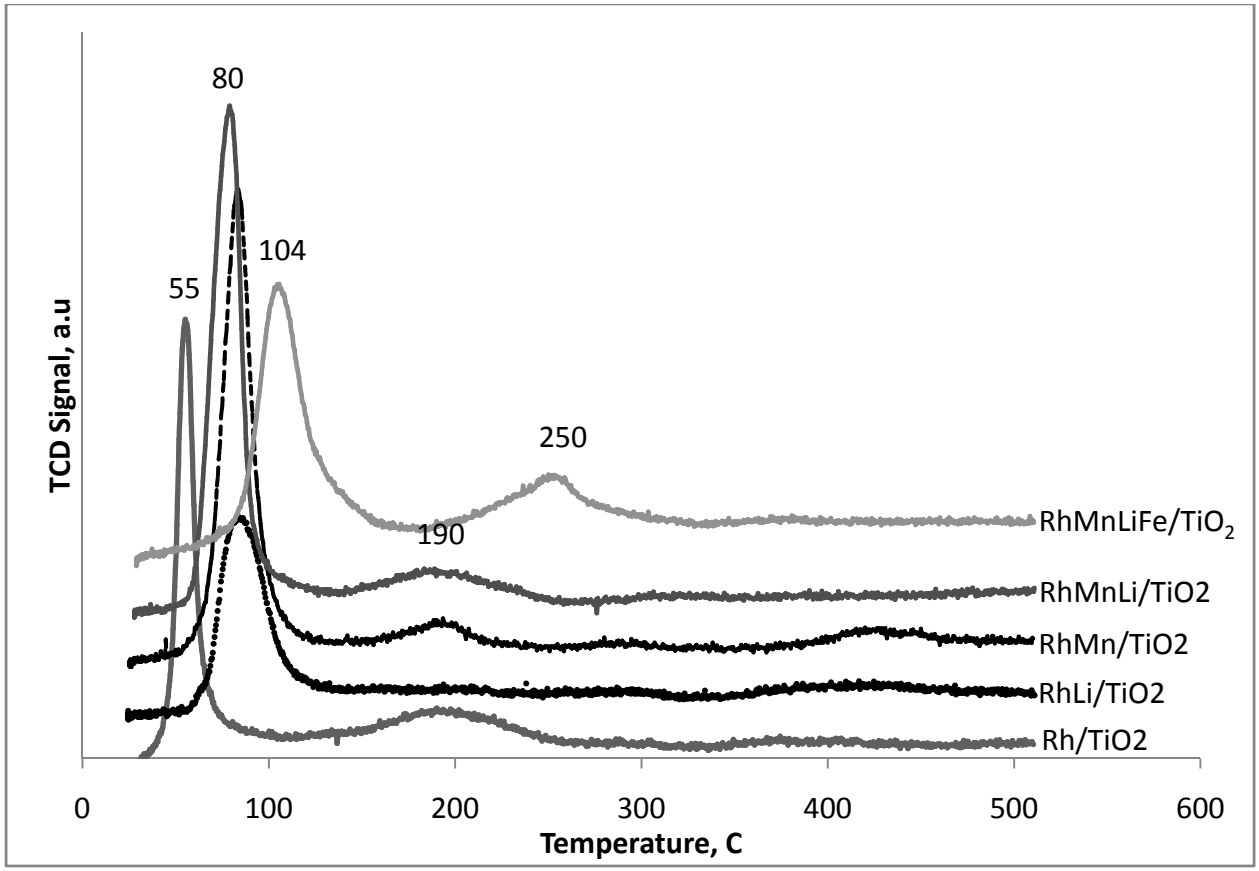

Figure 4.8: TPR profiles of the Rh/TiO, and promoted Rh/TiO, catalysts. TPR conditions: 5°C/min heating rate; room temperature to 500 °C; 10% H_2/Ar, 50 sccm; sample weight, 0.25 g-cat

The size of the first peak in comparison to the second peak can be used as an indication of how well dispersed the Rh atoms are. A larger low temperature peak indicates a well dispersed system while a larger high temperature peak suggests a poorly dispersed catalyst. Using Simpson's Rule, we calculated the area under the peaks of the TPR curves (Table 4.3).

Table 4.3. Area Counts of the TPR Peaks

	Area Counts (a.u.)				
	Rh	Rh-Li	Rh-Mn	Rh-Mn-Li	Rh-Mn-Li-Fe
Surface	220	215	375	410	301
Bulk	104	-	45	90	135
Total	324	215	420	500	436
Surface/Total	**0.7**	**1.0**	**0. 9**	**0.8**	**0.7**
CO Conv, mol %	0.8	2	1.4	0.6	0.6

The ratio of the surface Rh to total Rh can be used as rough estimate of the dispersion assuming that all the peaks are attributed to Rh. Rh-Li/TiO_2 shows no second peak suggesting few or no bulk Rh species, it could therefore be the most well dispersed catalyst tested here. Rh-Li/TiO_2 has a ratio of 0.98, which is higher than the unpromoted catalyst. This dispersion estimate seems to be proportional to CO conversion from the CO hydrogenation experiments at 260°C presented in Table 4.2 where Rh-Li/TiO_2 gave the highest conversion followed by Rh-Mn/TiO_2.

We recognize that CO chemisorption could be used for dispersion calculations, but with different promoters on our catalyst and the various adsorption modes of CO on Rh based catalysts, it is complicated to arrive at a suitable Rh:CO adsorption ratio and also to deconvolute how much has Rh contributed to CO chemisorption on the promoted catalysts.

4.3.5 TPO

Figure 4.9 shows the TPO profile of the catalysts. All the catalysts have a common large peak of CO_2 desorption. However some yield a much smaller shoulder peak adjoining the main

peak at about ~350 C. It also shows a major difference between the Mn promoted catalysts and those with no Mn because the three Mn promoted catalyst have a single peak for carbon oxidation to CO_2. We observe the shoulder peak on the TPO profiles of Rh/TiO_2 and $Rh\text{-}Li/TiO_2$ but not on $Rh\text{-}Mn/TiO_2$, $Rh\text{-}Mn\text{-}Li/TiO_2$ and $Rh\text{-}Mn\text{-}Li\text{-}Fe/TiO_2$, which only have single-peak profiles.

Mn has been reported to suppress the formation some more thermally-stable adsorbed CO species[4], so the second peak observed on Rh/TiO_2 or $Rh\text{-}Li/TiO_2$ might be due to carbon species related to that form of adsorbed CO. Another possible reason is that Mn, with its ability to reduce CO dissociation by weakening CO adsorption has shifted the second peak of the Mn-containing catalysts to a lower temperature, falling under this low temperature peak. This is consistent with the results of the CO-TPD suggesting the weakening effect of Mn on CO adsorption.

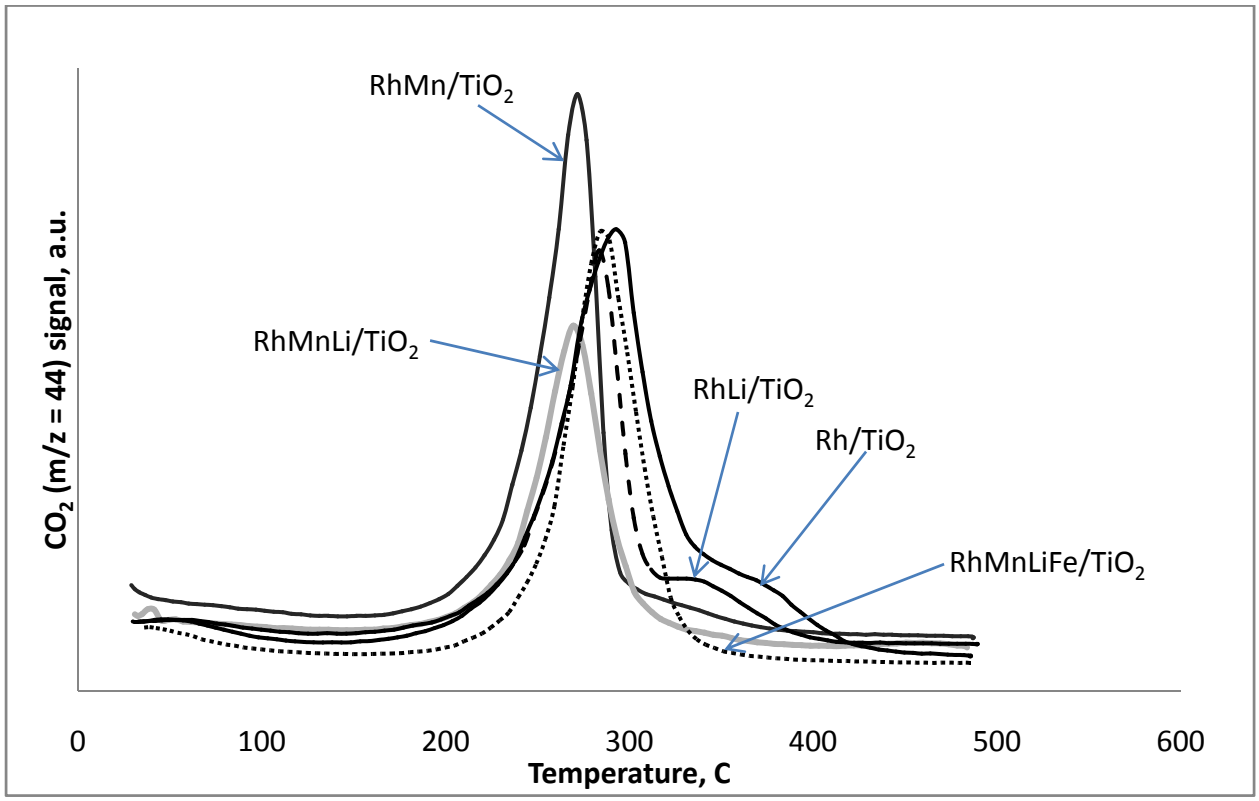

Figure 4.9: TPO profile of Rh/TiO_2 and promoted Rh/TiO_2 catalysts, following CO hydrogenation reaction

4.4 CONCLUSIONS

Below is what we concluded from these experiments:

1. Li enhances the dispersion of Rh, reducing the formation of large Rh atom ensembles on the surface that is required for the CO dissociation. This reduces the carbon coverage on the surface, increasing H_2 chemisorption on the surface leading to improved activity and selectivity to ethanol when compared to the unpromoted catalysts.
2. Mn promotion results in the weakening of the Rh-CO bond, leading to reduced carbon and more H_2 surface coverage. However, hydrogenation of surface intermediates to ethanol is limited.
3. Although, Mn and Li individually increased catalyst activity, loss of activity is observed when both promoters are combined. CO insertion is further improved but the hydrogenation ability of Rh-Li-Mn/TiO_2 is limited: the highest oxygenate selectivity of 38% (@260°C) and lowest methane formation was observed but with reduced catalyst activity.
4. Fe addition to Rh-Li-Mn/TiO_2 increases its hydrogenation activity – increasing methane selectivity versus C_2 oxygenates.

4.5 REFERENCES

1. H. Arakawa, T. Fukushima, M. Ichikawa, S. Natsushita, K. Takeuchi, T. Matsuzaki and Y. Sugi, *Chemistry Letters*, 1985, 881-884.
2. J. J. Spivey and A. A. Egbebi, *Chemical Society Reviews*, 2007, **36**, 1514-1528.
3. F. G. A. van den Berg, J. H. E. Glezer and W. M. H. Sachtler, *Journal of Catalysis*, 1985, **93**, 340-352.
4. K. P. De Jong, J. H. E. Glezer, H. P. C. E. Kuipers, A. Knoester and C. A. Emeis, *Journal of Catalysis*, 1990, **124**, 520-529.
5. M. Ojeda, M. L. Granados, S. Rojas, P. Terreros, F. J. Garcia-Garcia and J. L. G. Fierro, *Applied Catalysis a-General*, 2004, **261**, 47-55.

6. M. Ichikawa and T. Fukushima, *Journal of Physical Chemistry*, 1985, **89**, 1564-1567.

7. A. S. Lisitsyn, S. A. Stevenson and H. Knozinger, *Journal of Molecular Catalysis*, 1990, **63**, 201-211.

8. H. Kato, M. Nakashima, Y. Mori, T. Mori, T. Hattori and Y. Murakami, *Research on Chemical Intermediates*, 1995, **21**, 115-126.

9. S. C. Chuang, J. G. Goodwin and I. Wender, *Journal of Catalysis*, 1985, **95**, 435-446.

10. S. S. C. Chuang, R. W. Stevens and R. Khatri, *Topics in Catalysis*, 2005, **32**, 225-232.

11. H. Kusama, K. Okabe, K. Sayama and H. Arakawa, *Catalysis Today*, 1996, **28**, 261-266.

12. S. C. Chuang, J. G. Goodwin and I. Wender, *Journal of Catalysis*, 1985, **92**, 416-421.

13. H. Orita, S. Naito and K. Tamaru, *Chemistry Letters*, 1983, 1161-1164.

14. R. Burch and M. I. Petch, *Applied Catalysis a-General*, 1992, **88**, 39-60.

15. B. J. Kip, E. G. F. Hermans and R. Prins, *Applied Catalysis*, 1987, **35**, 141-152.

16. H. Y. Luo, W. Zhang, H. W. Zhou, S. Y. Huang, P. Z. Lin, Y. J. Ding and L. W. Lin, *Applied Catalysis a-General*, 2001, **214**, 161-166.

17. M. Ichikawa and T. Fukushima, *Journal of the Chemical Society-Chemical Communications*, 1985, 321-323.

18. H. M. Yin, Y. J. Ding, H. Y. Luo, D. P. He, W. M. Chen, Z. Y. Ao and L. W. Lin, *Journal of Natural Gas Chemistry*, 2003, **12**, 233-236.

19. M. P. Cabero, M. J. Holgado and V. Rives, *Materials Chemistry and Physics*, 1991, **27**, 181-188.

20. U. Usman, M. Takaki, T. Kubota and Y. Okamoto, *Applied Catalysis a-General*, 2005, **286**, 148-154.

21. I. E. Wachs, G. Deo, M. A. Vuurman, H. C. Hu, D. S. Kim and J. M. Jehng, *Journal of Molecular Catalysis*, 1993, **82**, 443-455.

22. R. Burch and M. J. Hayes, *Journal of Catalysis*, 1997, **165**, 249-261.

23. T. Ioannides and X. Verykios, *Journal of Catalysis*, 1993, **140**, 353-369.

24. H. M. Yin, Y. J. Ding, H. Y. Luo, W. M. Chen and L. W. Lin, in *Natural Gas Conversion Vii*, Editon edn., 2004, vol. 147, pp. 421-426.

25. H. M. Yin, Y. J. Ding, H. Y. Luo, H. J. Zhu, D. P. He, J. M. Xiong and L. W. Lin, *Applied Catalysis a-General*, 2003, **243**, 155-164.

26. K. K. Bando, K. Soga, K. Kunimori and H. Arakawa, *Applied Catalysis a-General*, 1998, **175**, 67-81.

27. D. G. Castner, R. L. Blackadar and G. A. Somorjai, *Journal of Catalysis*, 1980, **66**, 257-266.

28. P. R. Watson and G. A. Somorjai, *Journal of Catalysis*, 1982, **74**, 282-295.

29. D. H. Jiang, Y. J. Ding, Z. D. Pan, W. M. Chen and H. Y. Luo, *Catalysis Letters*, 2008, **121**, 241-246.

30. Y. Wang, Z. Song, D. Ma, H. Luo, D. Liang and X. Bao, *Journal of Molecular Catalysis A: Chemical*, 1999, **149**, 51-61.

31. R. Burch and M. I. Petch, *Applied Catalysis a-General*, 1992, **88**, 77-99.

32. R. Burch and M. I. Petch, *Applied Catalysis A: General*, 1992, **88**, 61-76.

33. A. Egbebi and J. J. Spivey, *Catalysis Communications*, 2008, **9**, 2308–2311.

34. C. Wong and R. W. McCabe, *Journal of Catalysis*, 1987, **107**, 535-547.

35. J. Hu, W. Chu and L. Shi, *Journal of Natural Gas Chemistry*, 2008, **17**, 159-164.

36. H.-Y. Luo, P.-Z. Lin, S.-B. Xie, H.-W. Zhou, C.-H. Xu, S.-Y. Huang, L.-W. Lin, D.-B. Liang, P.-L. Yin and Q. Xin, *Journal of Molecular Catalysis A: Chemical*, 1997, **122**, 115-123.

CHAPTER 5 : EFFECT OF CO_2 ON CO HYDROGENATION TO ETHANOL OVER PROMOTED Rh/TiO_2 CATALYSTS

5.1 INTRODUCTION

When biomass or coal is gasified, the resultant synthesis gas (syngas) contains considerable amounts of CO_2 in addition to CO and H_2 and steam. Ethanol, which can be used either as an energy carrier or a fuel additive, is a high value product that can be derived from such syngas[1].

Rhodium-based catalysts have been found to be active and selective for the formation of C_2 oxygenates from the hydrogenation of CO[2]. Their activity and selectivity for ethanol can be modified by a careful choice of promoters and support. Some Rh-based catalysts have also been tested for CO_2 hydrogenation to ethanol, which is thought to proceed through a CO intermediate[3, 4], so catalysts that have been found suitable for CO hydrogenation may in fact give comparable results for the hydrogenation of CO/CO_2 mixture. Most available relevant literature has focused on the hydrogenation of either CO or CO_2, rather than mixtures of the two[5-11].

We are aware of no literature in which realistic levels of CO, CO_2, H_2 and H_2O as contained in a biomass-derived syngas were studied for ethanol synthesis on Rh-based catalysts. Previous work done on hydrogenation of CO/CO_2 mixtures focuses on the effect of including small concentrations of CO_2 in CO hydrogenation experiments. Yields of methanol and ethanol have been reported to increase when a portion of CO in the feed was replaced with low levels of CO_2 during CO hydrogenation[12] and when small amounts of CO are added to the feed during CO_2 hydrogenation[13]. Increasing concentrations of CO_2 resulted in a maximum increase alcohol yield at about 5 - 10% CO_2 on 1% $Rh\text{-}Mo/ZrO_2$[12]. The authors attribute this to the r-WGS reaction, which presumably produces additional CO that is converted to the alcohols. However,

methane yield increased continuously over the range of CO_2 concentrations studied. The decline in alcohol yield at higher levels of CO_2 is attributed to strong adsorption of CO_2 on sites that form the alcohols, with the reaction then shifted toward methanation at higher concentrations of CO_2[12]. An alternative explanation is that CO_2 reacts more readily to form methane than CO over the entire range of CO_2 concentrations, causing the monotonic increase in methane yield with CO_2 content. Stronger adsorption and surface coverage of CO compared to CO_2 is said to be the reason for the difference in hydrogenation activities of CO and CO_2[14].

Here we examine the differences in the activity and product selectivity profiles of Rh/TiO_2, $Rh\text{-}Mn/TiO_2$, $Rh\text{-}Li/TiO_2$. $Rh\text{-}Mn\text{-}Li/TiO_2$ and $Rh\text{-}Mn\text{-}Li\text{-}Fe/TiO_2$ catalysts for hydrogenation of CO and of CO/CO_2 mixtures. The H/C ratio was kept at 2/1 for both set of experiments (i.e. $H_2/CO = H_2/(CO+CO_2) = 2/1$). This not only tests the effect of CO_2 on product selectivity, but also serves as a comparison between product distribution of conventional syngas (with little or no CO_2 content) and a representative biomass/coal-derived syngas which has much higher CO_2 content.

5.2 EXPERIMENTAL

CO Hydrogenation. Reaction tests at differential conversions were carried out in a ¼" glass-lined stainless steel fixed bed *Altamira 200R-HP* micro-reactor system at a total pressure of 20 bar. Prior to reaction tests the catalyst was reduced in-situ for 2 h in 75% H_2/25% He mixture. CO hydrogenation ($H_2/CO = 2/1$) reactions were run at GHSVs of 52800 scc hr^{-1} $gcat^{-1}$. For each run the syngas feed was diluted with He to reduce heat effects within the bed and to ensure that the conversion is low enough to keep the oxygenated products in vapor state for online GC/MS analysis. The total flow rate of the feed gas was maintained at 220 scc/min. The sum of the flow rates of H_2 + CO was 120 scc/min, with a constant flow rate of 100 scc/min He. Data were collected at furnace temperatures of 260°C and 270°C; reactions were allowed to run for at least

1.5 h at each temperature level to attain steady state before samples are injected into the GC for analysis.

Hydrogenation of CO + CO_2. These experiments were carried out after an oxidation/ reduction regeneration of the catalysts used in the CO hydrogenation experiments. Regeneration involves an oxidation step at 450°C in 10% O_2/He to remove surface carbon was followed by a reduction in diluted 75% H_2 /25% He gas stream at 350°C. The reaction conditions were exactly as for CO hydrogenation except the equimolar substitution of half of feed CO with CO_2 resulting in reactant feed rate of 80, 20 and 20 sccm/min for H_2, CO and CO_2 respectively. As before, the total flow rate of the feed gas was maintained at 220 scc/min, including a constant flow rate of 100 scc/min He. These flow rates ensured that the GSHV (52800 $scchr^{-1}gcat^{-1}$) and H/C ratio [$H_2/(CO+CO_2) = 2$] remains the same as in the previous CO hydrogenation in order to compare the results directly . Data were collected at furnace temperatures of 260°C and 270°C; reactions were allowed to run for at least 1.5 h at each temperature level to attain steady state before samples are injected into the GC.

5.3 RESULTS AND DISCUSSION

The composition of the synthesized catalysts measured by ICP-OES* is shown in previous chapter in Table 4.1.

Table 5.1 shows the selectivity of products for CO hydrogenation and the hydrogenation of CO/CO_2 mix at 260°C on Rh/TiO_2, $Rh-Mn/TiO_2$, $Rh-Li/TiO_2$. $Rh-Mn-Li/TiO_2$ and $Rh-Mn-Li-Fe/TiO_2$ catalysts. In general, the major products formed are methane, acetaldehyde, ethanol and methanol with trace amounts of n-propanol, n-butanol and ethane. The selectivity and activity of each catalyst is affected by the addition of CO_2 to the feed, the nature of such effects varies with the type of promoter used.

Table 5.1: Products Selectivity (mol %) for CO and CO/CO_2 Hydrogenation over Promoted and Unpromoted Rh/TiO_2 Catalysts (reaction conditions: 260°C, 20 bar, 52,800scc/hr-gcat., $H_2/[CO+CO_2] = 2/1$)

	Rh/ TiO_2		Rh-Li/ TiO_2		Rh-Mn/ TiO_2		Rh-Mn-Li/ TiO_2		Rh-Mn-Li-Fe/TiO_2	
	$CO+H_2$	**$(CO/CO_2)+H_2$**	**$CO+H_2$**	**$(CO/CO_2)+H_2$**	**$CO+H_2$**	**$(CO/CO_2)+H_2$**	**$CO+H_2$**	**$(CO/CO_2)+H_2$**	**$CO+H_2$**	**$(CO/CO_2)+H_2$**
methanol	8.3	6.9	5.0	3.2	4.4	4.0	10	5.6	9.1	8.7
acetaldehyde	5.1	3.8	10	5.5	12	5.3	17	10	10	5.7
ethanol	7.2	6.8	16	10	9.0	7.0	12	10	8.5	13
methane	71	80	62	78	69	81	56	72	63	69
CO_2	3.0	-	3.3	-	2.5	-	3.0	-	3.8	-
Total Oxy.	21	18	33	20	26	17	41	27	29	28
EtOH /Tot. Oxy	0.33	0.37	0.48	0.52	0.34	0.41	0.29	0.39	0.30	0.47
EtOH /CH_4	0.10	0.09	0.25	0.13	0.13	0.09	0.21	0.14	0.13	0.19
Conversion, *% C atom*	**0.8**	**1.0**	**2.0**	**2.4**	**1.4**	**2.2**	**0.6**	**0.7**	**0.6**	**0.7**

5.3.1 Rh/TiO_2: Effects of CO_2 on CO Hydrogenation

The selectivity to the major oxygenates (methanol, acetaldehyde and ethanol) decreased while methanation activity is increased on both catalysts when CO_2 is present in the reactant gas. For hydrogenation of CO only, unpromoted Rh/TiO_2 gave methane selectivity (71%). Upon adding CO_2, methane selectivity increased to 80% (although within the same margin of error) while oxygenates (methanol, ethanol and acetaldehyde) selectivities of methanol, ethanol and acetaldehyde remained fairly the same. The increase in methane selectivity is not unexpected because CO_2 has been reported to be more easily hydrogenated than CO to methane on Rh-based catalysts[3, 15, 16] – higher methanation activity from CO_2 hydrogenation has been shown on Rh/SiO_2[17] and Rh/Al_2O_3[18, 19]. The main differences have been in terms of higher methane selectivity, lower activation energy and higher methane formation rate for CO_2 hydrogenation than CO hydrogenation[17], so it is expected the partial substitution of CO with CO_2 in the feed would result in increased methane (or hydrocarbon) selectivity.

It appears that CO is an intermediate in the hydrogenation of CO_2 to products but the nature of CO obtained at the surface during CO_2 hydrogenation is different from adsorbed CO species during CO hydrogenation. Although CO_2 adsorbs sparingly on supported Rh catalysts, its chemisorption has been reported to be substantially enhanced in the presence of hydrogen (when either pre-adsorbed or co-adsorbed) on Rh/Al_2O_3 [19, 20] which would suggest the reaction:

(1)

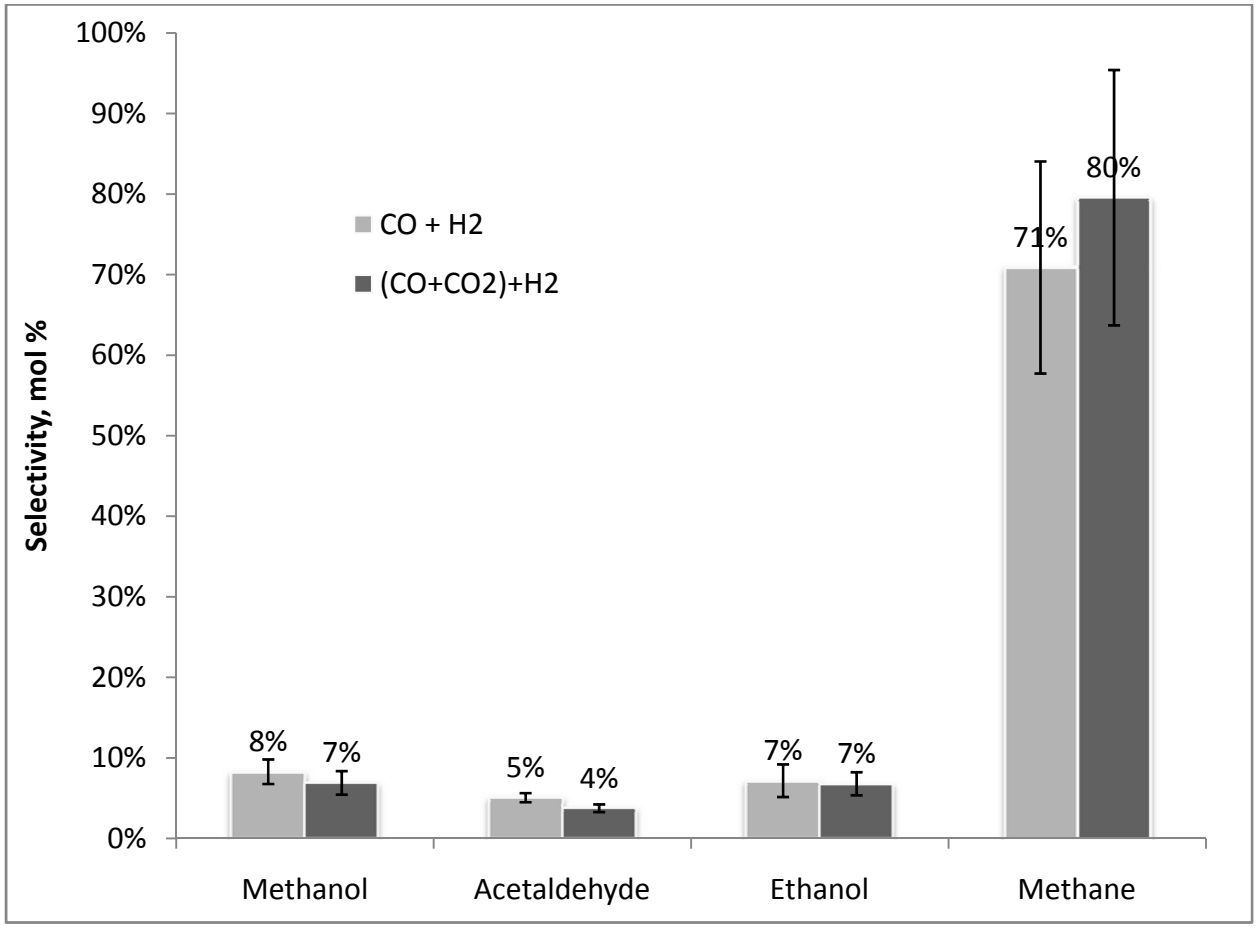

Figure 5.1: Products selectivity (mol %) for CO and CO/CO_2 hydrogenation over Rh/TiO_2 catalyst (reaction conditions: 260°C, 20 bar, 52,800scc/hr-gcat., $H_2/[CO+CO_2]$ = 2/1)

Reaction (1) is simply the reverse water-gas shift (r-WGS) reaction and it is thought to proceed through a formate intermediate on alumina-supported Rh[20]. This reaction shows that CO_2 hydrogenation proceeds via CO hydrogenation, with both having adsorbed CO as

intermediate[17]. Both CO and CO_2 hydrogenation reactions then proceed via CO dissociation and hydrogenation to methane. The exact route of CO dissociation is a subject of discussion in literature. One view holds that CO dissociation is hydrogen-assisted, which involves a carbonylhydride intermediate, formed when excess surface hydrogen suppresses the formation of di-carbonyl, Rh-$(CO)_2$, leading to Rh with CO and one or two hydrogen atoms bonded as shown below:

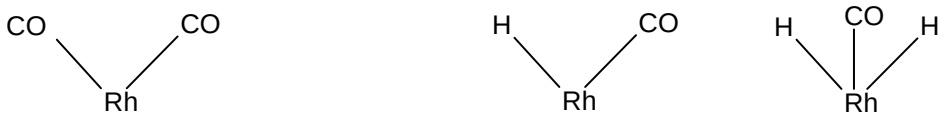

di-carbonyl carbonylhydride

The hydrogen(s) on the carbonylhydride intermediate is (are) electron-donating, thereby strengthening the Rh-C bond leading to a weakened C-O bond and an easier CO dissociation than via the alternative route where hydrogen is not involved in the CO dissociation[19, 20]. CO hydrogenation proceeds via the non-hydrogen assisted path to CO dissociation because the CO adsorbs in the di-carbonyl form, preventing the carbonylhydride formation. This might explain why CO_2 hydrogenation forms methane more easily than CO hydrogenation.

Conversely, tests on Rh/SiO_2 revealed that the mechanisms for CO_2 hydrogenation is not hydrogen-assisted but involves the dissociative adsorption of CO_2 on Rh[17]:

$$CO_{2(g)} \rightleftarrows CO_{2(a)} \rightleftarrows CO_{(a)} + O_{(a)} \qquad (2)$$

Reports have also shown that adsorbed formate species ($HCOO^-$) were observed on Rh supported on Al_2O_3, TiO_2 and MgO supports but not on Rh/SiO_2 when formic acid was decomposed on Rh dispersed on these various supports[21, 22]. The presence/absence of formate species may therefore determine or at least be an indication of the route of CO_2 adsorption i.e. whether it is via the hydrogen assisted route (reaction 1) or dissociative adsorption (reaction 2).

5.3.2 Rh-Mn/TiO_2: Effects of CO_2 on CO Hydrogenation

The effect of co-feeding CO_2 during CO hydrogenation on Rh-Mn/TiO_2 is essentially the same as on the unpromoted Rh/TiO_2: reduced oxygenate selectivity and more methane formation than the hydrogenation of CO only. Fig. 5.2 shows that methane selectivity increased from 69 to 81% while ethanol decreased from 9.0% to 7.0%, resulting in a decrease of the EtOH/CH_4 ratio from 0.13 to 0.09. Acetaldehyde selectivity decreased from 12% to 5.3% while methanol remains at 4.0%.

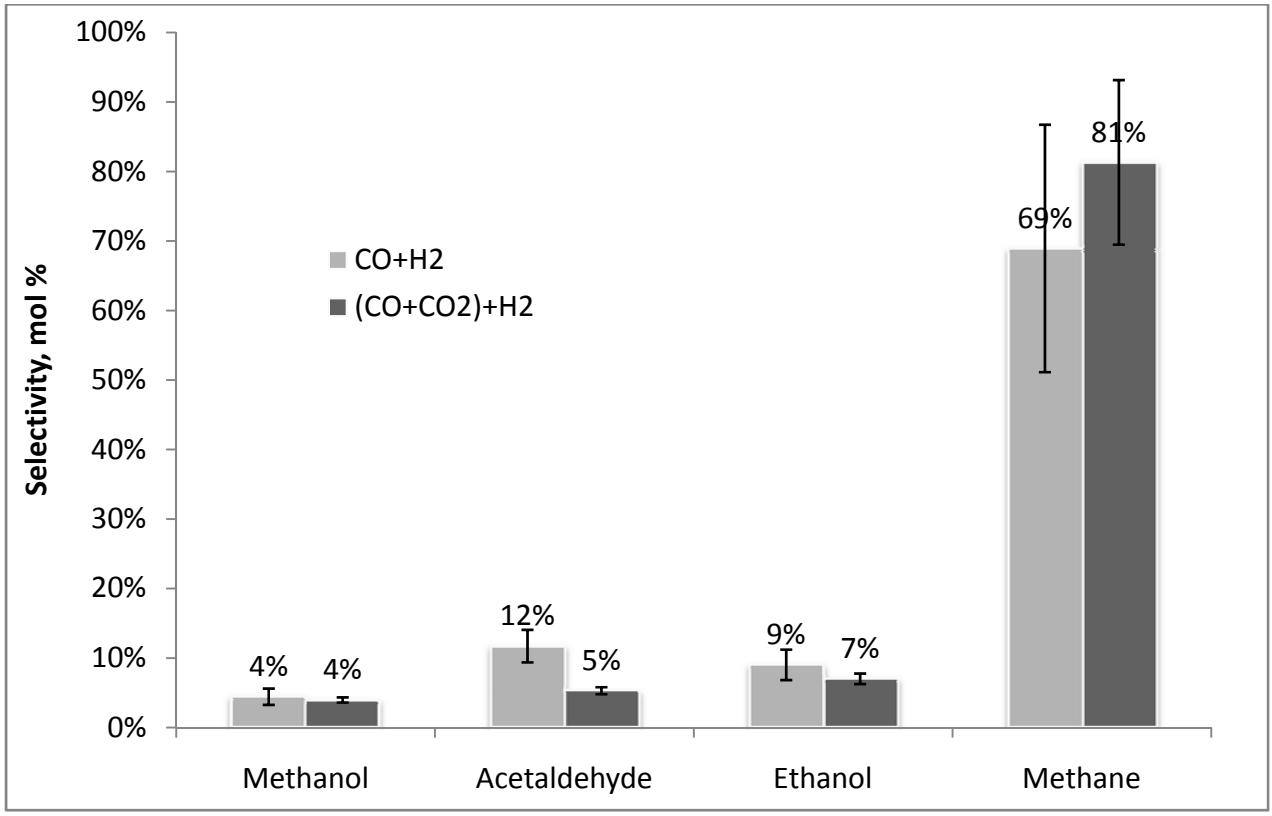

Figure 5.2: Products selectivity (mol %) for CO and CO/CO_2 hydrogenation over Rh-Mn/TiO_2 catalysts (reaction conditions: 260°C, 20 bar, 52,800scc/hr-gcat., H_2/[CO+CO_2] = 2/1)

5.3.3 Rh-Li/TiO_2: Effects of CO_2 on CO Hydrogenation

Replacing half of the CO in feed with CO_2 has a qualitatively similar effect on product selectivity as the unpromoted catalyst; Li promotion seems to have magnified the effects of CO_2

on CO hydrogenation. Methane selectivity increases from 62% to 78% (Fig. 5.3) while ethanol selectivity decreases from 16% to 10% and the $EtOH/CH_4$ ratio decreases from 0.25 to 0.13. With Li promotion, CO_2 co-feeding inhibits ethanol formation and enhances methane formation. Selectivity to other oxygenates decreases as well – methanol from 5.0% to 3.2% and acetaldehyde from 10.0% to 5.5%. The effect of of CO_2 addition in the feed on Rh-Li/TiO_2 seems to be more pronounced than on the unpromoted Rh/TiO_2.

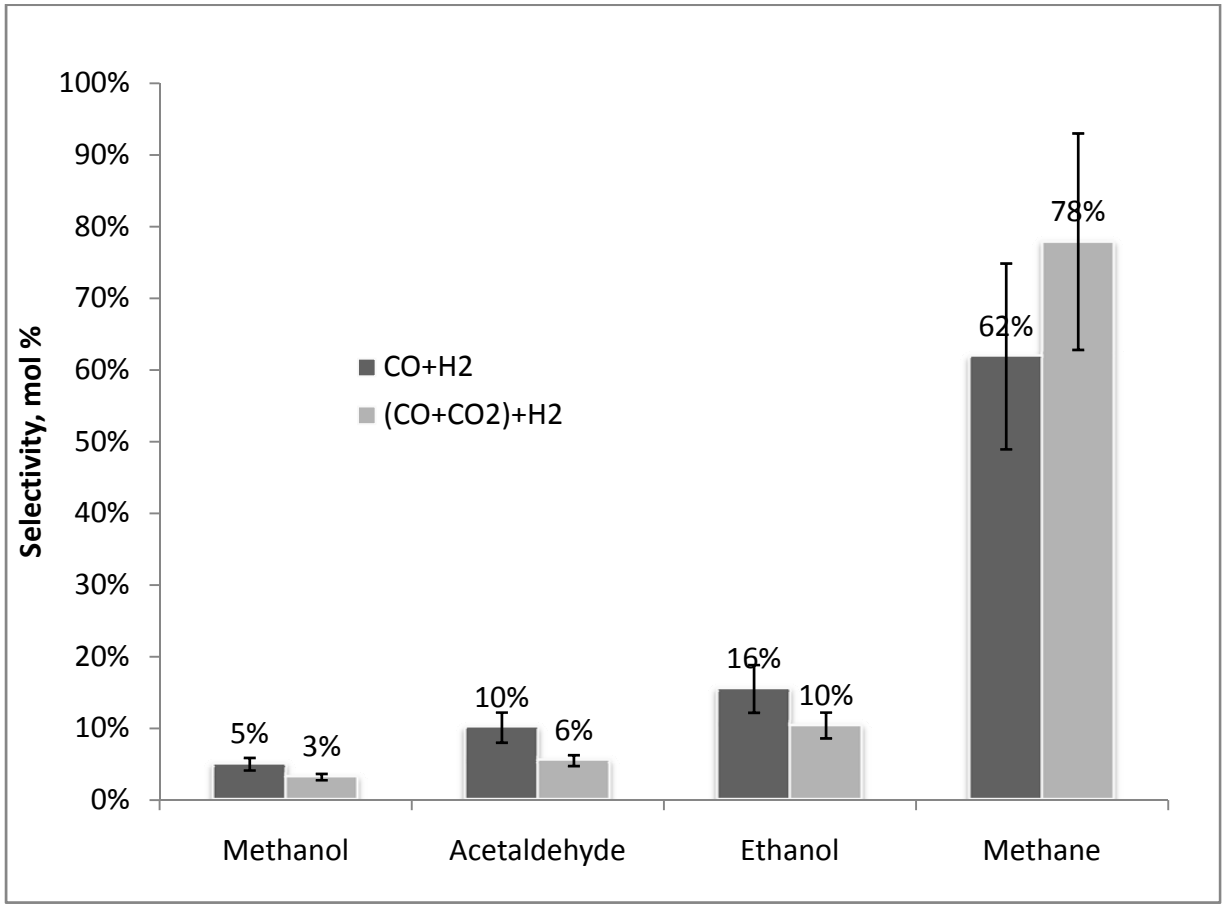

Figure 5.3: Product selectivity (mol %) for hydrogenation of CO_2 and CO/CO_2 over Rh-Li/TiO_2 catalyst (reaction conditions: 260°C, 20 bar, 52,800scc/hr-gcat., $H_2/(CO+CO_2)$ = 2/1)

5.3.4 Rh-Mn-Li/TiO_2: Effects of CO_2 on CO Hydrogenation

Increased methanation accompanied by decreased alcohols and oxygenates is the resultant effect of co-feeding CO with CO_2 on Rh-Mn-Li/TiO_2. Methane selectivity increases by

from 56% to 72%, while methanol decreases from 10% to 5.6% and acetaldehyde from 17% to 10% (Fig. 5.4). EtOH/CH_4 ratio decreases from 0.21 to 0.14 though the slight decrease in ethanol selectivity from 12% to 10% is within the margin of error.

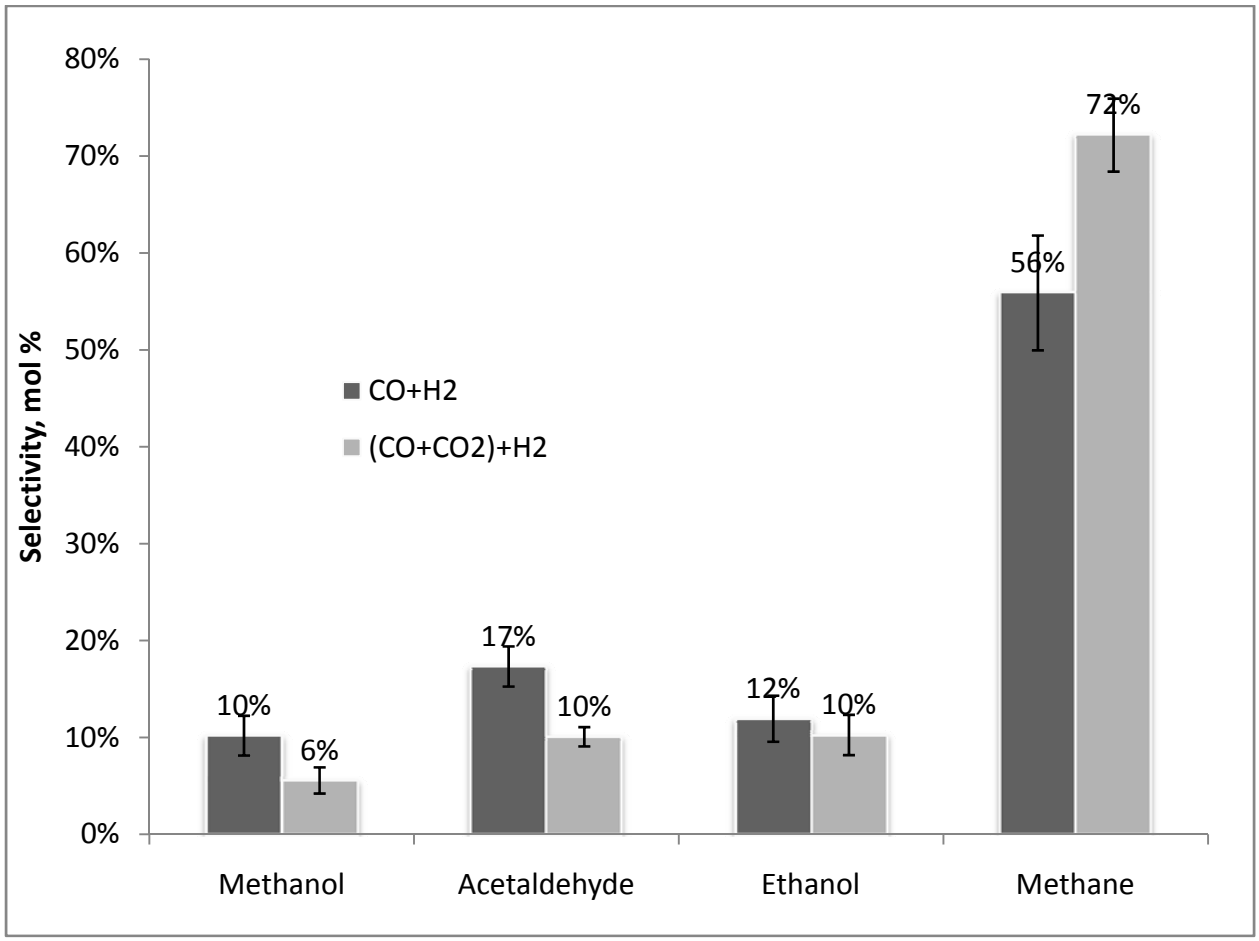

Figure 5.4: Product selectivity (mol %) for hydrogenation of CO_2 and CO/CO_2 over Rh-Mn-Li/TiO_2 catalyst (reaction conditions: 260°C, 20 bar, 52,800scc/hr-gcat., $H_2/(CO+CO_2)$ = 2/1)

5.3.5 Rh-Mn-Li-Fe/TiO_2: Effects of CO_2 on CO Hydrogenation

Rh-Mn-Li-Fe/TiO_2 gave a somewhat different response to the addition of CO_2 as feed to the CO hydrogenation reaction. Its methanol selectivity remains the same at 9.0% while acetaldehyde selectivity decreases (from 10% to 5%) upon CO_2 addition, along with increases in methane selectivity from 66% to 73% (Fig. 5.5). However, ethanol forming activity on this catalyst is higher for the hydrogenation of CO/CO_2 mixture than for only CO hydrogenation as

evident in ethanol selectivity increase from 8.5% to 13%. This results to a slight increase in $EtOH/CH_4$ ratio from 0.13 to 0.19.

This increase in ethanol selectivity upon CO_2 addition to feed is not expected because hydrogenation of only CO_2 on the same catalyst shows only trace amounts of ethanol (0.5% selectivity). This increase might be associated with the higher WGS/rWGS activity of the Fe-containing catalyst, which leads to the production of more CO adspecies for the ethanol forming reaction. Liu et al[24] recently reported that co-feeding CO_2 in Fischer-Tropsch synthesis over Fe-Mn catalyst (593 K, 1.5MPa) increases the formation rates of alcohols, ketones and aldehydes while methane (and hydrocarbon) selectivity remained fairly constant.

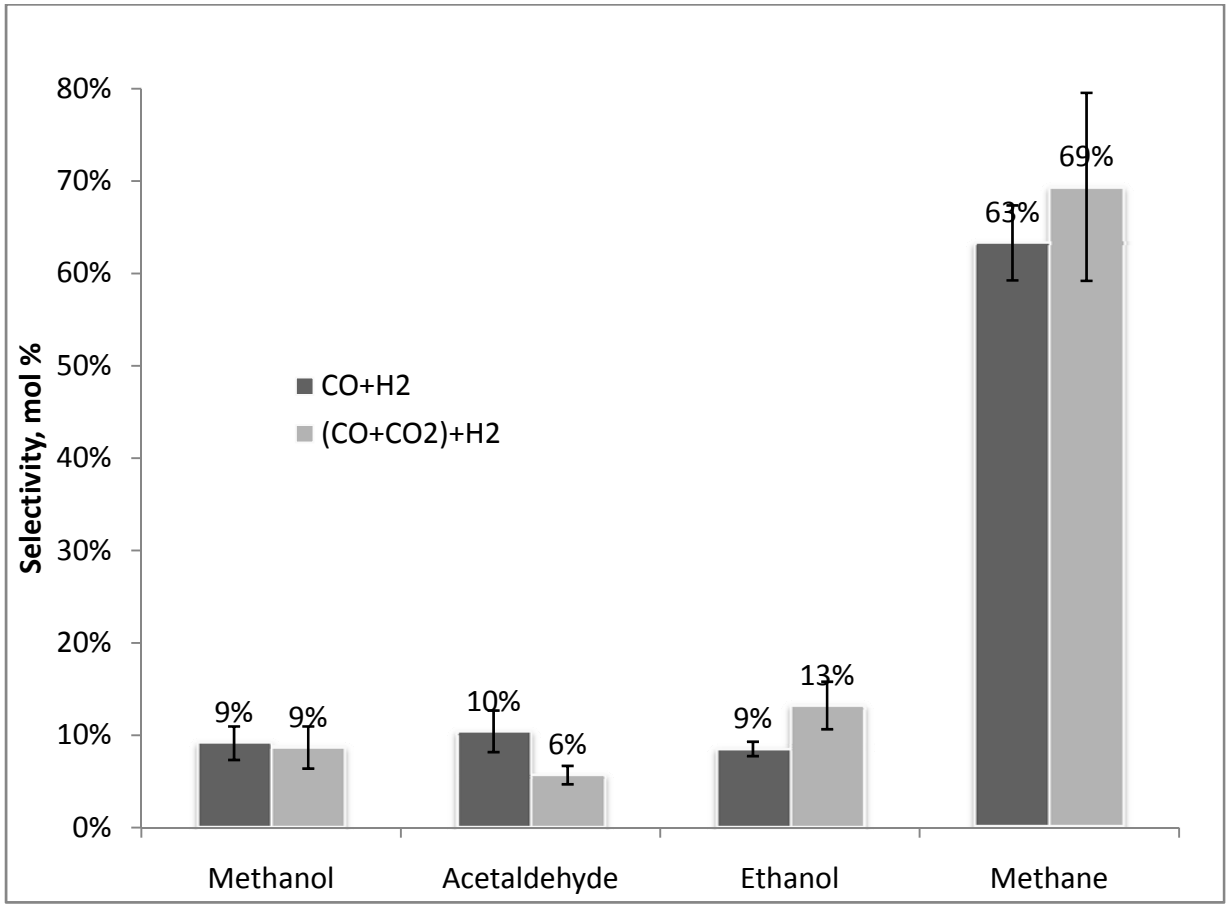

Figure 5.5: Product selectivity (mol %) for hydrogenation of CO_2 and CO/CO_2 over Rh-Mn-Li-Fe/TiO_2 catalyst (reaction conditions: 260°C, 20 bar, 52,800scc/hr-gcat., $H_2/(CO+CO_2)$ = 2/1)

They speculated that this is due to increased reverse WGS reaction upon CO_2 addition resulting in increased CO and decreased H species on the surface, hence increased CO insertion. However they did not specify the individual components of the product mix. Supported Fe catalysts have been shown to have lower WGS activity than bulk Fe, which are more frequently employed industrially in Fischer-Tropsch synthesis and WGS reactions[25, 26], because of a less efficient WGS mechanism[27]. Therefore the difference in WGS activity between our catalysts is therefore not a major one - CO_2 selectivity from CO hydrogenation is slightly more on Rh-Mn-Li-Fe/TiO_2 than on Rh-Mn-Li/TiO_2 (Fig. 4.5) and according to Xu et al[28], a lower carbon dioxide production can be taken as an indirect proof of lower water–gas shift activity.

In summary, Rh-Mn-Li-Fe/TiO_2 has the more favorable response (with respect to increased ethanol selectivity and EtOH/CH_4 ratio) to the co-feeding of CO_2 because the reverse WGS reaction is more rapid as a result of Fe addition.

5.4 CONCLUSIONS

The addition of the CO_2 to the feed during CO hydrogenation reaction generally increases methanation and reduces oxygenate formation, consistent with the observation that CO_2 is more easily hydrogenated to methane than CO at the same reaction conditions. Despite increased methanation as a result of the addition of CO_2 to the feed, Rh-Mn-Li-Fe/TiO_2 catalysts produced ethanol at a higher selectivity during the hydrogenation of a CO/CO_2 mixture than for the hydrogenation of only CO, which was not observed on Rh/TiO_2, Rh-Li/TiO_2, Rh-Mn/TiO_2 and Rh-Mn-Li/TiO_2. The Fe promoter is believed to increased reverse WGS reaction upon CO_2 addition, resulting in increased CO and decreased hydrogen species on the surface, leading to higher CO insertion activity than when Fe is not a promoter. The result is a higher increase in ethanol selectivity than in methanation activity, causing the EtOH/CH_4 to increase

5.5 REFERENCES

1. J. J. Spivey and A. A. Egbebi, *Chemical Society Reviews*, 2007, **36**, 1514-1528.

2. H. Arakawa, T. Fukushima, M. Ichikawa, S. Natsushita, K. Takeuchi, T. Matsuzaki and Y. Sugi, *Chemistry Letters*, 1985, 881-884.

3. T. Iizuka, Y. Tanaka and K. Tanabe, *Journal of Catalysis*, 1982, **76**, 1-8.

4. A. Trovarelli, C. Mustazza, G. Dolcetti, J. Kaspar and M. Graziani, *Applied Catalysis*, 1990, **65**, 129-142.

5. M. M. Bhasin, W. J. Bartley, P. C. Ellgen and T. P. Wilson, *Journal of Catalysis*, 1978, **54**, 120-128.

6. S. C. Chuang, J. G. Goodwin and I. Wender, *Journal of Catalysis*, 1985, **95**, 435-446.

7. P. Gronchi, E. Tempesti and C. Mazzocchia, *Applied Catalysis A: General*, 1994, **120**, 115-126.

8. M. Ichikawa and T. Fukushima, *Journal of the Chemical Society-Chemical Communications*, 1985, 321-323.

9. Y. H. Du, D. A. Chen and K. R. Tsai, *Applied Catalysis*, 1987, **35**, 77-92.

10. M. Ichikawa, T. Fukushima and K.Shikakura, Proc. 8th Int. Cong. Catal., Berlin, Germany, 1984.

11. A. Kiennemann, R. Breault, J. P. Hindermann and M. Laurin, *Journal of the Chemical Society-Faraday Transactions I*, 1987, **83**, 2119-2128.

12. S. Marengo, S. Martinengo and L. Zanderighi, *Chemical Engineering Science*, 1992, **47**, 2793-2798.

13. K. K. Bando, K. Soga, K. Kunimori and H. Arakawa, *Applied Catalysis a-General*, 1998, **175**, 67-81.

14. S. Ichikawa, *Journal of Molecular Catalysis*, 1989, **53**, 53-65.

15. T. Iizuka, Y. Tanaka and K. Tanabe, *Journal of Molecular Catalysis*, 1982, **17**, 381-389.

16. P. Reyes, I. Concha, G. Pecchi and J. L. G. Fierro, *Journal of Molecular Catalysis A: Chemical*, 1998, **129**, 269-278.

17. I. A. Fisher and A. T. Bell, *Journal of Catalysis*, 1996, **162**, 54-65.

18. F. Solymosi and A. Erdohelyi, *Journal of Molecular Catalysis*, 1980, **8**, 471-474.

19. F. Solymosi, A. Erdöhelyi and T. Bánsági, *Journal of Catalysis*, 1981, **68**, 371-382.

20. F. Solymosi, A. Erdohelyi and M. Kocsis, *Journal of Catalysis*, 1980, **65**, 428-436.

21. F. Solymosi and A. Erdöhelyi, *Journal of Catalysis*, 1985, **91**, 327-337.

22. J. J. Benítez, R. Alvero, M. J. Capitán, I. Carrizosa and J. A. Odriozola, *Applied Catalysis*, 1991, **71**, 219-231.

23. H. Kusama, K. K. Bando, K. Okabe and H. Arakawa, *Applied Catalysis A: General*, 2001, **205**, 285-294.

24. Y. Liu, C.-H. Zhang, Y. Wang, Y. Li, X. Hao, L. Bai, H.-W. Xiang, Y.-Y. Xu, B. Zhong and Y.-W. Li, *Fuel Processing Technology*, 2008, **89**, 234-241.

25. T. Herranz, S. Rojas, F. J. Pérez-Alonso, M. Ojeda, P. Terreros and J. L. G. Fierro, *Applied Catalysis A: General*, 2006, **308**, 19-30.

26. J. Kaspar, M. Graziani, A. M. Rahman, A. Trovarelli, E. J. S. Vichi and E. C. Dasilva, *Applied Catalysis a-General*, 1994, **117**, 125-137.

27. D. G. Rethwisch and J. A. Dumesic, *Journal of Catalysis*, 1986, **101**, 35-42.

28. L. G. Xu, S. Q. Bao, R. J. O'Brien, A. Raje and B. H. Davis, *Chemtech*, 1998, **28**, 47-53.

29. H. Kusama, K. Okabe, K. Sayama and H. Arakawa, *Catalysis Today*, 1996, **28**, 261-266.

30. H. Kusama, K. Sayama, K. Okabe and H. Arakawa, *Nippon Kagaku Kaishi*, 1995, 875-880.

31. H. Kusama, K. Okabe, K. Sayama and H. Arakawa, *Energy*, 1997, **22**, 343-348.

32. H. M. Yin, Y. J. Ding, H. Y. Luo, H. J. Zhu, D. P. He, J. M. Xiong and L. W. Lin, *Applied Catalysis a-General*, 2003, **243**, 155-164.

33. C. Wong and R. W. McCabe, *Journal of Catalysis*, 1987, **107**, 535-547.

34. H. T. Ma, Z. Y. Yuan, Y. Wang and X. H. Bao, *Surface and Interface Analysis*, 2001, **32**, 224-227.

35. F. G. A. van den Berg, J. H. E. Glezer and W. M. H. Sachtler, *Journal of Catalysis*, 1985, **93**, 340-352.

36. A. S. Lisitsyn, S. A. Stevenson and H. Knozinger, *Journal of Molecular Catalysis*, 1990, **63**, 201-211.

37. T. Ioannides and X. Verykios, *Journal of Catalysis*, 1993, **140**, 353-369.

38. K. P. De Jong, J. H. E. Glezer, H. P. C. E. Kuipers, A. Knoester and C. A. Emeis, *Journal of Catalysis*, 1990, **124**, 520-529.

CHAPTER 6 : EFFECT OF H_2/CO RATIO AND TEMPERATURE ON METHANE SELECTIVITY IN THE SYNTHESIS OF ETHANOL ON Rh-BASED CATALYST*

6.1 INTRODUCTION

Ethanol has found widespread use as both an energy carrier and a fuel additive[1]. A viable route for the manufacture of ethanol is the catalytic conversion of synthesis gas (syngas), which can be obtained by gasification of coal or a renewable resource like biomass. One key variable in syngas production is the H_2/CO ratio, which can be adjusted to maximize ethanol selectivity.

Supported Rh-based catalysts have been found to be most selective for the formation of ethanol from the hydrogenation of CO [2].

6.1.1 Thermodynamics

The reaction equation is given as:

$$2CO + 4H_2 \rightarrow C_2H_5OH + H_2O \qquad (1)$$

ΔH_r° = -61.20 kcal/mol

ΔG_r° = -29.32 kcal/mol

In Chapter 2, Fig. 2.1 shows a thermodynamic simulation (calculated using HSC Chemistry® software) of the equilibrium composition for reaction (1) as a function of temperature starting with a stoichiometric H_2/CO ratio of 2/1. Substantial amounts of ethanol can be observed at temperatures below 350°C with the products restricted to ethanol and water. However, when methane is allowed as an additional product, ethanol selectivity goes to zero at all temperatures (Fig. 2.3).

The reason for this difference is the methanation reaction:

$$CO + 3H_2 \rightarrow CH_4 + H_2O \qquad (2)$$

* This article was published in *Cat. Comm.,* 9, A. Egbebi and J. J. Spivey, Effect of H_2/CO ratio and temperature on methane selectivity in the synthesis of ethanol on Rh-based catalysts, 2308–2311, Copyright Elsevier (2008)

$\Delta H_r° = -49.27$ kcal/mol

$\Delta G_r° = -33.97$ kcal/mol

Methane is the most thermodynamically favored product, and is generally undesirable economically. In practice, the reaction kinetics therefore determines the observed selectivity to ethanol. The H_2/CO feed ratio and temperature are key adjustable variables in the overall conversion of syngas to ethanol /higher alcohols and it is of interest to determine their effects on the selectivity to ethanol, versus methane.

6.1.2 Kinetics

Previous work on CO hydrogenation to ethanol on Rh-based catalysts shows that point selectivities ($\boldsymbol{S = r_{EtOH}/r_{CH_4}}$) are typically poor, varying from 2/1 to 1/25, depending on the particular catalyst and reaction conditions[2-9]. There are several studies in which the kinetics of ethanol formation (eq. 1) and methanation (eq. 2) are measured. For example, Yin et al. give the following results for temperatures between 295 and 305°C, 30 atm, 15,000 h^{-1} for a Rh-Mn-Li-Fe/SiO_2 catalyst with a weight ratio among the metals of 1/1/0.075/0.05 [10] :

$$r_{EtOH} = 6.3 \times 10^{12}\, e^{-126.7/RT} P_{H_2}^{0.90} P_{CO}^{-0.76} \quad (4)$$

$$r_{CH_4} = 9.0 \times 10^{15}\, e^{-156.8/RT} P_{H_2}^{0.79} P_{CO}^{-0.60} \quad (5)$$

The point selectivity can then be calculated:

$$S = \frac{r_{EtOH}}{r_{CH_4}} = 7.0 \times 10^{-4}\, e^{+30.1/RT} P_{H_2}^{0.11} P_{CO}^{-0.16} \quad (6)$$

A qualitatively similar result, showing a positive dependence of ethanol selectivity on P_{H_2} and inverse dependence on P_{CO}, was found for an unpromoted 1.4%Rh/ZrO_2 catalyst[6]:

$$S = \frac{r_{EtOH}}{r_{CH_4}} = k P_{H_2}^{0.55} P_{CO}^{-0.45} \quad (7)$$

6.1.3 Effect of H_2/CO ratio on Selectivity

The effect of H_2/CO ratio can be shown from eq. (6), which can be re-written as:

$$S = \frac{r_{EtOH}}{r_{CH_4}} = 7.0 \times 10^{-4}\, e^{+30.1/RT} \left[\frac{P_{H_2}}{P_{CO}}\right]^{0.11} P_{CO}^{-0.05} \quad (8)$$

Similarly, eq. (7) can be re-written to show the effect of H_2/CO ratio explicitly:

$$S = \frac{r_{EtOH}}{r_{CH_4}} = k \left[\frac{P_{H_2}}{P_{CO}}\right]^{0.55} P_{CO}^{0.15} \quad (9)$$

Both eq. (8) and (9) show that increasing H_2/CO ratio has a small but positive effect on ethanol selectivity, whereas P_{CO} itself has relatively little effect. Eq. (8) and (9) also suggests that increasing the total pressure at constant P_{H_2}/P_{CO} does not significantly affect selectivity to ethanol.

6.1.4 Effect of Temperature on Ethanol Selectivity

The positive value of the activation energy in the expression for selectivity [eq. (6)] shows that at higher temperatures, selectivity to methane increases, which is consistent with experimental results over a wide range of temperatures, pressures, H_2/CO ratios, and catalyst formulations (see Table 6.1; see also ref.[7]).

Despite differences in the absolute value of the activation energies among the studies for the two individual reactions, there is striking agreement in the relative values - with the activation energy for ethanol being consistently lower than that for methane formation in any given study. This agrees with experimental results that uniformly show greater selectivity to methane with increasing temperatures.

6.1.5 Reaction Order in H_2 and CO

For the formation of both ethanol and methane, the reaction orders in H_2 are consistently positive, and are greater than those for CO, with CO values being negative or near zero except in one case (ref. [6]). This kinetic inhibition by CO has been attributed to preferential adsorption on Rh, which generally appears to inhibit ethanol formation more than methane.

Table 6.1: Comparison of Kinetics for Methanation and Ethanol Formation on Supported Rh Catalysts

Catalyst	**Temp, deg C**	**Press, atm**	$r_i = Ae^{-E_{a/RT}} P_{H_2}^a P_{CO}^b$								**Ref.**
			i=EtOH				*i*=CH_4				
			A	E_a	a	b	A	E_a	a	b	
1%Rh-Mn-Li-Fe/SiO_2	295-305	30	6.3 x 10^{12}	126.7	0.90	-0.76	9.0 x 10^{15}	156.8	0.79	-0.60	[10]
3%Rh-xMo/Al_2O_3	250	30	nr	101.7[a]	0.91 [a]	-0.47	nr	135.2	1.02	-0.32	[2]
Rh-Li/TiO_2 [b]	120-220	1	nr	87.9	nr	nr	nr	117.2	nr	nr	[5]
1.4% Rh/ZrO_2	200-280	1-25	nr	71.5-77.4	1.0	-1.0	nr	116-232	0.45	-0.55	[6]
Rh/La_2O_3, MgO, ZrO_2	nr	1	nr	96	1.0	0.3		121	0.8	-0.4	[6, c]
4%Rh-8%Mn/SiO_2	200-250	1	nr	60-125[a]	nr	nr	nr	120	nr	nr	[11]
2%RhSiO_2 [d]	270	5-15	nr	nr	0.33-1.73	0.07 to -1.52	nr	nr	0.75 to 1.0	-0.35 to -1.15	[12]

[A] = mol/mol Rh-hr-MPa^{a-b}l ; [E_a]=kJ/mol; nr=not reported

[a] This value is for the formation of all C_2 oxygenates; a separate value for ethanol is not provided. Table 1 within reference [2] shows that at least 70% of the C_2 oxygenate content in ethanol.
[b] Rh and Li loading not reported.
[c] As reported within [6], data of Ichikawa and Shikakura, 1981.
[d] A series of 2%Rh catalysts promoted with 1%Fe, 0.034%Li, 1%Mn were investigated. The kinetic parameters given here are the range of those reported for the entire series of catalysts.

We have conducted experiments to measure the effect of H_2/CO ratio on the selectivity ethanol with respect to methane for a 1% Rh /TiO_2 catalysts promoted with Mn and Li.

6.2 EXPERIMENTAL

Catalyst Preparation. Rh(1%)-Li(0.1%)-Mn(0.55%)/TiO_2 catalyst was prepared by incipient wetness impregnation of TiO_2 (Degussa Aerolyst, BET = 50 m^2/g) using nitrate precursors. Aqueous solutions of $Rh(NO_3)_3$, $Mn(NO_3)_2$ and $LiNO_3$ were co-impregnated on the support, dried overnight in an oven at 120 C and calcined for 4 h at 500°C.

Catalyst Activity Test. Reaction tests at differential conditions were carried out in a ¼" glass-lined stainless steel fixed bed micro-reactor system at 270°C and total pressure of 20 bar. Prior to reaction tests the catalyst was reduced in-situ for 2 h in 75% H_2/25% He mixture. CO

hydrogenation (H_2/CO = 1, 2 and 3) reactions were run at GHSVs of about 52800 $scchr^{-1}gcat^{-1}$. For each run the syngas feed was diluted with He to reduce heat effects within the bed and to ensure that the conversion is low enough to keep the oxygenated products in vapor state for online GC/MS analysis. The total flow rate of the feed gas was maintained at 220 scc/min, including a constant flow rate of 100 scc/min He. The sum of the flow rates of H_2 + CO was always 120 scc/min, with the H_2/CO ratio adjusted by changing the flow rates of H_2 and CO such that the total flow rate was 120 scc/min. Reactions are allowed to run for at least 1.5 h at each H_2/CO ratio level to attain steady state before samples are injected into the GC.

Analysis of products. This was done on an online Agilent GC/MS system (Agilent Technologies 6890N/5975B) equipped with two Thermal conductivity detectors (TCD). The line from the reactor exit to the sampling valves is heat traced to prevent products from condensing upstream of the GC/MS. The sampling valves are placed in an isothermal oven and maintained at a temperature of 250°C Oxygenates and C_2-C_4 hydrocarbon analysis was done using the mass selective detector (MSD) while hydrogen, CO, CO_2 and CH_4 were analyzed on the TCD. The columns are supplied by Wasson ECE Instrumentation that configured the GC/MS.

6.3 RESULTS AND DISCUSSION

Table 6.2 shows the selectivities to methane and ethanol at the three H_2/CO levels. Both methane and ethanol selectivities increase with H_2/CO, consistent with literature findings (Table 6.1). Methane and ethanol (and in general hydrocarbons and oxygenates) are thought to be formed by parallel reactions[1] and it would be expected to see reduced ethanol selectivity when methane selectivity increases. However, the total oxygenate selectivity follows the expected trend -- decreasing as the H_2/CO ratio increases. Acetaldehyde is the major oxygenate product (Table 6.2) and its selectivity decreases monotonically with increasing H_2/CO ratio. The reason why increasing the H_2/CO ratio increases ethanol selectivity, while it decreases the total

oxygenate selectivity, may be due to increased hydrogenation of acetaldehyde or an intermediate common to both ethanol and acetaldehyde.

Table 6.2. CO Hydrogenation[a]: Product Selectivities at different H_2/CO ratios on Rh-Mn-Li/TiO_2

Reaction product	Selectivity (mol %)		
	H_2/CO = 1	H_2/CO = 2	H_2/CO = 3
Methane	74	78	81
EtOH	3.5	4.3	4.8
Oxygenates[b]	25	21	19
Acetaldehyde	18	12	10
MeOH	3.3	3.4	3.4
$\boldsymbol{S = r_{EtOH}/r_{CH_4}}$	**0.048**	**0.054**	**0.060**
Total products, *ppm*	**909**	**1280**	**1633**
CO conversion, *mol %*	**0.5**	**0.9**	**1.6**
$\mathbf{r_{CO}}$**,** *mmol* hr^{-1} *gcat*$^{-1}$	**2.0**	**4.0**	**6.7**

[a]20 bar, 270 °C, 52 800 scc hr^{-1} $gcat^{-1}$
[b]sum of all observed oxygenate concentrations: methanol, ethanol, acetaldehyde, n-propanol, n-butanol

The reaction sequence leading to ethanol formation via CO hydrogenation on Rh-based catalysts can be depicted as shown in Fig. 6.1 [adapted from ref [1]]. In this sequence, the insertion of CO into a surface CH_x ($x \leq 3$) species, coupled with the addition of H atom(s) (step 2) leads to either an "enol" surface species, or an adsorbed acetaldehyde species, either of which can be formed by isomerization of the other. Further hydrogenation of either then leads to ethanol (step 4), while acetaldehyde can also be desorbed (step 5). Thus, increasing the H_2/CO ratio favors the "enol" path to ethanol.

It is safe to assume here that because acetaldehyde and ethanol selectivity follow opposite trends with H_2/CO ratio, they share the same intermediate, perhaps the "enol" species. Note that methanol selectivity remains essentially the same at all H_2/CO levels (Table 6.2), suggesting that methanol and ethanol are formed through different intermediates, which is not consistent with

the suggestion by Wang et al[13] that the two share a common intermediate. The ratio of the selectivity of EtOH to CH_4 also rises with H_2/CO in the same manner as EtOH and CH_4 selectivities individually, meaning that EtOH formation increases at a slightly higher rate than methane as H_2/CO ratio increases.

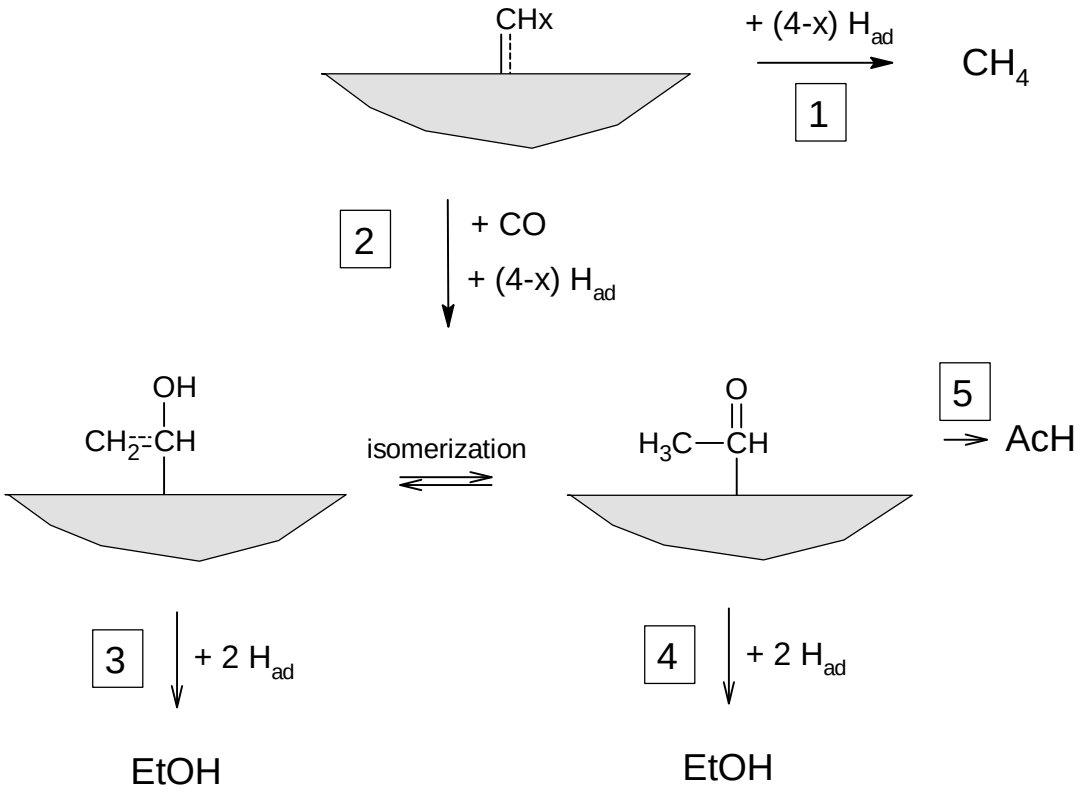

Figure 6.1. Reaction sequence from CO insertion to ethanol formation showing how Acetaldehyde comes into play (adapted from ref.[1])

To determine the point selectivity, *S*, relationship for the experiments reported here, we linearize equation (10):

$$S = \frac{r_{EtOH}}{r_{CH_4}} = \left(\frac{H_2}{CO}\right)^n \qquad (10)$$

and plot $\ln EtOH/CH_4$ vs $\ln H_2/CO$) to determine n (Fig. 8.4). This is found to be 0.20 ± 0.29 i.e.

$$S = \frac{r_{EtOH}}{r_{CH_4}} = \left(\frac{H_2}{CO}\right)^{0.20} \qquad (11)$$

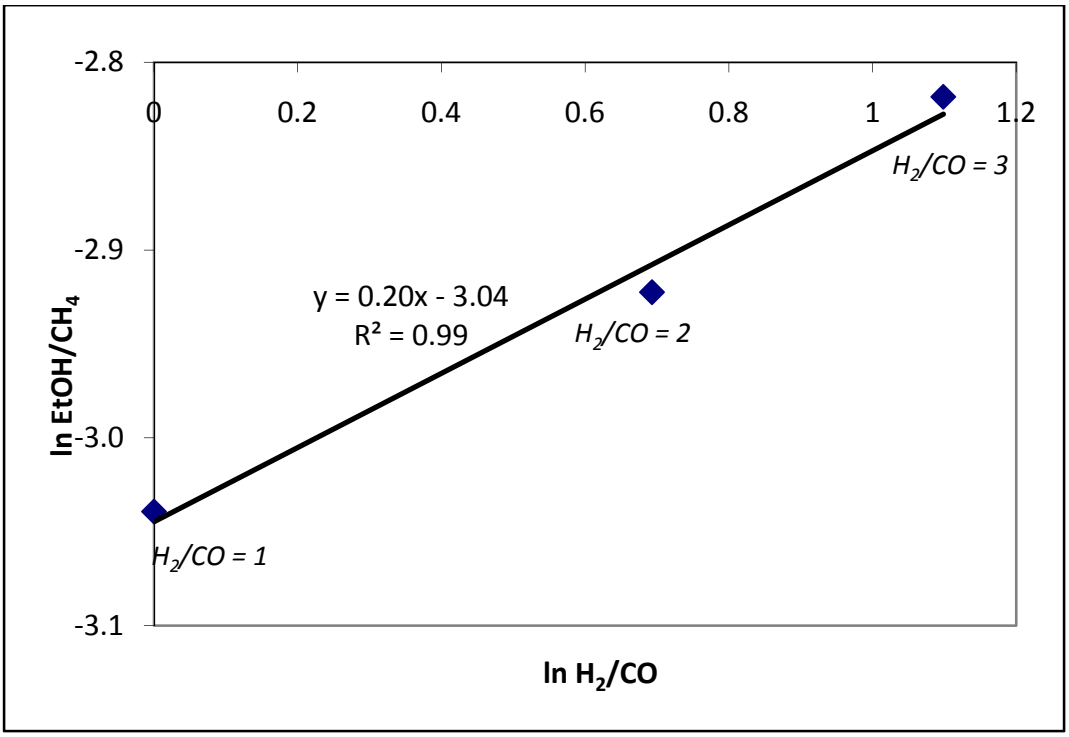

Figure 6.2: Plot of the dependence of $EtOH/CH_4$ ratio on H_2/CO ratio

This is within in the range of literature values of 0.11 and 0.55 from equations (8) and (9) respectively. This small but positive dependence is consistent with previous work and suggests that using excess hydrogen (i.e. more than H_2/CO ratio of 2) increases $EtOH/CH_4$ selectivity in syngas-to-ethanol reactors using Rh-based catalysts.

Effect of H_2/CO ratio on overall activity. The overall activity of the catalyst also increases with increasing H_2/CO ratio. This is in agreement with Burch and Petch[12] who proposed that the availability of hydrogen is key to the activity of Rh-based catalysts. However,

reducible oxide promoters like Fe make the activity less sensitive to feed H_2 concentration by increasing the effective population of surface hydrogen species on sites adjacent to the active sites. In order words, these promoters make more hydrogen species available at the surface than on unpromoted Rh catalysts by acting as reservoirs for spillover hydrogen[12].

6.4 CONCLUSION

Previous results show that increasing the H_2/CO feed ratio increases the selectivity for ethanol versus methane over a wide range of supported Rh catalysts. Experiments on a 1%Rh-0.1%Li-0.55% Mn/TiO_2 catalyst show the same effect, with a point selectivity ($S = r_{EtOH}/r_{CH_4}$) proportional to $(P_{H_2}/P_{CO})^{0.20}$ on this catalyst. Increasing H_2/CO ratio also increases hydrogenation of acetaldehyde (or C_2 a surface intermediate) to EtOH.

6.5 REFERENCES

1. J. J. Spivey and A. A. Egbebi, *Chemical Society Reviews*, 2007, **36**, 1514-1528.
2. N. A. Bhore, K. B. Bischoff, W. H. Manogue and G. A. Mills, *Abstracts of Papers of the American Chemical Society*, 1989, **198**, 43-Catl.
3. T. Koerts and R. A. Vansanten, *Journal of Catalysis*, 1992, **134**, 13-23.
4. H. Fujitsu, N. Ikeyama and I. Mochida, *Journal of Catalysis*, 1986, **100**, 279-286.
5. H. Orita, S. Naito and K. Tamaru, *Chemistry Letters*, 1983, 1161-1164.
6. C. Mazzocchia, E. Tempesti, P. Gronchi, L. Giuffre and L. Zanderighi, *Journal of Catalysis*, 1988, **111**, 345-352.
7. T. Inoue, T. Iizuka and K. Tanabe, *Applied Catalysis*, 1989, **46**, 1-9.
8. A. Trunschke, H. Ewald, D. Gutschick, H. Miessner, M. Skupin, B. Walther and H. C. Bottcher, *Journal of Molecular Catalysis*, 1989, **56**, 95-106.
9. Y. Mori, T. Mori, T. Hattori and Y. Murakami, *Applied Catalysis*, 1990, **66**, 59-72.
10. H. M. Yin, Y. J. Ding, H. Y. Luo, D. P. He, W. M. Chen, Z. Y. Ao and L. W. Lin, *Journal of Natural Gas Chemistry*, 2003, **12**, 233-236.
11. A. S. Lisitsyn, S. A. Stevenson and H. Knozinger, *Journal of Molecular Catalysis*, 1990, **63**, 201-211.

12. R. Burch and M. I. Petch, *Applied Catalysis a-General*, 1992, **88**, 77-99.

13. Y. Wang, H. Y. Luo, D. B. Liang and X. H. Bao, *Journal of Catalysis*, 2000, **196**, 46-55.

CHAPTER 7 : CONCLUSIONS AND RECOMMENDATIONS

7.1 CONCLUSIONS

The effects of Li, Mn and Fe on the hydrogenation of CO and of CO/CO_2 mixture have been studied. Li enhances the dispersion of Rh, reducing the formation of large Rh atom ensembles on the surface that is required for the CO dissociation. During CO hydrogenation, this reduces the carbon coverage on the surface, thereby increasing H_2 chemisorption on the surface leading to improved activity and selectivity to ethanol when compared to the unpromoted catalysts. Mn promotion results in the weakening of the Rh-CO bond, leading to reduced carbon and more H_2 surface coverage. However, hydrogenation of surface intermediates to ethanol is limited. Although, Mn and Li individually increased catalyst activity, when multiple promotion is used by combining Mn and Li, the CO insertion activity is further increased but the hydrogenation ability of $Rh\text{-}Li\text{-}Mn/TiO_2$ is limited: the highest oxygenate selectivity of 41% (at 260°C) and lowest methane selectivity (56%) was observed but with reduced catalyst activity. Fe addition to $Rh\text{-}Li\text{-}Mn/TiO_2$ increases its hydrogenation activity – increasing methane selectivity at the expense of C_2 oxygenates.

Despite increased methanation as a result of the addition of CO_2 to the feed, $Rh\text{-}Mn\text{-}Li\text{-}Fe/TiO_2$ catalysts produced ethanol at a higher selectivity during the hydrogenation of a CO/CO_2 mixture than for the hydrogenation of only CO, which was not observed on Rh/TiO_2, $Rh\text{-}Li/TiO_2$, $Rh\text{-}Mn/TiO_2$ and $Rh\text{-}Mn\text{-}Li/TiO_2$. The Fe promoter is believed to increased reverse WGS reaction upon CO_2 addition, resulting in increased CO and decreased hydrogen species on the surface, leading to higher CO insertion activity than when Fe is not a promoter. The result is a higher increase in ethanol selectivity than in methanation activity, causing the $EtOH/CH_4$ selectivity ratio to increase.

This work also establishes that ethanol formation from biomass/coal-derived syngas requires catalysts different from those used for conventional syngas which has little or no CO_2 content: Rh-Li/TiO_2 is the most selective for ethanol from CO hydrogenation while Rh-Mn-Li-Fe/TiO_2 gives the highest selectivity to ethanol from the hydrogenation of CO/CO_2 mixture.

Increasing the H_2/CO feed ratio increases the selectivity for ethanol versus methane over Rh-Mn-Li/TiO_2, with point selectivity ($S = r_{EtOH}/r_{CH_4}$) proportional to $(P_{H_2}/P_{CO})^{0.20}$. This catalyst this is consistent with some previous work over a wide range of supported Rh catalysts. Increasing H_2/CO ratio is thought to increase the population of hydrogen atoms on the surface of the catalyst resulting in hydrogenation of acetaldehyde (or a C_2 surface intermediate) to EtOH.

7.2 RECOMMENDATIONS

Based on the results presented here and the, the followings are recommended:

- Synthesis of Rh-Fe/TiO_2 to examine the effects of sole Fe promotion especially its activity for the r-WGS necessary for the synthesis of ethanol from CO_2 rich syngas
- FTIR studies to identify how the added promoters affect the population of various reaction intermediates or adsorbed CO species from both CO and CO_2 hydrogenation reactions
- Using higher Li loadings in Rh-Li/TiO_2 with a view to increasing catalyst activity and ethanol selectivity.
- The use of a more basic support can be explored for CO hydrogenation to reduce methane formation, which remained high on the TiO_2 supported catalysts. It appears increasing Li content on the catalyst can achieve the same result but too much alkali promotion may also cover the Rh surface sites leading to loss of activity.

- Optimization of the reaction conditions in terms of GHSV, temperature, pressure and H_2/CO ratio.
- Tests with H_2O in addition to CO + CO_2 + H_2 to examine ethanol formation with realistic syngas composition.

APPENDIX A : CALIBRATION OF GC/MS

A.1 CALIBRATION

The oxygenates are analyzed using the mass spectrometer as the detector. The calibration was done using three calibration levels of each component. To achieve this, two gaseous mixtures were used containing ~10 ppm and ~100 ppm of each oxygenate component. Higher concentrations of the oxygenates could not be purchased at higher concentrations so a liquid sample containing about 0.5 mol% (5000 ppm) of each component was used for the third calibration level. The calibration curves for the oxygenates are fitted quadratically and forced through zero. The gaseous components of CO, CO_2 and CH_4 are analyzed with the TCD using a single level calibration resulting in straight line fits of the calibration curve. Here, we present the calibration curves of the major components and the calculations leading to quantification of the reaction products and the estimation of error.

A.1.1 ETHANOL

The calibration data for ethanol is presented below along with the resultant calibration curve depicted in Figure A.1.

amount ppm (x)	Response area ct.(y)
9.3	8579
9.3	7612
9.3	7706
99.3	133394
99.3	133175
4921	4614175

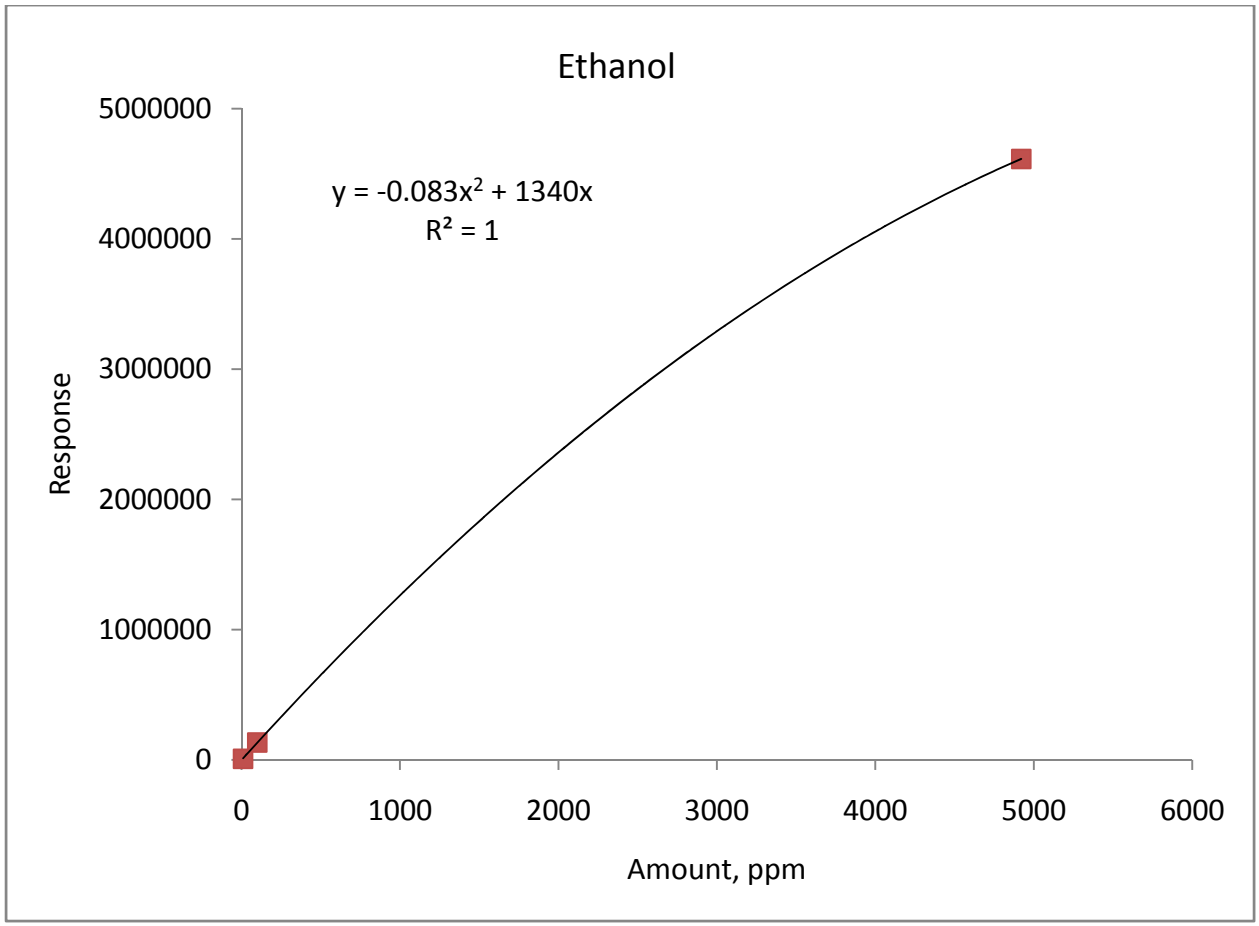

Figure A.1: Calibration curve for Ethanol

The calibration curve is fitted quadratically with the equation given as,

$$y = -0.083x^2 + 1340x$$

$$y = response$$

$$x = amount$$

Rearranging to,

$$-0.083x^2 + 1340x - y = 0$$

This is of the form,

$$ax^2 + bx + c = 0$$

With the solution given as

$$x = \frac{-b \pm \sqrt{b^2 - 4ac}}{2a}$$

Substituting $a = -0.083,\ b = 1340,\ c = -y$

$$\boldsymbol{x} = \frac{-1340 \pm \sqrt{1340^2 - 4(-0.083)(-\boldsymbol{y})}}{2(-0.083)}$$

There are two solutions, but only one is valid. We expect a zero amount (x) to give a zero response (y). Therefore setting y = 0, the solution that leads to x = 0 is the valid one, which is,

$$\boldsymbol{x_i} = \frac{-1340 + \sqrt{1340^2 - 4(-0.083)(-\boldsymbol{y_i})}}{2(-0.083)}$$

If x_i is the amount of ethanol measured and we took 3 repetitions, then x is the average of the 3 measurements taken at the same conditions and be expressed as the average, i.e.

$$x = \frac{\sum x_i}{n} = \frac{x_1 + x_2 + x_3}{3}$$

The selectivity of ethanol is therefore computed as

$$selectivity = \frac{x}{x + \alpha + \beta + \cdots \ldots \omega} \times 100\%$$

$$\alpha, \beta \ldots \ldots \omega \ are \ amounts \ of \ other \ product \ species$$

For example, for ethanol

$$\boldsymbol{x} = \frac{-1340 + \sqrt{1340^2 - 4(-0.083)(-\boldsymbol{y})}}{2(-0.083)}$$

And during the hydrogenation of CO/CO_2 at 260ºC, three GC/MS measurements were taken with responses 303096, 290336 and 306990 for ethanol resulting in a mean response of 300141

$$\boldsymbol{x} = \frac{-1340 + \sqrt{1340^2 - 4(-0.083)(-\boldsymbol{300141})}}{2(-0.083)}$$

$$= 227.18$$

The calibration curves and equation of the other oxygenate products are presented below in Figure A.2 through to Figure A.9

A.1.2 ACETALDEHYDE

amount ppm (x)	Response area ct.(y)
9	8497
9	10091
9	8178
99.8	85218
99.8	84315
4921	2354436

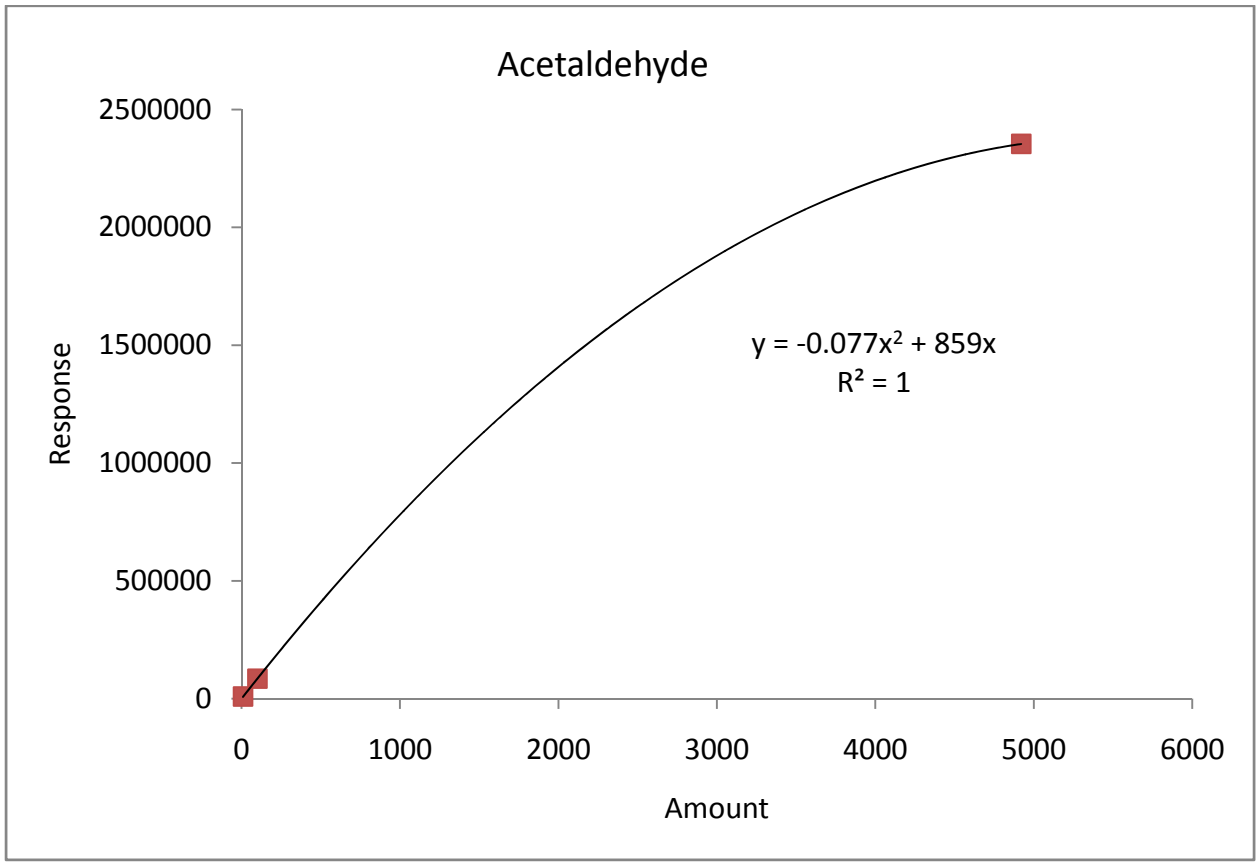

Figure A.2: Calibration curve for acetaldehyde

$$y = -0.077x^2 + 859x$$

$$\boldsymbol{x} = \frac{-859 + \sqrt{859^2 - 4(-0.077)(-\boldsymbol{y})}}{2(-0.077)}$$

A.1.3 METHANOL

Conc, ppm (x)	Response area ct.(y)
9.5	5035
9.5	4615
9.5	4723
109	71329
109	71774
4825	1977410

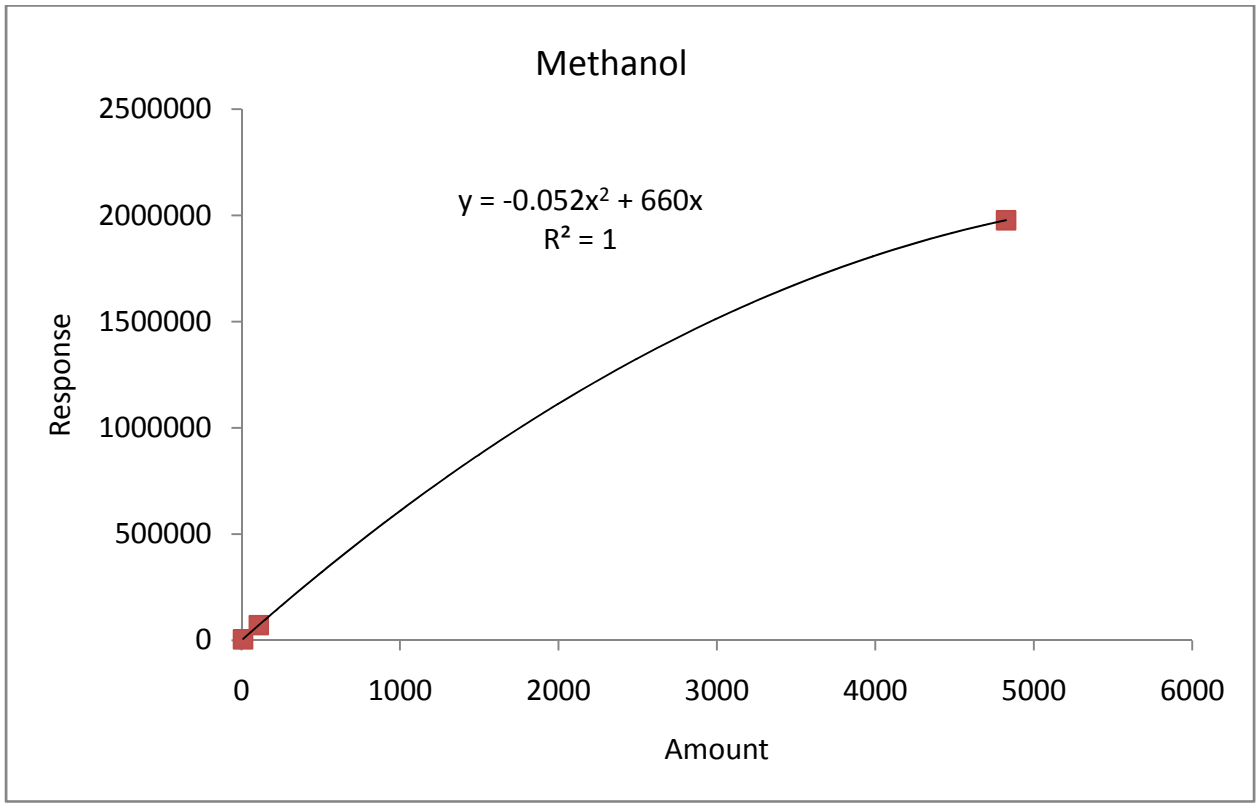

Figure A.3: Calibration curve for methanol

$$y = -0.052x^2 + 660x$$

$$\boldsymbol{x} = \frac{-660 + \sqrt{660^2 - 4(-0.052)(-\boldsymbol{y})}}{2(-0.052)}$$

A.1.4 ACETONE

Conc, mol % (x)	Response area ct.(y)
9.9	16769
9.9	17159
9.9	16704
93.2	176175
93.2	181369

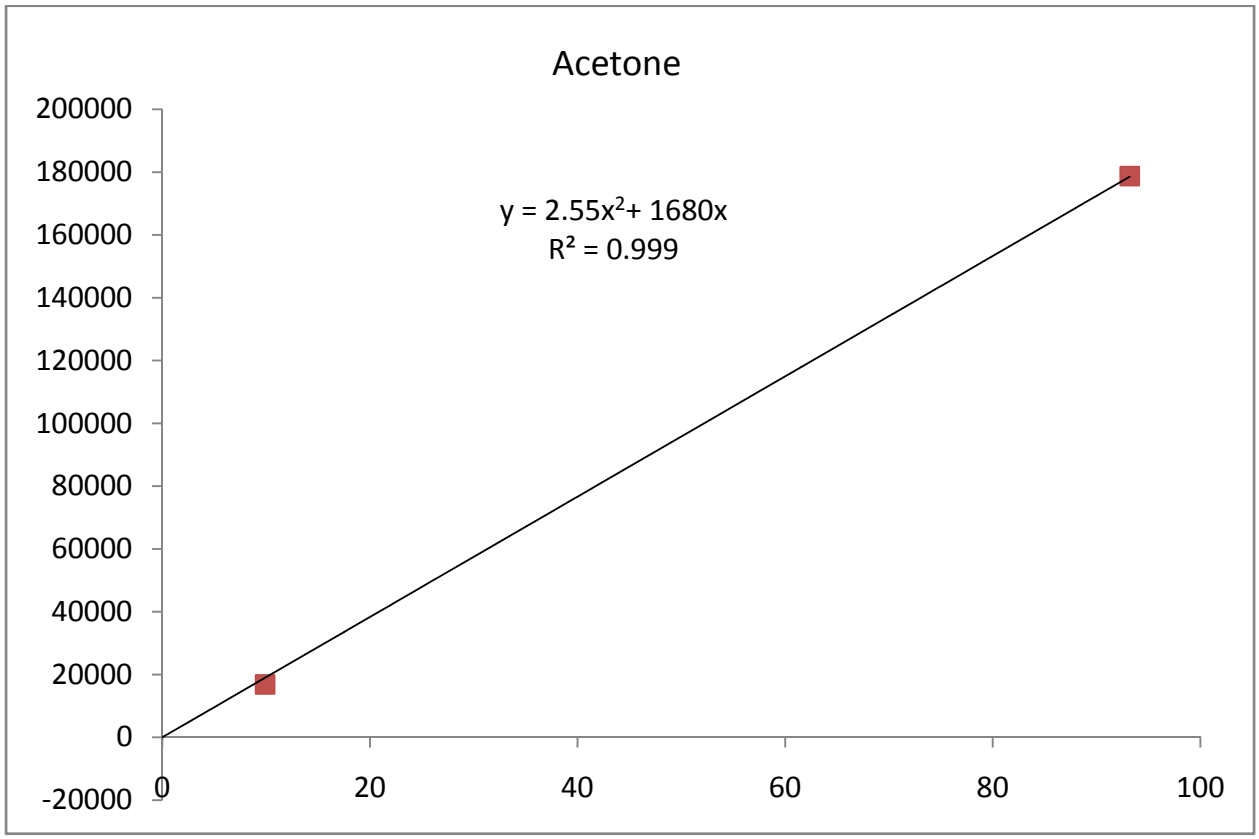

Figure A.4: Calibration curve for acetone

$$y = 2.55x^2 + 1680x$$

$$\boldsymbol{x} = \frac{-1680 + \sqrt{1680^2 - 4(2.55)(-\boldsymbol{y})}}{2(2.55)}$$

A.1.5 N-PROPANOL

Conc, ppm (x)	Response area ct.(y)
8.9	10667
8.9	9458
8.9	10371
100	197537
100	205783
4825	10792907

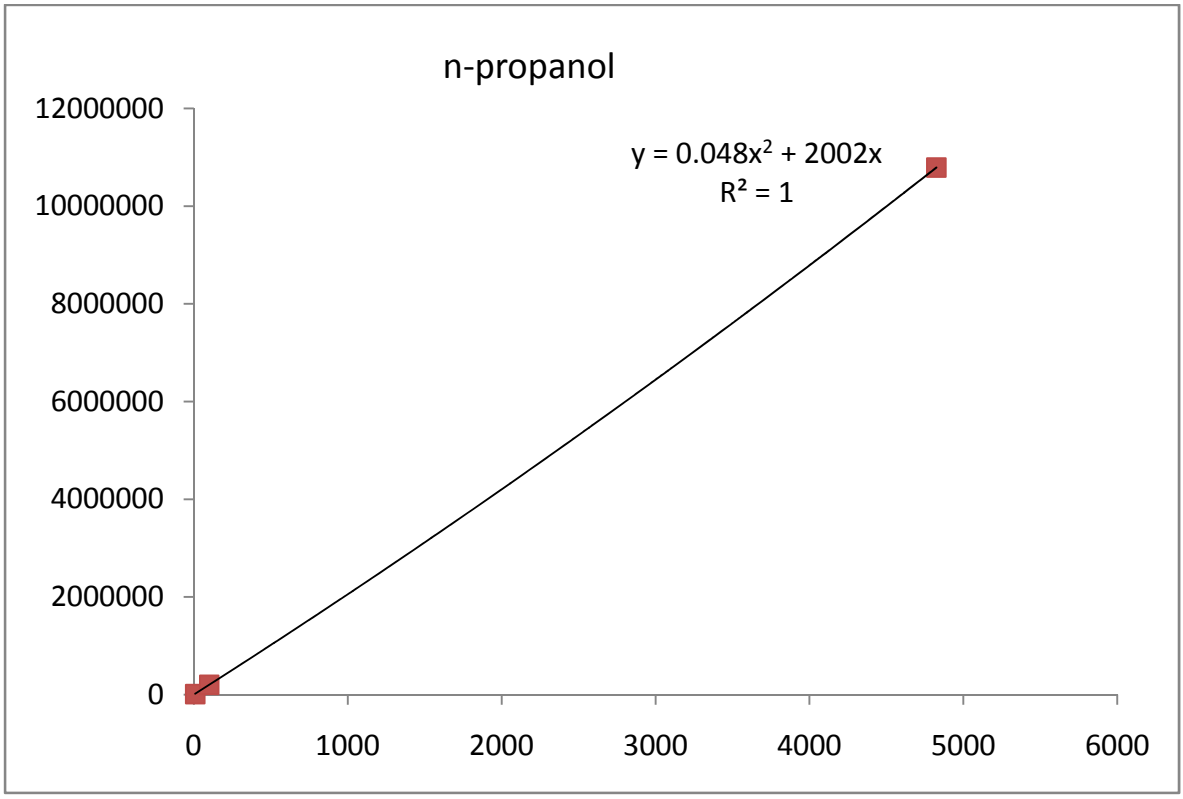

Figure A.5: Calibration curve for n-propanol

$$y = 0.048x^2 + 2002x$$

$$\boldsymbol{x} = \frac{-2002 + \sqrt{2002^2 - 4(0.048)(-\boldsymbol{y})}}{2(0.048)}$$

A.1.6 N-BUTANOL

Concentration, ppm (x)	Response area ct.(y)
8.9	4671
8.9	3072
8.9	4328
100	101827
100	101465
4825	5698186

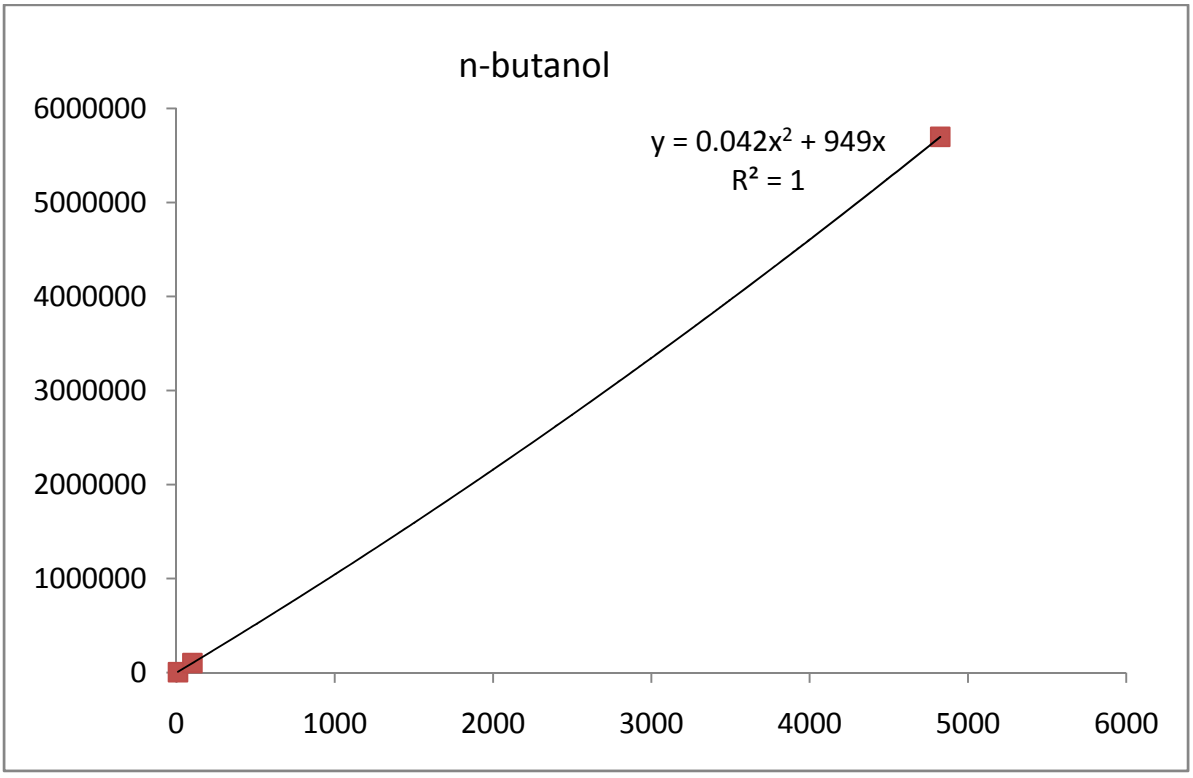

Figure A.6: Calibration curve for n-butanol

$$y = 0.042x^2 + 949x$$

$$\boldsymbol{x} = \frac{-949 + \sqrt{949^2 - 4(0.042)(-\boldsymbol{y})}}{2(0.042)}$$

A.1.7 METHANE

Conc, mol % (x)	Response area ct.(y)
6	3388142
6	3397470
0	0

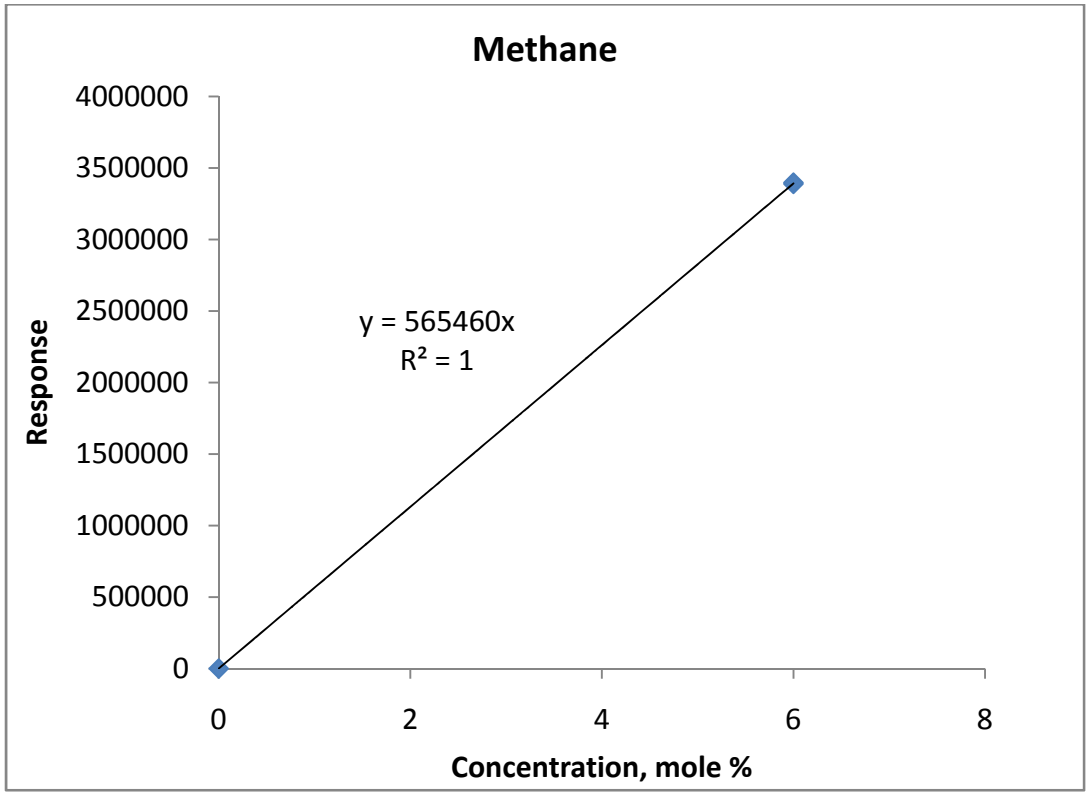

Figure A.7: Calibration curve for methane

$$y = 565460\, x$$

$$x = \frac{y}{565460}$$

A.1.8 CARBON DIOXIDE

Conc, mol % (x)	Response area ct.(y)
100	52306363
100	52409638
0	0

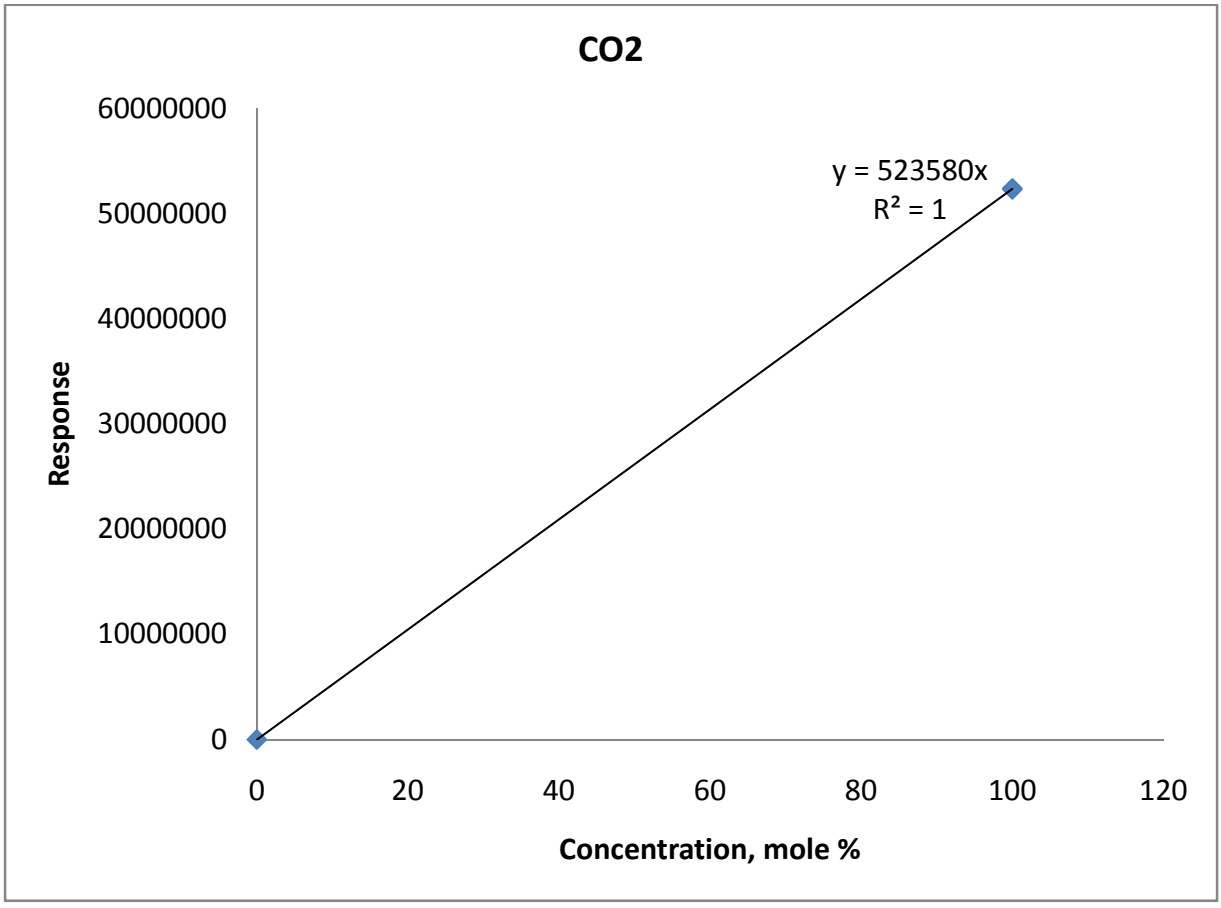

Figure A. 8: Calibration curve for Carbon dioxide

$$y = 523580\,x$$

$$x = \frac{y}{523580}$$

A.1.9 CARBON MONOXIDE

Conc, mol % (x)	Response area ct.(y)
100	42761080
100	42766165
0	0

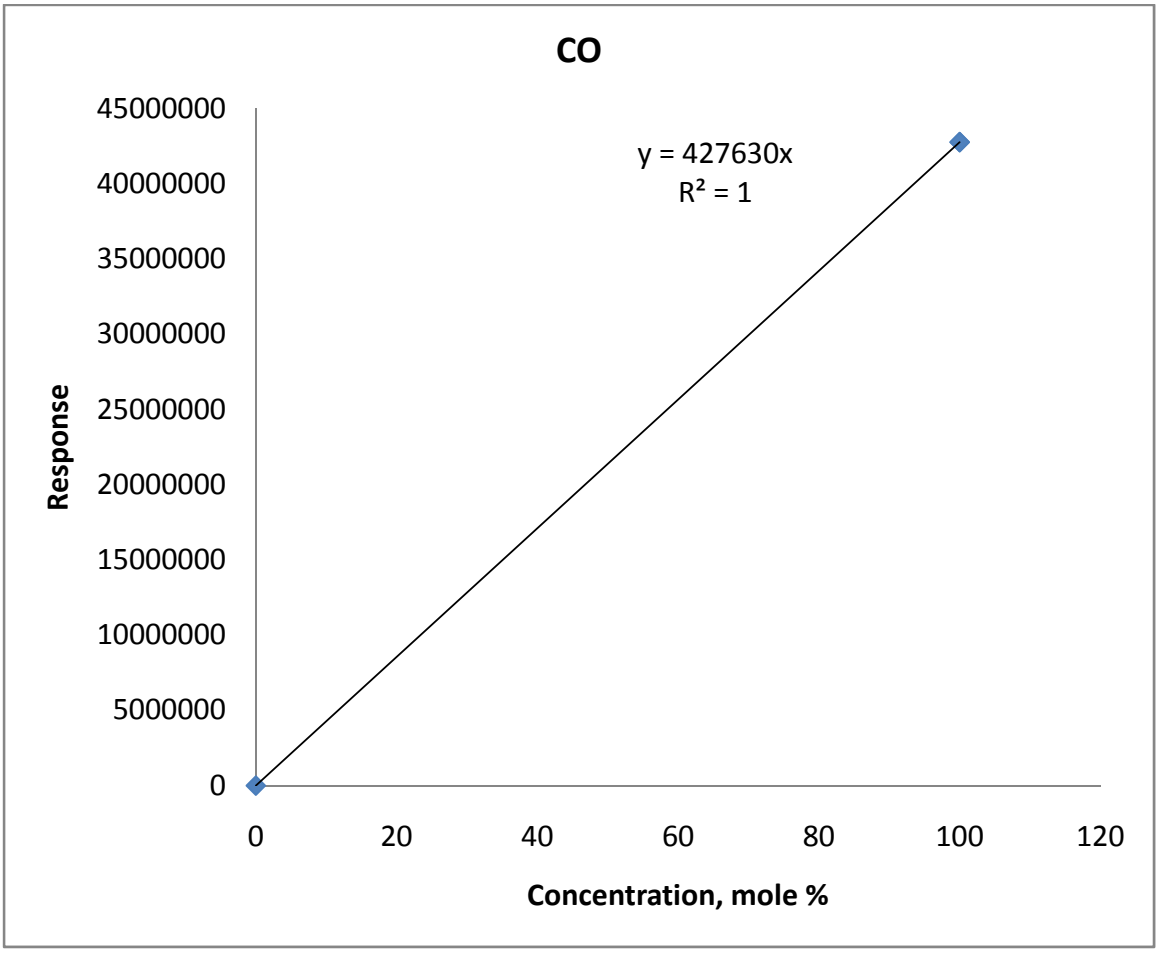

Figure A. 9: Calibration curve for carbon monoxide

$$y = 427630\,x$$

$$x = \frac{y}{427630}$$

A.2 ERROR ESTIMATION

For error estimation, the quadratic term is negligible in our concentration range; therefore the response is essentially linear with amount of component being measure. This reduces the calibration equation for ethanol to.

$$y = \ 1335x$$

$$x = \ \frac{y}{1335} = \frac{y}{c}$$

From Engineering Statistics by Montgomery et al, the approximate mean, *E(Y)* and variance, *V(Y)* of a non linear function can be computed as.

$$E(Y) = \mu_Y \cong h(\mu_1, \mu_2 \ldots\ldots \mu_n)$$

$$V(Y) = \sigma^2{}_Y \cong \sum \left(\frac{\partial h}{\partial X_i}\right)^2 \sigma_i^2$$

……..where$\mu_i$and $\sigma^2{}_i$ are the mean and variance of variable X_i respectively.

The derivative $dh/\partial X_i$ is evaluated at μ_i.

Applying to our case,

$$E(Y) \ \equiv x = \frac{y}{c}$$

$$V(Y) \equiv \ \sigma^2{}_x = \left(\frac{dx}{dc}\right)^2 \sigma^2{}_c + \left(\frac{dx}{dy}\right)^2 \sigma^2{}_y$$

……..where

$$\frac{dx}{dc} = \ \frac{-y}{c^2}$$

$$\frac{dx}{dy} = \ \frac{1}{c}$$

σ_c and σ_y are the standard deviations of the slope of the straight line of fit and responses of same component measured at the same reaction conditions respectively. The variance of *x*, σ_x therefore accounts for the error due to calibration as well as that due to the repeat measurements at same reaction condition.

Table A.1 shows the calibration equations of the major components and the corresponding linear approximation. While Table A.2 shows an example of the matrix of calculations leading to estimation of error associated with the concentration measurement.

Table A.1: Summary of Calibration Equations of the Major Components and the Corresponding Linear Approximation

Component	Quadratic fit	Linear approximation
Methanol	$y = -0.052x^2 + 660x$	$y = 654x$
Ethanol	$y = -0.083x^2 + 1340x$	$y = 1335x$
Acetaldehyde	$y = -0.077x^2 + 859x$	$y = 851x$
Acetone	$y = 2.55x^2 + 1680x$	$y = 1914x$
Propanol	$y = 0.048x^2 + 2002x$	$y = 2006x$
Butanol	$y = 0.042x^2 + 949x$	$y = 1009x$
CO	-	$y = 427636x$
CO_2	-	$y = 523580x$
CH_4	-	$y = 565467x$

Table A.2: Calculations leading to Estimation of Error using the Linear Approximation for CO hydrogenation on Rh/TiO_2

	y_1	y_2	y_3	y	σ_y	c	σ_c	$\frac{dx}{dc} = \frac{-y}{c^2}$	$\frac{dx}{dc} = \frac{1}{c}$	$x = \frac{y}{c}$	${\sigma_x}^2$	σ_x	$CI = 1.96\sigma_x$
										[ppm]			**[ppm]**
Methanol	55514.	60785	52459.81	56253.13	4211.68	654.72	11.55	-0.13123	0.00153	**85.9**	43.677	6.609	**12.95**
Acetaldehyde	44817	44400	45367.01	44861.74	484.59	851.07	13.52	-0.06194	0.00117	**52.7**	1.025	1.013	**1.98**
Ethanol	97126	113403	87400.22	99310.28	13138.52	1335.93	39.14	-0.05564	0.00075	**74.3**	101.465	10.073	**19.74**
Acetone	6515.78	7658	6236.82	6803.56	753.06	1914.60	27.57	-0.00186	0.00052	**3.55**	0.157	0.397	**0.77**
n_Propanol	1098.22	1095	725.96	973.22	214.14	2006.33	72.89	-0.00024	0.00050	**0.49**	0.012	0.108	**0.21**
n-Butanol	5046.23	6164.81	4466.46	5225.83	863.31	1009.83	43.48	-0.00512	0.00099	**5.17**	0.781	0.883	**1.73**
												[mol %]	
Carbon Dioxide	1652.4	1703.68	1509.7	1621.93	100.5163	523580	3347.53	-5.916E-09	1.91E-06	**30.98**	3.724E-08	0.00019	**3.782**
Methane	41418.83	44594.311	38221.06	41411	3186.633	565467	2364.98	-1.295E-07	1.768E-06	**732.34**	3.185E-05	0.00564	**110.61**

A.3 GC/MS INSTRUMENT CONTROL PARAMETERS.

This appendix contains the control parameters of the GC/MS system and also the MSD acquisition parameters for each method employed in the analysis of our products

A.3.1 Analysis of Oxygenates and Heavier Hydrocarbons

C:\MSDCHEM\1\METHODS\Oxygenates.m

Sample Inlet : GC
Injection Source : Valve/Immediate Start
Injection Location: Valve 8
Mass Spectrometer : Enabled

OVEN
Initial temp: 35°C (On) Maximum temp: 165°C
Initial time: 1.50 min Equilibration time: 0.70 min
Ramps:

#	Rate	Final temp	Final time
1	4.00	70	0.00
2	15.00	160	2.00
3	0.0(Off)		

Post temp: 145 'C
Post time: 1.75 min
Run time: 18.25 min

FRONT INLET (SPLIT/SPLITLESS)
Mode: Split
Initial temp: 300 'C (On)
Pressure: 45.56 psi (On)
Split ratio: 20:1
Split flow: 46.9 mL/min
Total flow: 51.4 mL/min
Gas saver: On
Saver flow: 20.0 mL/min
Saver time: 2.00 min
Gas type: Helium

BACK INLET (SPLIT/SPLITLESS)
Mode: Split
Initial temp: 220 'C (On)
Pressure: 4.00 psi (On)
Split ratio: 6:1
Split flow: 55.4 mL/min
Total flow: 67.1 mL/min
Gas saver: On
Saver flow: 20.0 mL/min
Saver time: 2.00 min
Gas type: Helium

COLUMN 1
Capillary Column
Model Number: Wasson KC40
100 x 250 x 0.50
Max temperature: 350 'C
Nominal length: 100.0 m
Nominal diameter: 250.00 um
Nominal film thickness: 0.50 um
Mode: constant flow
Initial flow: 1.7 mL/min

COLUMN 2
Capillary Column
Model Number: Wasson KC134
14 x 530 x20
Max temperature: 165 'C
Nominal length: 14.0 m
Nominal diameter: 530.00 um
Nominal film thickness: 20.00 um
Mode: ramped pressure
Initial pressure: 4.00 psi

Nominal init pressure: 36.63 psi

Average velocity: 26 cm/sec
Inlet: Front Inlet
Outlet: MSD
Outlet pressure: vacuum

Initial time: 2.10 min

#	Rate	Final pres	Final time
1	0.65	2.00	0.00
2	0.0(Off)		

Post pressure: 4.00 psi
Nominal initial flow: 9.2 mL/min
Average velocity: 74 cm/sec
Inlet: Back Inlet
Outlet: Front Detector
Outlet pressure: ambient

FRONT DETECTOR (TCD)
Temperature: 250 'C (On)
Reference flow: 10.0 mL/min (On)
Mode: Constant makeup flow
Makeup flow: 7.0 mL/min (Off)
Makeup Gas Type: Helium
Filament: On
Negative polarity: Off

BACK DETECTOR (TCD)
Temperature: 250 'C (On)
Reference flow: 38.0 mL/min (On)
Mode: Constant makeup flow
Makeup flow: 7.0 mL/min (Off)
Makeup Gas Type: Nitrogen
Filament: On
Negative polarity: On

SIGNAL 1
Data rate: 5 Hz
Type: front detector
Save Data: On
Zero: 0.0 (Off)
Range: 0
Fast Peaks: Off
Attenuation: 0

SIGNAL 2
Data rate: 20 Hz
Type: back detector
Save Data: On
Zero: 0.0 (Off)
Range: 0
Fast Peaks: Off
Attenuation: 0

COLUMN COMP 1
Derive from front detector

COLUMN COMP 2
Derive from back detector

THERMAL AUX 1
Use: Valve Box Heater
Description:
Initial temp: 150 'C (On)
Initial time: 0.00 min

#	Rate	Final temp	Final time
1	0.0(Off)		

THERMAL AUX 2
Use: MSD Transfer Line Heater
Description:
Initial temp: 280 'C (On)
Initial time: 0.00 min

#	Rate	Final temp	Final time
1	0.0(Off)		

AUX PRESSURE 3
Description:
Gas Type: Helium
Initial pressure: 5.00 psi (On)
Initial time: 0.00 min

#	Rate	Final pres	Final time
1	0.0(Off)		

AUX PRESSURE 4
Description:
Gas Type: Helium
Initial pressure: 3.80 psi (On)
Initial time: 0.00 min

#	Rate	Final pres	Final time
1	0.0(Off)		

AUX PRESSURE 5
Description:
Gas Type: Helium
Initial pressure: 5.00 psi (Off)

VALVES
Valve 1 Switching Off
Description:
Valve 2 Switching Off
Description:
Valve 3 Switching Off
Description:
Valve 4 Switching On
Description:
Valve 8 Gas Sampling
Description:
Loop Volume: 1.000 mL
Load Time: 0.50 min
Inject Time: 0.50 min
Inlet: Front Inlet

POST RUN
Post Time: 1.75 min
Oven Temperature: 145 'C
Column 1 Flow: 1.7 mL/min
Column 2 Pressure: 4.0 psi

TIME TABLE

Time	Specifier	Parameter & Setpoint
0.01	Valve 2:	On
0.01	Valve 3:	On
0.40	Valve 1:	On
0.50	Valve 2:	Off
0.60	Valve 1:	Off
4.50	Valve 3:	Off

MS ACQUISITION PARAMETERS

General Information

Tune File : atune.u
Acquistion Mode : SIM

MS Information

Solvent Delay : 0.00 min
EM Absolute : False
EM Offset : 0
Resulting EM Voltage : 1858.8

[SIM Parameters]

GROUP 1
Group ID : 1
Resolution : Low
Plot 1 Ion : 27.00

Ions/Dwell In Group	(Mass, Dwell)	(Mass, Dwell)	(Mass, Dwell)
	(18.00, 100)	(27.00, 100)	(29.00, 100)
	(31.00, 100)	(32.00, 100)	(33.00, 100)
	(41.00, 100)	(42.00, 100)	(43.00, 100)
	(44.00, 100)	(45.00, 100)	(46.00, 100)
	(55.00, 100)	(56.00, 100)	(57.00, 100)
	(58.00, 100)	(59.00, 100)	(60.00, 100)

[MSZones]

MS Quad : 150 C maximum 200 C
MS Source : 230 C maximum 250 C

TUNE PARAMETERS

EMISSION : 34.610
ENERGY : 69.922
REPELLER : 29.788
IONFOCUS : 90.157
ENTRANCE_LE : 32.000
EMVOLTS : 1858.824
AMUGAIN : 1146.000
AMUOFFSET : 119.688
FILAMENT : 1.000
DCPOLARITY : 0.000
ENTLENSOFFS : 17.569
MASSGAIN : -716.000
MASSOFFSET : -39.000

A.3.2 Analysis of Light Components

C:\MSDCHEM\1\METHODS\Light-Gases.M

Control Information
------- -----------

Sample Inlet : GC
Injection Source : Valve/Immediate Start
Injection Location: Valve 8
Mass Spectrometer : Enabled

OVEN
Initial temp: 55°C (On) Maximum temp: 165°C
Initial time: 3.00 min Equilibration time: 0.70 min

Ramps:

#	Rate	Final temp	Final time
1	15°C	160°C	20.00 min
2	0.0(Off)		

Post temp: 145°C
Post time: 1.00 min
Run time: 30.00 min

FRONT INLET (SPLIT/SPLITLESS)
Mode: Split
Initial temp: 300 'C (On)
Pressure: 5.00 psi (On)
Split ratio: 500:1
Split flow: 112.7 mL/min
Total flow: 115.4 mL/min
Gas saver: On
Saver flow: 20.0 mL/min
Saver time: 2.00 min
Gas type: Helium

BACK INLET (SPLIT/SPLITLESS)
Mode: Split
Initial temp: 220 'C (On)
Pressure: 4.00 psi (On)
Split ratio: 6:1
Split flow: 49.9 mL/min
Total flow: 60.6 mL/min
Gas saver: On
Saver flow: 20.0 mL/min
Saver time: 2.00 min
Gas type: Helium

COLUMN 1
Capillary Column
Model Number: Wasson KC40
100 x 250 x 0.50
Max temperature: 350°C
Nominal length: 100.0 m
Nominal diameter: 250.00 µm
Nominal film thickness: 0.50 µm
Mode: ramped pressure
Initial pressure: 5.00 psi
Initial time: 22.50 min

#	Rate	Final pres	Final time
1	2.00	2.00	0.00
2	0.0(Off)		

Post pressure: 4.99 psi
Nominal initial flow: 0.2 mL/min
Average velocity: 9 cm/sec
Inlet: Front Inlet
Outlet: MSD
Outlet pressure: vacuum

COLUMN 2
Capillary Column
Model Number: Wasson KC134
14 x 530 x20
Max temperature: 165°C
Nominal length: 14.0 m
Nominal diameter: 530.00 µm
Nominal film thickness: 20.00 µm
Mode: ramped pressure
Initial pressure: 4.00 psi
Initial time: 2.10 min

#	Rate	Final pres	Final time
1	0.65	2.00	0.00
2	0.0(Off)		

Post pressure: 4.00 psi
Nominal initial flow: 8.3 mL/min
Average velocity: 71 cm/sec
Inlet: Back Inlet
Outlet: Front Detector
Outlet pressure: ambient

FRONT DETECTOR (TCD)
Temperature: 250 'C (On)
Reference flow: 10.0 mL/min (On)
Mode: Constant makeup flow
Makeup flow: 7.0 mL/min (Off)
Makeup Gas Type: Helium
Filament: On

BACK DETECTOR (TCD)
Temperature: 250 'C (On)
Reference flow: 38.0 mL/min (On)
Mode: Constant makeup flow
Makeup flow: 7.0 mL/min (Off)
Makeup Gas Type: Nitrogen
Filament: On

Negative polarity: Off

Negative polarity: On

SIGNAL 1
Data rate: 5 Hz
Type: front detector
Save Data: On
Zero: 0.0 (Off)
Range: 0
Fast Peaks: Off
Attenuation: 0

SIGNAL 2
Data rate: 20 Hz
Type: back detector
Save Data: On
Zero: 0.0 (Off)
Range: 0
Fast Peaks: Off
Attenuation: 0

COLUMN COMP 1
Derive from front detector

COLUMN COMP 2
Derive from back detector

THERMAL AUX 1
Use: Valve Box Heater
Description:
Initial temp: 150 'C (On)
Initial time: 0.00 min
Rate Final temp Final time
1 0.0(Off)

THERMAL AUX 2
Use: MSD Transfer Line Heater
Description:
Initial temp: 280 'C (On)
Initial time: 0.00 min
Rate Final temp Final time
1 0.0(Off)

AUX PRESSURE 3
Description:
Gas Type: Helium
Initial pressure: 35.00 psi (On)
Initial time: 0.00 min
Rate Final pres Final time
1 0.0(Off)

AUX PRESSURE 4
Description:
Gas Type: Helium
Initial pressure: 3.80 psi (On)
Initial time: 0.00 min
Rate Final pres Final time
1 0.0(Off)

AUX PRESSURE 5
Description:
Gas Type: Helium
Initial pressure: 4.00 psi (On)
Initial time: 22.50 min
Rate Final pres Final time
1 0.50 9.00 0.00
2 0.0(Off)

VALVES
Valve 1 Switching Off
Description:
Valve 2 Switching Off
Description:

POST RUN
Post Time: 1.00 min
Oven Temperature: 145 'C
Column 1 Pressure: 5.0 psi
Column 2 Pressure: 4.0 psi

Valve 3 Switching Off
Description:
Valve 4 Switching Off
Description:
Valve 8 Gas Sampling
Description:
Loop Volume: 1.000 mL
Load Time: 0.50 min
Inject Time: 0.50 min
Inlet: Front Inlet

TIME TABLE

Time	Specifier	Parameter & Setpoint
0.01	Valve 2:	On
0.01	Valve 3:	On
0.40	Valve 1:	On
0.50	Valve 2:	Off
0.60	Valve 1:	Off
4.50	Valve 3:	Off

MS ACQUISITION PARAMETERS

General Information

Tune File : atune.u
Acquistion Mode : SIM

MS Information

Solvent Delay : 0.00 min
EM Absolute : False
EM Offset : 0
Resulting EM Voltage : 1764.7

[SIM Parameters]

GROUP 1
Group ID : 1
Resolution : Low
Plot 1 Ion : 16.00
Ions/Dwell In Group (Mass, Dwell) (Mass, Dwell) (Mass, Dwell)
(15.00, 20) (16.00, 20) (28.00, 20)
(29.00, 20) (30.00, 20) (44.00, 20)

GROUP 2
Group ID : 2
Resolution : Low

Group Start Time : 11.50
Plot 1 Ion : 37.00

Ions/Dwell In Group	(Mass, Dwell)	(Mass, Dwell)	(Mass, Dwell)
	(37.00, 20)	(38.00, 20)	(39.00, 20)
	(41.00, 20)	(42.00, 20)	(43.00, 20)
	(44.00, 20)		

[MSZones]

MS Quad : 150 C maximum 200 C
MS Source : 230 C maximum 250 C

TUNE PARAMETERS

EMISSION : 34.610
ENERGY : 69.922
REPELLER : 30.793
IONFOCUS : 90.157
ENTRANCE_LE : 28.500
EMVOLTS : 1764.706
AMUGAIN : 1154.000
AMUOFFSET : 119.250
FILAMENT : 1.000
DCPOLARITY : 0.000
ENTLENSOFFS : 18.573
MASSGAIN : -720.000
MASSOFFSET : -39.000

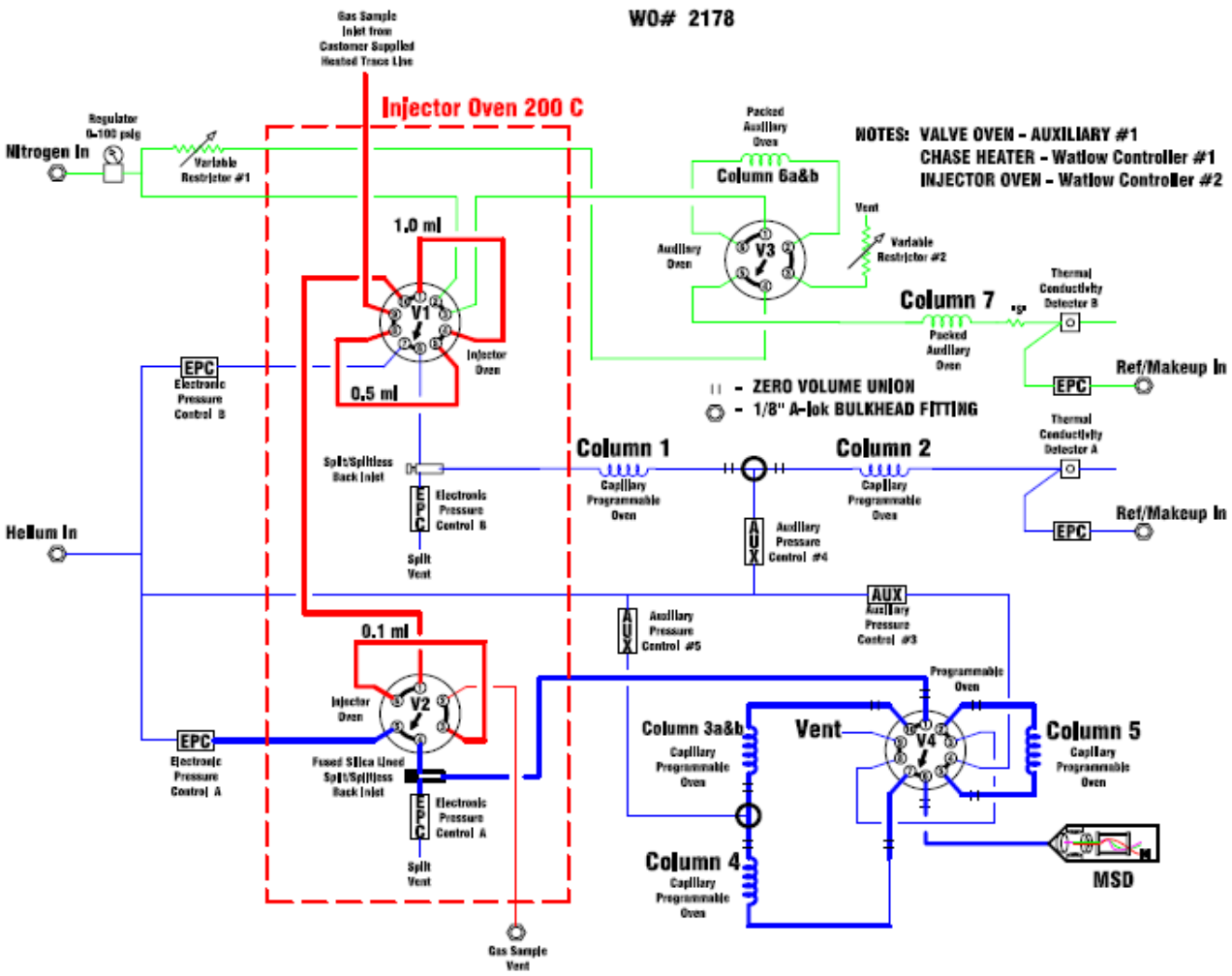

Gas Type	Required Purity	Required Pressure
Helium	99.999%+	100 psig
Nitrogen	99.999%	60 psig
Perm Tube Cal Gas	Not Applicable	
Gas Samples	Not Applicable	
Liquid Samples	Not Applicable	

Column #	Part # or Column Code
Column 1	KC 134 1m
Column 2	KC134 13m
Column 3 a&b	a: KC090 15m b: KC134 1m
Column 4	KC080 50m
Column 5	KC066 100 m
Column 6 a&b	a: K1 6 ft b: K2 7 ft
Column 7	K2S 2 ft
Color denotes Gas Type (Ie. Blue - Helium)	

Valve #	Valve Part #
Valve 1	15500
Valve 2	15300
Valve 3	15320
Valve 4	15531
Voltage/Power Requirements	120 Vac/20 Amps

Agilent Technologies SN:	Agilent Technologies 7973 SN:	Wasson ECE Instrumentation SN:
US10710006	US65135535	070741

Figure A.10: Schematic of the switching valves and columns installed in the GC/MS system

APPENDIX B: PERMISSION LETTERS

B.1. Permission Letter for Chapter 2

Adefemi Egbebi

From: CONTRACTS-COPYRIGHT (shared) [Contracts-Copyright@rsc.org]
Sent: Thursday, July 03, 2008 1:52 AM
To: aegbeb1@lsu.edu
Subject: RE: Permission Request Form: Adefemi Egbebi

Dear Adefemi Egbebi

The Royal Society of Chemistry (RSC) hereby grants permission for the use of your paper(s) specified below in the printed and microfilm version of your thesis. You may also make available the PDF version of your paper(s) that the RSC sent to the corresponding author(s) of your paper(s) upon publication of the paper(s) in the following ways: in your thesis via any website that your university may have for the deposition of theses, via your university's Intranet or via your own personal website. We are however unable to grant you permission to include the PDF version of the paper(s) on its own in your institutional repository. The Royal Society of Chemistry is a signatory to the STM Guidelines on Permissions (available on request).

Please note that if the material specified below or any part of it appears with credit or acknowledgement to a third party then you must also secure permission from that third party before reproducing that material.

Please ensure that the published article states the following:

Reproduced by permission of The Royal Society of Chemistry

Regards

Gill Cockhead
Contracts & Copyright Executive

Gill Cockhead (Mrs), Contracts & Copyright Executive
Royal Society of Chemistry, Thomas Graham House
Science Park, Milton Road, Cambridge CB4 0WF, UK
Tel +44 (0) 1223 432134, Fax +44 (0) 1223 423623
http://www.rsc.org

B.2. Completed permission request form for the use of Chapter 2

-----Original Message-----
From: aegbeb1@lsu.edu [mailto:aegbeb1@lsu.edu]
Sent: 02 July 2008 18:50
To: CONTRACTS-COPYRIGHT (shared)
Subject: Permission Request Form: Adefemi Egbebi

Name : Adefemi Egbebi
Address :

Department of Chemical Engineering
Louisiana State University
S. Stadium Drive
Baton Rouge
LA 70820

Tel : 225-578-7032
Fax : 225-578-1476
Email : aegbeb1@lsu.edu

I am preparing the following work for publication:

Article/Chapter Title : Dissertation (Ph.D)
Journal/Book Title :
Editor/Author(s) : Adefemi Egbebi

Publisher :

I would very much appreciate your permission to use the following material:

Journal/Book Title : Chemical Society Reviews
Editor/Author(s) : J.J. Spivey, Adefemi Egbebi
Volume Number : 36
Year of Publication : 2007
Description of Material : entire paper
Page(s) : 1514-1528

Any Additional Comments :

This review paper will be included in the Literature Review section of my dissertion with minor modifications.

B.3. Permission Letter for Chapter 6

Adefemi Egbebi

From: Steward, Laura (ELS-OXF) [L.Steward@elsevier.com]
Sent: Friday, July 04, 2008 4:50 AM
To: Adefemi Egbebi
Subject: RE: Permission Request - Adefemi Egbebi
Attachments: image001.gif

Dear Dr Egbebi,

We hereby grant you permission to reprint the material below at no charge **in your thesis** subject to the following conditions:

1. If any part of the material to be used (for example, figures) has appeared in our publication with credit or acknowledgement to another source, permission must also be sought from that source. If such permission is not obtained then that material may not be included in your publication/copies.

2. Suitable acknowledgment to the source must be made, either as a footnote or in a reference list at the end of your publication, as follows:

   "This article was published in Publication title, Vol number, Author(s), Title of article, Page Nos, Copyright Elsevier (or appropriate Society name) (Year)."

3. Your thesis may be submitted to your institution in either print or electronic form.

4. Reproduction of this material is confined to the purpose for which permission is hereby given.

5. This permission is granted for non-exclusive world **English** rights only. For other languages please reapply separately for each one required. Permission excludes use in an electronic form other than submission. Should you have a specific electronic project in mind please reapply for permission.

6. This includes permission for UMI to supply single copies, on demand, of the complete thesis. Should your thesis be published commercially, please reapply for permission.

Kind regards
Laura Steward

Laura Steward
Rights Assistant
Elsevier Ltd.
Tel: +44 (0) 1865 843517
Fax: +44 (0) 1865 843950

B.4. Letter requesting permission for the use of Chapter 6

From: Adefemi Egbebi [mailto:aegbeb1@paws.lsu.edu]
Sent: 03 July 2008 18:01
To: Rights and Permissions (ELS)
Subject: Permission Request - Adefemi Egbebi
Importance: High

Adefemi Egbebi
Department of Chemical Engineering
Louisiana State University
S. Stadium Drive
Baton Rouge
LA 70820

Dear Sir/Madam,

I would very much appreciate the permission to use the following material, which is to be published in Catalysis Communications. I plan to include this paper in its entirely as a chapter in my dissertation (Ph.D). This could not be done through Rightslink

"Effect of H_2/CO ratio and temperature on methane selectivity in the synthesis of ethanol on Rh-based catalysts"

Adefemi Egbebi and James J. Spivey

http://dx.doi.org/10.1016/j.catcom.2008.05.011

Thank you.

Regards

Adefemi Egbebi.

Catalysis Communications 9 (2008) 2308–2311

Contents lists available at ScienceDirect

Catalysis Communications

journal homepage: www.elsevier.com/locate/catcom

Effect of H_2/CO ratio and temperature on methane selectivity in the synthesis of ethanol on Rh-based catalysts

Adefemi Egbebi, James J. Spivey *

Cain Department of Chemical Engineering, Louisiana State University, S. Stadium Drive, Baton Rouge, LA 70803, USA

ARTICLE INFO

Article history:
Received 25 February 2008
Received in revised form 2 May 2008
Accepted 5 May 2008
Available online 17 May 2008

Keywords:
Ethanol
Methane
C_2^+ oxygenates
H_2/CO ratio
Syngas
Biomass
Rhodium catalyst

ABSTRACT

The hydrogenation of CO to form ethanol is thermodynamically limited if methane is allowed as a reaction product. The literature confirms this – selectivity to ethanol versus methane is limited even on Rh-based catalysts, which are the most selective for ethanol. Although it might be anticipated that increasing H_2/CO ratio would favor methane, the kinetic studies in the literature, and our results reported here, show that the point selectivity for ethanol ($S = r_{EtOH}/r_{CH_4}$) actually increases with increasing H_2/CO ratio on Rh-based catalysts. This may be attributed to the increased hydrogenation of the surface acetaldehyde intermediate to ethanol.

1. Introduction

Ethanol has found widespread use as both an energy carrier and a fuel additive [1]. A viable route for the manufacture of ethanol is the catalytic conversion of synthesis gas (syngas), which can be obtained by gasification of coal or a renewable resource like biomass. One key variable in syngas production is the H_2/CO ratio, which can be adjusted to maximize ethanol selectivity.

Supported Rh-based catalysts have been found to be most selective for the formation of ethanol from the hydrogenation of CO [1]:

$$2CO + 4H_2 \rightarrow C_2H_5OH + H_2O, \quad (1)$$
$$\Delta H_r^\circ = -61.20 \text{ kcal/mol},$$
$$\Delta G_r^\circ = -29.32 \text{ kcal/mol}.$$

1.1. Thermodynamics

Fig. 1 shows the equilibrium composition for reaction (1) as a function of temperature starting with a stoichiometric H_2/CO ratio of 2/1. Substantial amounts of ethanol can be observed at temperatures below 350 °C with the products restricted to ethanol and water. However, when methane is allowed as an additional product, ethanol selectivity goes to almost zero at all temperatures (Fig. 2).

The reason for this difference is the methanation reaction:

$$CO + 3H_2 \rightarrow CH_4 + H_2O, \quad (2)$$
$$\Delta H_r^\circ = -49.27 \text{ kcal/mol},$$
$$\Delta G_r^\circ = -33.97 \text{ kcal/mol}.$$

Methane is the most thermodynamically favored product, and is generally undesirable economically. In practice, the reaction kinetics determine the observed selectivity to ethanol. The H_2/CO feed ratio and temperature are key adjustable variables in the overall conversion of syngas to ethanol/higher alcohols and it is of interest to determine their effects on the selectivity to ethanol, versus methane.

1.2. Kinetics

Previous work on CO hydrogenation to ethanol on Rh-based catalysts shows that point selectivities ($S = r_{EtOH}/r_{CH_4}$) are typically poor, varying from 2/1 to 1/25, depending on the particular catalyst and reaction conditions [2–9]. There are several studies in which the kinetics of ethanol formation (Eq. (1)) and methanation (Eq. (2)) are measured. For example, Yin et al. give the following results for temperatures between 295 and 305 °C, 30 atm, 15,000 h^{-1} for a Rh–Mn–Li–Fe/SiO_2 catalyst with a weight ratio among the metals of 1/1/0.075/0.05 [10]:

$$r_{EtOH} = 6.3 \times 10^{12} e^{-126.7/RT} P_{H_2}^{0.90} P_{CO}^{-0.76}, \quad (3)$$
$$r_{CH_4} = 9.0 \times 10^{15} e^{-156.8/RT} P_{H_2}^{0.79} P_{CO}^{-0.60}. \quad (4)$$

* Corresponding author. Tel.: +225 578 3690; fax: +225 578 1476.
E-mail address: jjspivey@lsu.edu (J.J. Spivey).

1566-7367/$ - see front matter © 2008 Elsevier B.V. All rights reserved.
doi: 10.1016/j.catcom.2008.05.011

Heterogeneous catalytic synthesis of ethanol from biomass-derived syngas

James J. Spivey* and Adefemi Egbebi

Received 30th December 2006
First published as an Advance Article on the web 7th March 2007
DOI: 10.1039/b414039g

The selective catalytic conversion of biomass-derived syngas into ethanol is thermodynamically feasible at temperatures below roughly 350 °C at 30 bar. However, if methane is allowed as a reaction product, the conversion to ethanol (or other oxygenates) is extremely limited. Experimental results show that high selectivities to ethanol are only achieved at very low conversions, typically less than 10%. The most promising catalysts for the synthesis of ethanol are based on Rh, though some other formulations (such as modified methanol synthesis catalysts) show promise. (*Critical review*—173 references.)

1. Introduction

1.1 Biomass

Potential of biomass as an energy source. The use of biomass and other renewables to provide energy and chemicals is receiving increased attention because these resources can supplement existing supplies of raw materials and have less net environmental impact, according to some studies.[1] Worldwide, renewable energy sources (including biomass) account for about 19% of total energy usage,[2] and have the potential to supply 50% of world energy demand in the next century.[3] In the US, biomass supplied roughly 3% of a total energy demand of 98 quads in 2003,[4] and is projected to grow to at a rate of 1.5% per year through to 2025.[5,6]

Biomass gasification. Virtually all of the energy derived from biomass (98% by one estimate[7]) is currently produced by direct combustion. Gasification is an alternative that offers a number of advantages, *e.g.*, the potential for higher thermal efficiency.[8,9] Large scale biomass gasification plants ranging in size from 15–70 MW_{th}[10] are being developed in Europe, primarily for power generation.

Louisiana State University, Cain Department of Chemical Engineering, Baton Rouge, LA 70803, USA. E-mail: jjspivey@lsu.edu; Fax: (225) 578-1476; Tel: (225) 578-3690

Gasification is a thermochemical process in which biomass reacts with air (or oxygen) and steam to produce synthesis gas, a mixture consisting primarily of CO, CO_2, H_2, and H_2O (Fig. 1). This mixture can be used to produce a range of products using well-established technologies, such as fuels *via* the Fischer–Tropsch process.[11–14] However, the use of biomass-derived syngas to produce higher alcohols has received relatively little attention, despite the potential to produce valuable compounds such as ethanol.[13,15,16] Challenges that remain include novel catalytic reactor designs tailored to the typically smaller scale of biomass conversion

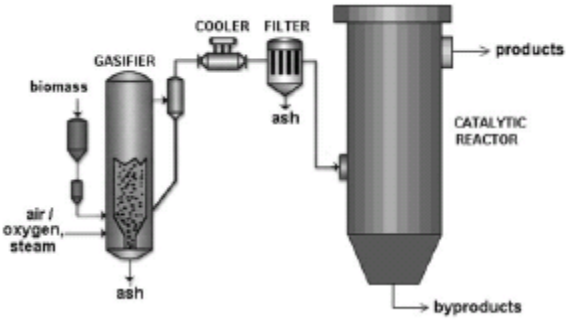

Fig. 1 Generic biomass gasification process.

James J. Spivey

James J. Spivey received BS and MS degrees in Chemical Engineering from NC State University and a PhD in the same field from Louisiana State University (1980). He is currently the James Shrivers Professor of Chemical Engineering at LSU, where his research interests focus on the use of heterogeneous catalysts for the conversion of syngas and low molecular weight hydrocarbons to both energy and higher value chemicals.

Adefemi Egbebi

Adefemi Egbebi was born in 1975 in Lagos, Nigeria. He received his BSc in Chemical Engineering from Obafemi Awolowo University, Ife, Nigeria in 1999. He moved to the Louisiana State University in Baton Rouge, USA where he his presently working on his doctoral degree on the conversion of biomass-derived syngas to oxygenated fuels under the supervision of Dr James Spivey.

VITA

Adefemi Adelanwa Egbebi was born in Lagos, Nigeria, on September 13, 1975. He obtained a Bachelor of Science (Honors) degree in chemical engineering from Obafemi Awolowo University, Ife, Nigeria in 1999. He moved to the Louisiana State University in Baton Rouge, USA, in 2002 after working with Total Nigeria as an LPG sales assistant and doing a two-year stint as an analyst at the then Universal Trust Bank, Nigeria. He is presently a candidate for the doctorate degree in chemical engineering.